UNIVERSIDADE FEDERAL DO CEARÁ
CENTRO DE TECNOLOGIA
DEPARTAMENTO DE ENGENHARIA DE TELEINFORMÁTICA
PROGRAMA DE PÓS-GRADUAÇÃO EM ENGENHARIA DE TELEINFORMÁTICA

EDUARDO DE OLIVINDO CAVALCANTE

SUM-POWER MINIMIZATION BEAMFORMING FOR DENSE NETWORKS

FORTALEZA
2018

EDUARDO DE OLIVINDO CAVALCANTE

SUM-POWER MINIMIZATION BEAMFORMING FOR DENSE NETWORKS

Dissertação apresentada ao Programa de Pós-Graduação em Engenharia de Teleinformática da Universidade Federal do Ceará, como parte dos requisitos para obtenção do Título de Mestre em Engenharia de Teleinformática. Área de concentração: Sinais e Sistemas

Orientador: Prof. Dr. Yuri Carvalho Barbosa Silva

FORTALEZA
2018

Dados Internacionais de Catalogação na Publicação
Universidade Federal do Ceará
Biblioteca Universitária
Gerada automaticamente pelo módulo Catalog, mediante os dados fornecidos pelo(a) autor(a)

C364s Cavalcante, Eduardo de Olivindo.
Sum-Power Minimization Beamforming For Dense Networks / Eduardo de Olivindo Cavalcante. – 2018.
79 f. : il. color.

Dissertação (mestrado) – Universidade Federal do Ceará, Centro de Tecnologia, Programa de Pós-Graduação em Engenharia de Teleinformática, Fortaleza, 2018.
Orientação: Prof. Dr. Yuri Carvalho Barbosa Silva.

1. Formação de Feixes. 2. Minimização de Potência. 3. Redes Densas. 4. TDD dinâmico. I. Título.
CDD 621.38

EDUARDO DE OLIVINDO CAVALCANTE

SUM-POWER MINIMIZATION BEAMFORMING FOR DENSE NETWORKS

Dissertation presented to the Graduate Program in Teleinformatics Engineering at the Federal University of Ceará, as part of the requirements for obtaining the Master's Degree in Teleinformatics Engineering.m Concentration area: Signal and Systems

Approved in: 06/02/2018.

EXAMINATION BOARD

Prof. Dr. Yuri Carvalho Barbosa Silva (Advisor)
Universidade Federal do Ceará

Prof. Dr. Walter da Cruz Freitas Júnior
Universidade Federal do Ceará

Prof. Dr. Carlos Héracles Morais de Lima
Universidade Estadual de São Paulo

ACKNOWLEDGEMENTS

Firstly above all, I would like to thank God, for guiding each of my steps, and for supporting me with strength and peace.

To my parents, João and Joselita, for the unconditional love and for all the sacrifices they made to raise me and my brothers. To my beloved wife Rebeca, who is always by my side, supporting me with love, patience and encouragement. To my brothers, Eider and Erivan, for all the good example and inspiration they give me.

To my advisor Prof. Dr. Yuri Silva and to Prof. Dr. Walter and Dr. Gábor Fodor, who have a great part on this work. Without your great effort none of this was possible.

To all my colleagues from UFC and GTEL, for all the many joyful moments and for the productive talks, advices and suggestions that helped me on the development of this work.

Finally, I acknowledge the technical and financial support from CAPES, and from the Innovation Centre, Ericsson Telecomunicações S/A, Brazil.

RESUMO

O emprego de redes densas é uma solução promissora para os futuros sistemas 5G. O uso de um maior número de BSs (do inglês, *base station*) por unidade de área provê uma redução na distancia de transmissão e pode melhorar significativamente a multiplexação espacial. Porém, a densificação traz preocupações principalmente relacionadas à maior interferência, devido às distâncias reduzidas. Esta dissertação visa apresentar formas de gerir interferência em cenários densos através do uso da formação de feixes para minimização da soma de potências. Mais especificamente, focamos em dois aspectos das redes densas: A solução de problemas de larga-escala e a gerência de interferências de enlace cruzado em redes densas que utilizam TDD (do inglês, *time division duplexing*) dinâmico. Para o primeiro aspecto, nós apresentamos uma análise de desempenho para uma solução de formação de feixes baseada em ADMM (do inglês, *alternating directions method of multipliers*) que é considerada ser bem adaptada para otimização em larga-escala. Por simulações, nós comparamos esta solução com a bem conhecida solução via SDP (do inglês, *semidefinite programming*) em diversas configurações de rede. Os resultados indicam que a solução ADMM proporciona convergência rápida com acurácia modesta. Para cenários TDD dinâmico, nós propomos dois problemas de formação de feixes. No primeiro, nós almejamos proteger a comunicação UL (do inglês *uplink*) forçando uma limitação na potência de interferência entre BSs, enquanto garantimos uma SINR (do inglês, *signal-to-interference-plus-noise ratio*) mínima para o DL (do inglês, *downlink*). Propomos uma solução centralizada e uma distribuída baseada em decomposição primal. Os resultados de simulação mostram que o desempenho do UL é melhorado e os alvos de SINR para o DL são garantidos, e que a solução distribuída itera em direção à centralizada, enquanto soluções realizáveis podem ser obtidas em iterações intermediárias ao custo de potência subótima. No segundo problema para TDD dinâmico, nós visamos garantir uma SINR mínima para usuários em UL e DL. Propomos uma solução centralizada e uma solução distribuída baseada em ADMM. Os resultados de simulação mostram que ambas as abordagens alcançam bom desempenho e que a solução distribuída itera em direção à centralizada, enquanto a carga de sinalização pode ser controlada fixando o número de iterações ao custo de desempenhos de SINR e potência próximos ao ótimo.

Palavras-chave: Formação de Feixes, Minimização de Potência, Redes Densas, TDD dinâmico

ABSTRACT

The employment of dense networks is a promising solution for the upcoming 5G systems. The use of a larger number of base stations (BSs) per unit area provides a reduction in transmission distance and can significantly improve spatial multiplexing. However, the densification also brings worries mainly related to higher interference due to the reduced distances. This master thesis aims to present ways to manage interference in dense scenarios by using sum-power minimization beamforming. More specifically, we focus in two aspects of dense networks: The solution of large-scale problems and the management of the cross-link interferences in dense networks that employ dynamic time division duplex (TDD). For the first aspect, we present an performance analysis for a alternating direction method of multipliers (ADMM)-based solution for the beamforming,which is considered to be well adapted to large-scale optimization. In the simulations we compare the ADMM solution to a well known semidefinite programming (SDP) solution in several network configurations. The results indicate that the ADMM approach has faster convergence for large-scale scenarios when modest accuracy is required. For dynamic TDD scenarios, we propose solutions for different beamforming problems. In the first case, we aim to protect the uplink (UL) communication by forcing a constraint on the BS to BS interference power while guaranteeing downlink (DL) signal-to-interference-plus-noise ratio (SINR). We propose a centralized and a primal decomposition based distributed solution. The simulation results show that UL performance is improved and DL SINR targets are guaranteed, and that the distributed solution iterates towards the centralized one, while feasible beamformers can be obtained at intermediate iterations at the cost of suboptimal power. In the second dynamic TDD problem, we aim to guarantee a minimum SINR for UL and DL users. We propose a centralized and an ADMM-based distributed solution. The simulation results show that both approaches achieve good performance and the distributed solution iterates towards the centralized one, while the signaling load can be controlled by fixing the number of iterations at the cost of close to optimal power and SINR performance.

Keywords: Beamforming, Power Minimization, Dense Networks, Dynamic TDD

LIST OF FIGURES

LIST OF TABLES

LIST OF ABBREVIATIONS AND ACRONYMS

5G	fifth generation
ADMM	alternating direction method of multipliers
AWGN	additive white Gaussian noise
BBU	baseband unit
BS	base station
CBOP	coordinated beamforming optimization problem
CDF	cumulative distribution function
C-RAN	cloud radio access network
CDMA	code division multiple access
CS	channel sounding
CSI	channel state information
DL	downlink
FDMA	frequency division multiple access
HSD	homogeneous self-dual
ICIC	intercell interference cordination
KKT	Karush-Kuhn-Tucker
LoS	line-of-sight
MIMO	multiple-input multiple-output
MISO	multiple-input single-output
MMSE	minimum-mean-square error
MRT	maximum ratio transmission
PIC	parallel interference cancellation
QoS	quality-of-service
RRU	remote radio unit
SDP	semidefinite programming
SIC	successive interference cancellation
SINR	signal-to-interference-plus-noise ratio
SOCP	second-order-cone programming
SVD	singular value decomposition
TDD	time division duplex
TDMA	time division multiple access
UE	user equipment
UL	uplink
ZF	zero-forcing

TABLE OF CONTENTS

1 INTRODUCTION

1.1 Thesis Scope and Motivation

During the past few years, the mobile communications systems experienced a huge increase in data rate and a great improvement in many other quality-of-service (QoS) indicators. This was achieved in order to provide sufficient connection to the large and growing number of users. Beyond that, this improvement also aimed to support new services and applications, which required more and more capacity, reliability and flexibility of connection. This network growth continues in the present days, and it tends to advance even more in the near future. Recent studies affirm that the number of mobile subscribers of the broadband mobile networks will keep rising in a rate of 30% per year. It has also been stated, that by the year 2020, around 90% of the people older than 6 will own a mobile phone [1]. These new requirements for reliable connection, anytime and everywhere, make the research of new technologies for wireless communications one of the main focuses of the current technological development.

A new generation of mobile communication systems, also known as fifth generation (5G), is in its specification process, with plans to start its deployment by the year 2020 [2]. This new generation is projected based on forecasts of the future user requirements, which also indicate a huge increase in the demand of data rate per user. This growth is generated by the emergence of new scenarios and applications which require very high transfer rates. Therefore, 5G systems must largely exceed the performance of the past generations, and increase the possibilities for the use of the mobile systems.

Furthermore, in 5G, the communication will not be made only between people. In a near future machine-type communication will be a constituent part of new systems and countless types of devices will need to have access to the network in order to perform the more diverse tasks. These communicating equipments range from simple technological accessories, such as toys or smart-devices (watches, glasses, clothing and many others), to very critical devices, such as industrial actuators or autonomous vehicles. All of them will access the networks and must have guaranteed their specific requirements of capacity, latency, mobility and reliability.

Based on that, the basic requirements that the 5G systems must fulfill are described in [3], and are listed as follows:

- Massive system capacity.
- Very high data rates everywhere.
- Very low latency.
- Ultra-high reliability and availability.
- Very low device cost and energy consumption.
- Energy-efficient networks.

In order to fulfill these requirements it is necessary to achieve an unprecedented growth in system capacity. Such increase is directly related to some key factors that can be seen in (1.1), which are shown by the capacity upper-bound equation for a cellular mobile system with additive white Gaussian noise (AWGN) channels [4] .

$$R < C = m\left(\frac{W}{n}\right)\log_2\left(1+\frac{S}{I+N}\right), \tag{1.1}$$

where m is the spatial multiplexing factor, W denotes the available bandwidth, n is the number of users sharing the same resource, S is the power of the received signal, I is the interference power and N is the noise power.

Therefore, the system capacity can be increased by the use of larger bandwidths (W), by increasing the spatial multiplexing term (m), by the reduction of the number of users sharing the same resource (n) or by increasing the SINR. Lately, some technologies and solutions targeting each of these key factors are subject to a great interest from the scientific community. This interest is motivated by the intention of standardizing such technologies as constituent parts of the future 5G systems. Among the main upcoming technologies we can highlight the following:

• **New frequency bands:** In order to achieve the higher rates and capacity in 5G it is necessary to expand the widths of the transmission bands (W) to some hundreds of MHz. Currently, the frequency bands used by the cellular systems are below 6 GHz. However, the 5G requirement for higher bandwidths, makes it necessary to allocate frequencies far beyond this threshold, reaching frequencies up to the order of 100 GHz [5]. In these higher frequencies, it is possible to find wide unused frequency bands. For example, 1 GHz wide unused bands can be found in the spectrum between 28 GHz and 30 GHz [6]. However, in these higher frequency bands the transmitter waves (commonly called millimeter waves, for its smaller wave-length) present high path and penetration losses, which makes necessary the study and characterization of new channel models [7].

• **Massive MIMO:** The concept of massive multiple-input multiple-output (MIMO) is defined as the use of a large number of antennas in order to serve many users using the same frequency-time resource [8]. With the employment of massive MIMO, a 10-fold increase in system capacity and a 100 times improvement in energy efficiency are expected, when compared to previous systems [9]. This increase in capacity and energy efficiency comes from the aggressive spatial multiplexing (m), provided by the excessive number of antennas and by the formation of extremely narrow beams.

• **Dense networks:** The employment of dense networks reduces the number of users sharing the same resources (n). For that, it proposes networks with larger numbers of BSs per unit area, which would manage a smaller number of users [4]. These users, on the other hand, will be closer to its BS, what makes the system capacity increase and decrease the transmit power for BSs and user equipments (UEs). Thus, denser networks are expected to provide improvement in energy efficiency and to enable better exploitation of spectrum.

Each of these technologies for the 5G systems present their specific technical issues, which still need lots of research in order to achieve the target gains. Therefore, in this master's thesis we focus on techniques to manage interference levels generated by the network densification in the upcoming 5G networks. Network densification brings, beyond its clear benefits, some worries mainly related to: the higher interference due to the reduced space between the increased number of nodes; the solution of larger-scale optimization problems with very large number of variables; the amount of signaling among the larger number of network entities; and to the variation and asymmetry of the UL and DL traffic requirements between neighboring cells.

In this work, we seek to study the impact of using sum-power minimization beamforming to combat interference in dense networks. More specifically, we focus in two different aspects. The first one is the difficulty to perform optimization tasks with the larger number of variables that are due to the massive amount of coordinated nodes. For this, we present a performance analysis for a beamforming solution based on ADMM that is well adapted for large-scale problems. The second aspect, is the effect of the different interference links created in dense networks that employ Dynamic TDD in order to adapt to the unbalanced traffic requirements. For this, we propose two different centralized and decentralized beamforming approaches in order to manage such interferences.

1.2 State of the Art

Interference management schemes play a very important role in dense scenarios, since they result in more interference sources whose proximity can achieve extreme levels. Such schemes are commonly classified in three categories: interference avoidance, interference cancellation and interference coordination [10].

- Interference avoidance: interference is managed by avoiding using interfering resources of time, frequency, code or space. This is achieved by allocating orthogonal portions of each resource to each transmitting link. Examples of techniques are multiple access methods [11] such as time division multiple access (TDMA), frequency division multiple access (FDMA) and code division multiple access (CDMA), which allocate separate resources of time, frequency and code, respectively. Also, another technique is based on spatial frequency reuse methods [12], which manages interference by avoiding allocating a same frequency resource to neighbor cells. Power control techniques also fall in this category, since they try to adapt the transmitted power to avoid interfering with other communications.

- Interference cancellation: receivers take advantage of the structure of the interfering signals in order to reconstruct them by demodulation and decodification. This is done so that interference can be subtracted from the complete signal [13]. This interfering signals extraction can be done using successive interference cancellation (SIC) solutions, in which the signal of each user is sequentially extracted from the original signal [14], or using parallel interference cancellation (PIC) solutions in which the interference from all users is extracted simultaneously

Figure 1.1 – Beamforming filtering.

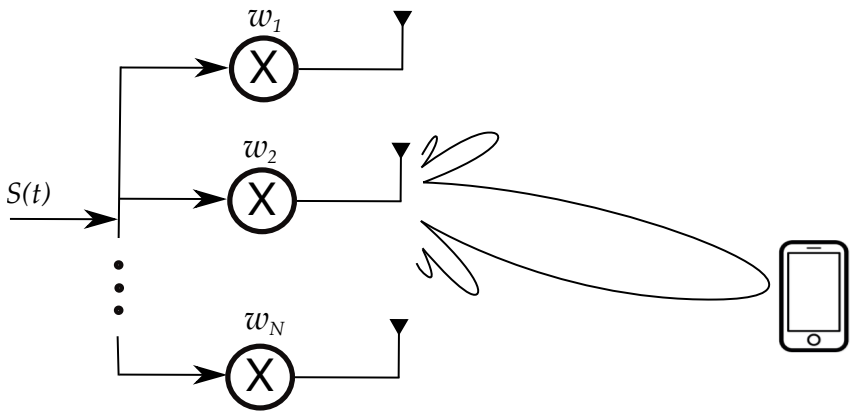

Source: Created by the author.

from the original signal [15].

- Interference coordination: multiple transmitters and receivers are coordinated among themselves in order to mitigate the effects of interference. In a multi-antenna deployment, interference can be managed by using a spatial filtering technique called coordinated beamforming. Beamforming filtering is performed in such a way to combine the signals from each antenna in order to focus a signal beam in a desired direction, or in order to avoid transmitting signal to unintended directions. This can be done, in the simplest case, by building a transmit filter such that its inner product with the steering vector of the desired direction is large, while its inner product with all the other steering vectors are small [16]. The coordination among the different nodes is done in order to jointly design the filters with the objective of optimizing some network performance indicator.

Therefore, this work focuses on the beamforming strategy to coordinate the transmissions and manage interference, in order to achieve the promised performance gains in super-dense scenarios. The next subsection discusses the main concepts and works related to the beamforming technologies.

1.2.1 Beamforming

A beam is formed by the constructive and destructive combination of the signals transmitted by each element in the antenna array. This is achieved by a spatial filtering strategy that assigns complex weight factors (w_n) that are multiplied to the signals transmitted by each antenna. Figure 1.1 illustrates a simple beamforming process, where the weight factors are designed to focus a beam of maximum power in the direction of the user. This can be done by a simple maximum ratio transmission (MRT) approach that maximizes the signal power in the receiver direction, without taking into account interferences [17].

Alternatively, in a multi-user scenario the beamforming can be designed in a way that the BS serves each of its users while avoiding interference between them. A well known

approach to accomplish that is zero-forcing (ZF), which is designed to achieve zero inter-user interference [18]. However, ZF may not be optimal for all cases, since permitting some small degree of interference can allow an increase in other performance aspects, such as power and complexity, without compromising capacity. Another classic beamforming approach that takes into account interference is minimum-mean-square error (MMSE), which aims to minimize the difference between the received and the decoded symbol [19].

In a multi-cell scenario, if each BS performs its beamforming strategies independently, the network performance can be degraded due to the inter-cell interference that occurs between the transmissions of neighboring cells using the same radio resources. Therefore, some coordination among the cells can exist, such that the beamforming weights can be designed to control inter-cell interference in order to improve the overall system performance. This coordination can be performed in a centralized or distributed manner.

In the centralized coordination approach a master entity (a simple central node or a cloud radio access network (C-RAN)) is in charge of performing all the beamforming computation, taking into account the relationship among the cells. In order to do this, the central controller must acquire knowledge of the channels between all BSs and all users in the system, i.e., global channel state information (CSI), which can be achieved by each BS sending its local CSI to a central controlling unit via backhaul. Beyond that, the filters resulting from the beamforming computations must be sent back to the respective transmitters. Alternatively, centralized approaches are also commonly defined with each BS performing its computations. For this, every BS must have access to global CSI via backhaul sharing.

With distributed coordination each node takes its own decisions relying on the availability of local CSI, i.e., knowledge of the channels between itself and other nodes in the system. In addition to local CSI, a small amount of information exchange can be allowed via backhaul and/or over-the-air signaling in order to better coordinate the nodes. The coordination using backhaul exchange is conventionally done to allow intercell interference cordination (ICIC), and can take place for example, by control plane signaling via the X2 interface. The over-the-air signaling is conventionally done for the estimation of effective channels, and can be designed by a channel sounding (CS) strategy using precoded pilot signaling.

The choice between centralized and decentralized solutions is highly scenario dependent. This decision must take into account the trade-off regarding the amount of necessary signaling and the optimality of the beamforming computation, since decentralized algorithms offer the possibility of reduced signaling overhead, while there is the cost of a degradation in performance. Decentralized schemes are often more viable than centralized ones, and they can be designed in a way to achieve minimum performance losses in comparison with centralized schemes. However, if the decentralized scheme is not well designed it may cause delay and increase signaling overhead. This way, it is very important to take these issues into account.

The design of the beams using coordinated beamforming can be done with respect to a variety of network objectives, which depend on the scenario where it is applied and on its

respective QoS requirements. Classical beamforming approaches MRT, ZF and MMSE can also be used in multi-cell coordinated scenarios. However, other optimization-based beamforming approaches have very high importance, since they can be used do optimize more complex network objectives. The most common are sum-rate maximization [20, 21, 22], energy efficiency maximization [23, 24, 25, 26] and sum-power minimization [27, 28, 29, 30, 31, 32, 33, 34, 35].

In conventional sum-rate maximization algorithms the goal of the beamforming procedure is to maximize the total throughput of the network while satisfying some maximum transmit power constraints at each BS. This approach may not be fair with all users, since users with good channel conditions may be favored. This way, in order to add fairness to the beamforming procedure, weights can be assigned to the sum-rate of different users. Weighted sum-rate maximization is conventionally not convex, then global optimality cannot be guaranteed. However, many studies proposed reformulations and approximations to efficiently solve it. In this sense, [20] proposed a weighted sum rate maximization approach for multiple-input single-output (MISO) systems that can be implemented in a distributed way. For the MIMO case [21] proposed a centralized solution to find transmit and receive filter, which is experimentally shown to reach a local optimum. The authors in [22] proposed centralized and distributed solutions based on an iterative process where transmit and receive filters are alternatively optimized, which are proven to converge to a local optimum.

Energy efficiency maximization aims to maximize the ratio between sum-rate of the coordinated BSs and the corresponding power consumption. The authors in [23] proposed a suboptimal centralized design procedure based on the Karush-Kuhn-Tucker (KKT) conditions for a MISO scenario. Other solutions for the MISO scenarios are presented in [24], which proposed a decentralized solution that is proven to converge to a stable point, and by [25], which presented a solution that can be applied in a decentralized or parallel manner. A solution for MIMO scenarios is proposed by [26], which jointly optimizes the transmit powers and beamforming vectors in an iterative alternating algorithm.

In this master's thesis we use the beamforming with objective to minimize the sum-power, which aims to minimize the total network transmission power, while guaranteeing some quality target (most commonly SINR) for each user. Such solution is highly desirable, since the reduction in power consumption is one of the key factors for the development of new technologies, in order to provide less operational costs and to achieve a greener network. Sum-power minimization beamforming was introduced by [27] for a multi-cell MISO scenario, which proposed a solution based on uplink-downlink SINR duality that can be implemented in a distributed form if channel reciprocity is assumed in TDD.

Alternative centralized solutions for the sum-power minimization problem were proposed by [28] and [29], based on convex optimization. Such solutions provided reformulations of the original problem in convex relaxed-SDP and second-order-cone programming (SOCP) forms, respectively. These reformulations provide the possibility of using standard convex optimization numerical tools such as CVX [36] and SCS [37], in order to efficiently solve the

beamforming problem with a guarantee of global optimality.

Other distributed solutions for the MISO case were proposed by [30] and [31]. The decentralization procedure employed by these solutions is based on primal and dual decomposition methods, respectively. Differently from [28] these solutions provide feasible beamformers at intermediate iterations, with the cost of suboptimal performance, what can be very desired in order to reduce delay in networks with timing restrictions.

For MIMO scenarios the problems can no longer be directly reformulated in a convex form for transmitters and receivers. This way, more complex algorithms were proposed to optimize transmit and receive filters. In [32] authors proposed a solution based on an uplink-downlink duality. In [33] a solution is proposed to iteratively optimize transmitters and receivers. Such solutions must be performed in a centralized manner, since they required global CSI knowledge. However, the authors in [34] were capable of providing a decentralized solution which requires only local CSI and a combination of pilot and backhaul signaling.

Beyond conventional studies on the sum-power minimization solution, which normally do not consider very large numbers of BS and UEs, [35] proposed an ADMM based solution that is better suited for large-scale optimization. Such solution is highly desirable for super-dense scenarios, since the number of nodes tends to greatly increase.

1.2.2 Dynamic TDD

In dense networks, another very important issue arises, related to the larger amount of signaling among the massive number of entities coordinated in the network. For that reason, the use of TDD was proposed as the standard way to duplex direct (downlink) and reverse (uplink) links in dense networks, since it provides channel reciprocity, what greatly reduces the signaling overhead used for channel estimation.

In previous generations, the systems that employed TDD, used fixed time intervals for each link direction, and neighbor cells should transmit in the same direction. This was made with the intention to avoid creating interference between BSs and between UEs transmitting in contrary directions [38]. However, the reduced cell size in dense networks makes the instantaneous traffic demands vary significantly between cells [39]. Therefore, the dynamic reconfiguration between uplink and downlink can allow an increase in the system efficiency for systems with varying or unbalanced data requirements in both directions.

However, beyond the high interference levels generated by the proximity between the entities in dense networks, the coexistence of different link directions in neighbor cells creates new types of interference between BSs (BS to BS interference) and between UEs (UE to UE interference) located in cells with opposite directions. Figure 1.2 exemplifies these interferences in a three cell scenario, where two BSs are transmitting in downlink and they generate BS to BS interference to the BS receiving uplink communication. On the other hand, the UE transmitting in uplink generates UE to UE interference for the other two UEs in the contrary direction. This way, in order to achieve the gains obtained by the use of dynamic reconfiguration between downlink

Figure 1.2 – Interferences in a dynamic TDD scenario.

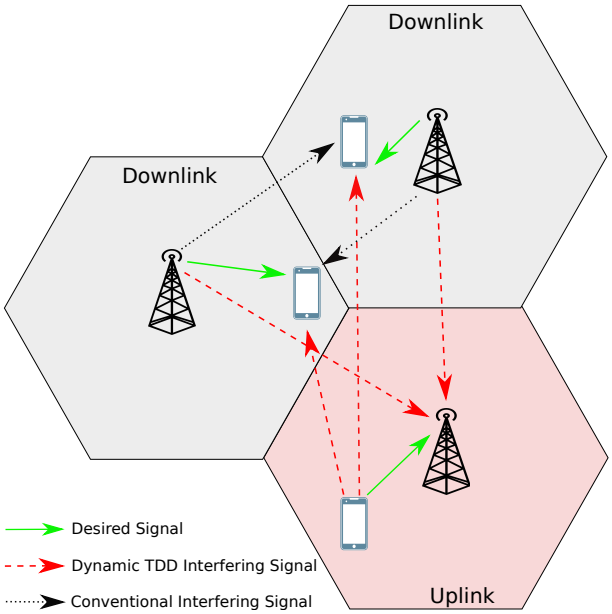

Source: Created by the author.

and uplink in dense networks, it is crucial to manage the effects of such interferences.

Some strategies to treat interference in systems that employ dynamic TDD were recently proposed, including clustering schemes, power control techniques and time slot allocation strategies. Clustering schemes are proposed in [40], where neighboring cells are grouped to use the same link direction, in a way to eliminate cross link interference. However, this solution has a drawback with respect to unbalanced traffic adaptation, since even if two neighbor cells have totally different traffic demands they must still choose the same direction.

Power control solutions are proposed in [41], which controls BS to BS interference by reducing the transmission power of the aggressor BS, and in [42], which increases the transmission power of the UE that has its communication affected by interference. However, both approaches are not optimal, since reducing BS power directly affects downlink capacity, and increasing UE transmit power leads to a growth in battery consumption, which is an important issue for mobile transceivers. Time slot allocation algorithms have also been proposed to manage dynamic TDD interference, such as in [43], that avoids allocating adjacent time slots to UEs located in the borders of the cells.

The previous interference management techniques do not make use of the multi-antenna ability to provide more degrees of freedom in order to deal with interference. Thus, beamforming techniques, that by combining the signals from each antenna focus a signal beam in a desired direction, while avoiding others, can provide better interference management performance. However, to the best of our knowledge only few beamforming solutions were proposed to directly combat these interferences considering different optimization objectives, and most of them consider single antenna UEs.

Beamforming solutions for the MISO case were presented in [44] to maximize the

energy efficiency. However, this solution requires a central entity to compute the solution, and is based on non-linear fractional programming, which has very high computational complexity. The authors in [45] presented a solution using a pricing approach that penalizes the DL BSs that cause interference. However, by using this approach the DL capacity suffers in order to provide less interference in the UL. In [46] a sum-power minimization decentralized approach using ADMM is presented. A beamforming solution for MIMO systems is presented in [47], which maximizes the weighed sum rate.

However, in the case of sum-power minimization beamforming, which is well-motivated in static duplex systems, since it helps to reduce the operational expenditures, it is still an open question whether it can be employed to mitigate the dynamic TDD cross-link interferences and provide good performance in MIMO scenarios. Thus, in this work we also seek to study ways to use the sum-power minimization beamforming to manage the cross-link interferences in MIMO dynamic TDD networks.

1.3 Objectives and Main Contributions

The main objective of this master's thesis is to analyze and propose coordinated beamforming solutions to manage the higher interference levels in dense scenarios. More specifically, we focus in two aspects: the solution of large-scale optimization problems and the different interference links in dynamic TDD dense networks. The main contributions of this work can be listed as:

- Present a performance analysis for an ADMM large-scale beamforming solution, assessing its scalability when applied to different network configurations.
- Simulation results indicate that the ADMM method can provide solutions for large-scale problems in much less time than the SDP method, when modest accuracy is required.
- Formulate a non-trivial and novel optimization problem to optimize the beamformers in a Dynamic TDD scenario. The objective of this problem is to minimize the network sum-power while providing a minimum SINR for DL users and limiting the BS to BS interference power to some threshold.
- Present a centralized and a decentralized solution for the proposed problem. The decentralization is based on the primal decomposition method.
- Provide a signaling scheme to enable the primal decomposition decentralized beamforming calculation.
- Show that the decentralized solution approaches the same result as the centralized one if the algorithm is performed until convergence. However, feasible beamformers can be obtained at intermediate steps, at the cost of sub-optimal power minimization performance.

- Formulate another non-trivial and novel optimization problem to optimize the beamformers in a Dynamic TDD scenario. The objective of this new problem is to minimize the network total sum-power while providing a minimum SINR for DL and UL users.
- Present a centralized and a decentralized solution for the proposed problem. The decentralization is based on ADMM.
- Provide a signaling scheme to enable the ADMM decentralized beamforming calculation. This scheme is based on over-the-air pilot signaling and the backhaul exchange of a small number of scalars.
- Show that the decentralized solution approaches the same result as the centralized one if the algorithm is performed until convergence. However, approximate solutions can be obtained with a reduced amount of iterations.

1.4 Thesis Organization

In Chapter 2, we describe the mathematical tools required for the solutions presented in this work. More specifically, we present the ADMM method that is used by the solutions presented in chapters 3 and 5, and the primal decomposition method, that is used in the decentralization of the solution presented in Chapter 4.

In Chapter 3, we focus on the issues related to the solution of the sum-power minimization beamforming problem with large numbers of variables. We present an ADMM-based solution for the coordinated beamforming optimization problem (CBOP), based on the solution proposed by [35], and we compare it, via simulations, with a well known SDP solution for the CBOP presented in [16].

In Chapter 4, we propose a sum-power minimization problem for a Dynamic TDD MIMO network which protects the UL communication from BS to BS interference, while guaranteeing a minimum SINR target for DL users. We propose a centralized and a decentralized iterative solutions for this problem. The decentralized solution is based on primal decomposition and requires only local CSI and a light-weight pilot and backhaul signaling scheme. We show that both solutions can improve the UL performance while guaranteeing DL SINR targets, and the decentralized solutions iterate toward the centralized ones, while feasible solutions can be obtained at intermediate iterations with the cost of suboptimal power.

In Chapter 5, we propose another sum-power minimization problem for a Dynamic TDD MIMO network. This problem tries to guarantee a minimum SINR threshold for DL and UL users. We propose a centralized and an ADMM-based decentralized solution. The decentralized solution also requires only local CSI and a light-weight pilot and backhaul signaling scheme. We also show that the centralized solution iterates towards the centralized one and that the signaling load can be controlled by fixing the number of iterations at the cost of close to optimal performance.

In Chapter 6, we summarize this master's thesis main conclusions and we point future research directions that can be considered as extensions to this work.

1.5 Scientific Production

The content and contributions of this Master's thesis were submitted with the following information.

- **Eduardo de O. Cavalcante**; Yuri C. B. Silva ; Walter C. Freitas Jr, "A Performance Analysis of ADMM Applied to Coordinate Beamforming". XXXV Simpósio Brasileiro de Telecomunicações e Processamento de Sinais (SBrT), 2017.
- **Eduardo de O. Cavalcante**; Gabor Fodor; Yuri C. B. Silva ; Walter C. Freitas Jr, "Distributed Beamforming in Dynamic TDD MIMO Networks with BS to BS Interference Constraints". IEEE Wireless Communications Letters (under review).

In parallel to the development of the Master course the author has been working on other research projects related to interference management in 5G networks. In the context of these projects, the author participated on the following technical reports:

- Khaled Ardah; Francisco R. V. Guimarães; Darlan C. Moreira; László R. Costa; **Eduardo de O. Cavalcante**; Elvis M. G. Stancanelli; Walter C. Freitas Jr.; Yuri C. B. Silva; and Francisco R. P. Cavalcanti; Interference management for super-dense scenarios – Link and System Level Aspects; GTEL-UFC-Ericsson UFC.42; Fourth Technical Report, October 2016.
- Khaled Ardah; Francisco R. V. Guimarães; **Eduardo O. Cavalcante**; Walter C. Freitas Jr.; Yuri C. B. Silva; and Francisco R. P. Cavalcanti; TIDE5G - Dynamic Time Division Duplexing Evolution for 5G Systems – Interference Mitigation in DTDD Multiple Antenna Systems; GTEL-UFC-Ericsson TIDE5G; First Technical Report, May 2017.
- Khaled Ardah; Francisco R. V. Guimarães; **Eduardo O. Cavalcante**; Walter C. Freitas Jr.; Yuri C. B. Silva; and Francisco R. P. Cavalcanti; TIDE5G - Dynamic Time Division Duplexing Evolution for 5G Systems – Interference Mitigation in DTDD and Hybrid Beamforming; GTEL-UFC-Ericsson TIDE5G; Second Technical Report, November 2017.

2 MATHEMATICAL TOOLS

2.1 Introduction

In this chapter, we discuss two numerical methods that are used by the solutions proposed in this master's thesis. The alternating direction method of multipliers (ADMM) is discussed in Section 2.2 and applied to the beamforming solution for large-scale systems in Chapter 3 and to the decentralized solution proposed in Chapter 5. The primal decomposition method is discussed in Section 2.3 and used by the decentralized solution proposed in Chapter 4.

2.2 Alternate Direction Method of Multipliers

ADMM is described by [48] as a simple but powerful algorithm that is well suited to distributed convex optimization and takes the form of a decomposition-coordination procedure, in which the solutions to small subproblems are coordinated to find a solution to a large global problem. In the next chapters, we seek benefit from two well known characteristics of ADMM, its ability to solve large-scale problems with moderate accuracy, within a reasonably low amount of time, and to allow parallel processing.

The ADMM algorithm tries to mix the benefits of other two preceding optimization methods. It tries to implement the parallelism provided by the Dual Decomposition Method (Dual Ascent) and the robustness of the Augmented Lagrangians and Method of Multipliers, by implementing a combination of both algorithms. For that reason, in order to better understand ADMM, it is necessary to begin our description by briefly revising these other two older methods.

2.2.1 Dual Ascent

For the dual ascent method, consider a simple convex optimization problem

$$\begin{aligned} &\text{minimize} && f(\mathbf{x}) \\ &\text{subject to} && \mathbf{Ax} = \mathbf{b}, \end{aligned} \tag{2.1}$$

with $\mathbf{x} \in \mathbf{R}^n$, $\mathbf{A} \in \mathbf{R}^{m \times n}$, and $f : \mathbf{R}^n \rightarrow \mathbf{R}$ being a strictly convex function.

The Lagrangian for this problem is

$$L(\mathbf{x}, \mathbf{y}) = f(\mathbf{x}) + \mathbf{y}^T(\mathbf{Ax} - \mathbf{b}), \tag{2.2}$$

where $\mathbf{y}$ is the dual variable. The dual of the problem in (2.1) is

$$\text{maximize} \quad \inf_{\mathbf{x}} L(\mathbf{x}, \mathbf{y}), \tag{2.3}$$

where $\inf_{\mathbf{x}}(f(\mathbf{x}))$ denotes the infimum of $f(\mathbf{x})$ in relation to the variable $\mathbf{x}$.

If it is assumed that strong duality holds in this case, i.e. the primal and dual optimal solutions are the same, it is possible to obtain the primal optimal point ($\mathbf{x}^*$) from the dual optimal point ($\mathbf{y}^*$) by doing

$$\mathbf{x}^* = \underset{\mathbf{x}}{\operatorname{argmin}} L(\mathbf{x}, \mathbf{y}^*). \tag{2.4}$$

The dual ascent method solves iteratively the dual problem, by first minimizing the Lagrangian and then updating the dual variable, as shown in

$$\begin{aligned} \mathbf{x}^{k+1} &= \underset{\mathbf{x}}{\operatorname{argmin}} L(\mathbf{x}, \mathbf{y}^k), \\ \mathbf{y}^{k+1} &= \mathbf{y}^k + \alpha^k(\mathbf{A}\mathbf{x}^{k+1} - \mathbf{b}), \end{aligned} \tag{2.5}$$

where $\alpha^k > 0$ is the step size, and the term between parentheses in the dual variable update step is the gradient of the dual function.

One of the main features of dual ascent is the possibility of distributing the calculations. For example, in cases when the objective function can be split in N different parts, the algorithm is written as

$$\begin{aligned} \mathbf{x}_i^{k+1} &= \underset{\mathbf{x}_i}{\operatorname{argmin}} L(\mathbf{x}_i, \mathbf{y}^k), \qquad i = 1, \ldots, N. \\ \mathbf{y}^{k+1} &= \mathbf{y}^k + \alpha^k(\mathbf{A}\mathbf{x}^{k+1} - \mathbf{b}), \end{aligned} \tag{2.6}$$

where each of the N instances of the Lagrangian minimization step can be done independently in a parallel fashion, while the dual variable update step is done in a centralized manner, after gathering the results from each independent calculation. This distributed version of the Dual Ascent Method is called the Dual Decomposition Method.

Although useful for some applications, the Dual Decomposition Method fails to converge in many other cases, for example when f is not strictly convex or reaches $+\infty$.

2.2.2 Augmented Lagrangian and the Method of Multipliers

Methods that use augmented Lagrangians are designed to provide robustness to the dual ascent method, in order to converge in a larger amount of cases. The augmented Lagrangian of the problem in (2.1) is

$$L_\rho(\mathbf{x}, \mathbf{y}) = f(\mathbf{x}) + \mathbf{y}^T(\mathbf{A}\mathbf{x} - \mathbf{b}) + (\rho/2)||\mathbf{A}\mathbf{x} - \mathbf{b}||_2^2, \tag{2.7}$$

where $\rho > 0$ is a penalty parameter, which is included in order to make the dual function, $g_\rho(\mathbf{y}) = \inf_{\mathbf{x}} L_\rho(\mathbf{x}, \mathbf{y})$, differentiable in more cases.

Applying the Dual Ascent method to the new Lagrangian we obtain the algorithm known as the Method of Multipliers

$$\begin{aligned} \mathbf{x}^{k+1} &= \underset{\mathbf{x}}{\operatorname{argmin}} L_\rho(\mathbf{x}, \mathbf{y}^k), \\ \mathbf{y}^{k+1} &= \mathbf{y}^k + \rho(\mathbf{A}\mathbf{x}^{k+1} - \mathbf{b}). \end{aligned} \tag{2.8}$$

The differences from this method to the dual ascent are the use of the augmented Lagrangian in the first step and the substitution of the step size term with the penalty parameter. These changes make it a more robust algorithm, in the sense that it can converge under more general conditions. However, by using the augmented Lagrangian in the first step, it becomes no longer possible to use parallel independent partitions when f is separable.

2.2.3 ADMM

In this sense, ADMM was developed in order to blend the benefits from the aforementioned methods, i.e. ADMM should be robust and allow parallel calculation.

The optimization problem in (2.1) can be rewritten by splitting the variable $\mathbf{x}$ in two, $\mathbf{x}$ and $\mathbf{z}$, related as shown in the constraint part of (2.9), with the objective function separable across this splitting.

$$\begin{aligned} &\text{minimize} && f(\mathbf{x}) + g(\mathbf{z}) \\ &\text{subject to} && \mathbf{A}\mathbf{x} + \mathbf{B}\mathbf{z} = \mathbf{c}, \end{aligned} \tag{2.9}$$

with $\mathbf{x} \in \mathbf{R}^n$, $\mathbf{z} \in \mathbf{R}^m$, $\mathbf{A} \in \mathbf{R}^{p \times n}$, $\mathbf{B} \in \mathbf{R}^{p \times m}$, and $\mathbf{c} \in \mathbf{R}^p$. Assuming that f and g are convex functions.

Writing the augmented Lagrangian for the problem in (2.9) we obtain

$$L_\rho(\mathbf{x}, \mathbf{y}) = f(\mathbf{x}) + g(\mathbf{z}) + \mathbf{y}^T(\mathbf{A}\mathbf{x} + \mathbf{B}\mathbf{z} - \mathbf{c}) + (\rho/2)||\mathbf{A}\mathbf{x} + \mathbf{B}\mathbf{z} - \mathbf{c}||_2^2, \tag{2.10}$$

where $\mathbf{y}$ is the dual variable and ρ is the penalty parameter.

The ADMM algorithm is similar to the dual decomposition and the method of multipliers and consists of the three steps shown below: the minimization of the augmented Lagrangian over each of the two variables, $\mathbf{x}$ and $\mathbf{z}$, and the update of the dual variable.

$$\begin{aligned} \mathbf{x}^{k+1} &= \underset{\mathbf{x}}{\operatorname{argmin}} L_\rho(\mathbf{x}, \mathbf{z}^k, \mathbf{y}^k), \\ \mathbf{z}^{k+1} &= \underset{\mathbf{z}}{\operatorname{argmin}} L_\rho(\mathbf{x}^{k+1}, \mathbf{z}, \mathbf{y}^k), \\ \mathbf{y}^{k+1} &= \mathbf{y}^k + \rho(\mathbf{A}\mathbf{x}^{k+1} + \mathbf{B}\mathbf{z}^{k+1} - \mathbf{c}). \end{aligned} \tag{2.11}$$

ADMM can also be written in a more convenient form by using a scaled version of the dual variable, $\lambda = (1/\rho)y$.

$$\begin{aligned}
\mathbf{x}^{k+1} &= \underset{\mathbf{x}}{\operatorname{argmin}}\,(f(\mathbf{x}) + (\rho/2)||\mathbf{A}\mathbf{x} + \mathbf{B}\mathbf{z}^k - \mathbf{c} + \boldsymbol{\lambda}^k||_2^2), \\
\mathbf{z}^{k+1} &= \underset{\mathbf{z}}{\operatorname{argmin}}\,(g(\mathbf{z}) + (\rho/2)||\mathbf{A}\mathbf{x}^{k+1} + \mathbf{B}\mathbf{z} - \mathbf{c} + \boldsymbol{\lambda}^k||_2^2), \\
\boldsymbol{\lambda}^{k+1} &= \boldsymbol{\lambda}^k + \mathbf{A}\mathbf{x}^{k+1} + \mathbf{B}\mathbf{z}^{k+1} - \mathbf{c}.
\end{aligned} \tag{2.12}$$

The difference between the method of multipliers and ADMM is that the updates of $\mathbf{x}$ and $\mathbf{z}$ are done jointly in the former ($(\mathbf{x}^{k+1}, \mathbf{z}^{k+1}) := \operatorname{argmin}_{\mathbf{x},\mathbf{z}} L_\rho(\mathbf{x}, \mathbf{z}, \mathbf{y}^k)$), but in an alternate fashion in the latter ($\mathbf{z}^{k+1}$ depends on $\mathbf{x}^{k+1}$), and this is what allows the decomposition when f or g are separable. In this sense, ADMM is a robust method for solving large-scale optimization problems, which has the aptitude to be applied in a parallel manner.

We use ADMM trying to benefit from its robustness and large-scale adaptation in Chapter 3 as a means to speed up calculations for large-scale problems. ADMM is also used in Chapter 5 to solve the proposed optimization problem in a distributed approach, with each node performing its necessary calculations to find the optimal precoders.

2.3 Primal Decomposition

Decomposition methods are designed to solve a problem by decomposing it in many subproblems of smaller dimension that are easier to solve and can be calculated in a parallel distributed fashion [49]. For example, it can be applied to decouple the interference terms linking two (or more) BSs in the beamforming optimization problem, and allow that each BS can independently compute its subproblems. In order to coordinate these subproblems, a high-level master problem is considered to manage the necessary information sharing between each subproblem. Figure 2.1 illustrates the decomposition of a problem in this two-level approach.

Figure 2.1 – Two-level decomposition.

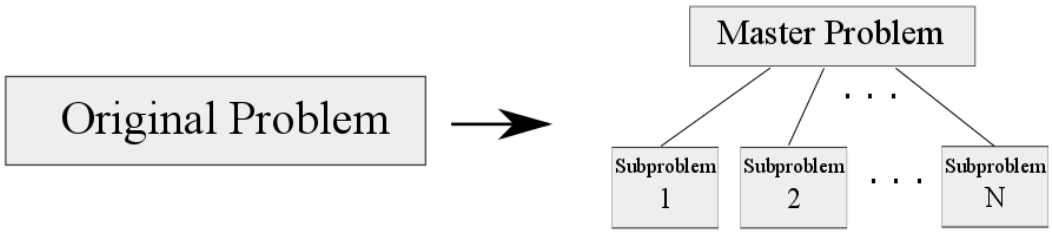

Source: Adapted from [50]

A well known category of decomposition methods is the primal decomposition, which divides the original primal problem in many subproblems coordinated by a master problem [50]. Primal decomposition works when an original problem has coupling terms such that, when

fixed to some value, decouples the rest of the problem into smaller subproblems. Consider, for example, this general optimization problem:

$$\begin{aligned} \underset{\mathbf{y},\{\mathbf{x}_i\}\forall i}{\text{maximize}} \quad & \sum_i f_i(\mathbf{x}_i) \\ \text{subject to} \quad & \mathbf{A}_i\mathbf{x}_i \leq \mathbf{y}, \quad \forall i \\ & \mathbf{y} \in \mathcal{Y}. \end{aligned} \tag{2.13}$$

The variable $\mathbf{y}$ couples the problem, since the calculation of every $\mathbf{x}_i$ depends on the optimal value of $\mathbf{y}$. This way, if $\mathbf{y}$ can be fixed to some value the problem would decouple. Thus, we could use primal decomposition to solve this problem, by having the subproblems for each i with $\mathbf{y}$ fixed written as:

$$\begin{aligned} \underset{\mathbf{x}_i}{\text{maximize}} \quad & f_i(\mathbf{x}_i) \\ \text{subject to} \quad & \mathbf{A}_i\mathbf{x}_i \leq \mathbf{y}. \end{aligned} \tag{2.14}$$

At the higher level, the master problem has the role of updating the values to which $\mathbf{y}$ must be fixed to by solving

$$\begin{aligned} \underset{\mathbf{y}}{\text{maximize}} \quad & \sum_i f_i^*(\mathbf{y}) \\ \text{subject to} \quad & \mathbf{y} \in \mathcal{Y}, \end{aligned} \tag{2.15}$$

where $f_i^*(\mathbf{y})$ is the optimal objective value of the problem in (2.13) given $\mathbf{y}$.

The primal decomposition solves the original problem by solving the master problem with the gradient or subgradient methods. And after that, by solving all subproblems in order to obtain the gradients or subgradients for the next master problem update.

If the original primal problem is convex, so are the respective subproblems and the master problem. Thus, each subproblem can be solved separately using standard convex optimization tools, or the interior-point method. To solve the master problem the gradient method can be used if the master problem objective, $\sum_i f_i^*(\mathbf{y})$, is differentiable. However, this function in general is not differentiable and a subgradient method, which only requires knowledge about the subgradients, may be used. If a subgradient method is applied to solve the master problem in (2.15), then a sequence of feasible points $\mathbf{y}(t)$ are generated as

$$\mathbf{y}(t+1) = [\mathbf{y}(t) + \alpha(t)\mathbf{s}(t)]_{\mathcal{Y}}, \tag{2.16}$$

where $\mathbf{s}(t)$ is a valid subgradient of the objective function of (2.15) at the point $\mathbf{y}(t)$, $[\cdot]_{\mathcal{Y}}$ is a projection onto the feasible set $\mathcal{Y}$, and $\alpha(t)$ is the step-size. The subgradient method is guaranteed to converge if a diminishing step size is used, for example $\alpha(t) = 1/\sqrt{t}$ [51]. However, monotonicity is not guaranteed by the subgradient method, then the best solutions must be stored at each iteration.

The Primal decomposition method is used in Chapter 4 in order to decouple the terms in the proposed optimization problem and allow its distributed computation. In the scenario of Chapter 4, the coupling terms are the inter-cell interference values. These values will be fixed in the local subproblems, while the master problem updates them. There are, however, other categories of decomposition methods, including the dual decomposition method, which is based on decomposing the Lagrangian dual problem instead of the primal problem [52] and it is normally applied to problems that become decoupled when a constraint is relaxed.

3 A PERFORMANCE ANALYSIS OF LARGE-SCALE BEAMFORMING

3.1 Introduction

The larger number of cells and users combined with the more strict QoS requirements in future mobile systems will lead to optimization problems with high dimensions and large numbers of variables and constraints, as well as very strict latency requirements. However, conventional algorithms that solve the beamforming problem have their performance demonstrated for systems with small numbers of cells, typically less than a dozen. This fact motivates the search for optimization methods that could be used to solve the beamforming problem in large-scale scenarios.

A promising method to optimize the beamforming was proposed by [35], which uses an ADMM based algorithm. This method is said to solve large-scale problems with moderate accuracy, within a reasonably low amount of time. ADMM also allows parallel processing, what is very desirable for C-RAN systems, in which the baseband processing is centralized and shared among sites in a virtualized baseband unit (BBU) pool [53].

In this chapter we present an ADMM-based solution for the beamforming problem, based on the one proposed by [35], without considering joint transmission, which is a more practical assumption and allows for a fair comparison with the well known SDP solution for the beamforming problem, presented in [16]. The main contributions of this chapter are the performance analysis, that assesses the scalability of the ADMM solution applied to different network configurations, and the convergence analysis, that shows how the ADMM solution iterates to find an optimal solution.

The rest of the chapter is organized as follows. Section 3.2 defines the signal model. Section 3.3 defines the problem and presents the ADMM-based solution for the beamforming problem. Section 3.4 shows and analyzes the simulation results. Finally, Section 3.5 draws the main conclusions.

3.2 Signal Model

The scenario where beamforming is applied is exemplified in Figure 3.1. It is formed by a set of K single-antenna UEs and L remote radio units (RRUs) with N antennas, managed by one single BBU pool. The signal received by a UE k, which is assigned to an RRU l, is $y_k \in \mathbb{C}$, and it is expressed as

$$y_k = \underbrace{\mathbf{h}_{kl}^H \mathbf{v}_{kl} s_k}_{\text{desired signal}} + \underbrace{\sum_{\substack{j=1 \\ j \neq k}}^{K} \mathbf{h}_{kl}^H \mathbf{v}_{jl} s_j}_{\text{intra-RRU interference}} + \underbrace{\sum_{\substack{i=1 \\ i \neq l}}^{L} \sum_{\substack{j=1 \\ j \neq k}}^{K} \mathbf{h}_{ki}^H \mathbf{v}_{ji} s_j}_{\text{inter-RRU interference}} + n_k, \ \forall k, \tag{3.1}$$

Figure 3.1 – Illustration of an example scenario.

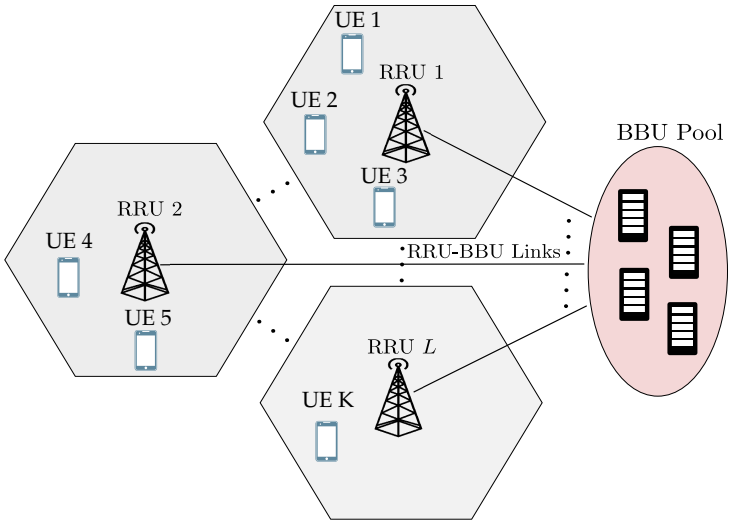

Source: Created by the author.

where $\mathbf{h}_{kl}^H \in \mathbb{C}^{N\times 1}$ is the channel vector between RRU l and UE k, $\mathbf{v}_{kl} \in \mathbb{C}^{N\times 1}$ is the beamforming vector from RRU l to UE k (we assume that if an user j is not assigned to an RRU i, then $\mathbf{v}_{ji}$ is a zero vector), $s_k \in \mathbb{C}$ is the data sent to user k, which is assumed to have unit variance, and $n_k \in \mathbb{C}$ is the additive white Gaussian noise at user k, with variance σ_k^2.

The SINR of each UE is given by

$$\Gamma_k = \frac{|\mathbf{h}_{kl}^H \mathbf{v}_{kl}|^2}{\sum\limits_{\substack{j=1 \\ j\neq k}}^{K} |\mathbf{h}_{kl}^H \mathbf{v}_{jl}|^2 + \sum\limits_{\substack{i=1 \\ i\neq l}}^{L} \sum\limits_{\substack{j=1 \\ j\neq k}}^{K} |\mathbf{h}_{ki}^H \mathbf{v}_{ji}|^2 + \sigma_k^2}, \ \forall k. \tag{3.2}$$

3.3 ADMM based Coordinated Beamforming

We define the beamforming problem as a power minimization problem, with an independent SINR constraint, γ_k, for each receiver

$$\begin{aligned} \text{minimize} \quad & \sum_{i=1}^{L} \sum_{j=1}^{K} \|\mathbf{v}_{ji}\|_2^2 \\ \text{subject to} \quad & \Gamma_k \geq \gamma_k, \ \forall k. \end{aligned} \tag{3.3}$$

However, in order to use the ADMM algorithm to solve this problem, we rewrite it into another form, called HSD embedding [37]. This new embedding is obtained by transforming a *primal-dual* pair of a convex conic optimization problem into an equivalent feasibility problem of finding a nonzero point in the intersection of a subspace and a cone. HSD has a very desirable feature of providing certificates of infeasibility when the solution is not attainable. In this sense, the problem in (3.3) should be first rewritten in a standard conic form to then be transformed into the equivalent HSD embedding.

3.3.1 Conic Reformulation and Matrix Stuffing

The first step is to transform the problem in (3.3) into its conic version. The desired standard SOCP form can be expressed as

$$\begin{aligned} &\text{minimize} && \boldsymbol{c}^T\boldsymbol{\nu} \\ &\text{subject to} && \mathbf{A}\boldsymbol{\nu}+\boldsymbol{\mu}=\boldsymbol{b} \\ & && (\boldsymbol{\nu},\boldsymbol{\mu})\in\mathbb{R}^n\times\mathcal{K}, \end{aligned} \tag{3.4}$$

with variables $\boldsymbol{\nu}\in\mathbb{R}^n$ and $\boldsymbol{\mu}\in\mathbb{R}^m$. $\boldsymbol{A}\in\mathbb{R}^{m\times n}$, $\boldsymbol{b}\in\mathbb{R}^m$ and $\boldsymbol{c}\in\mathbb{R}^n$ are the problem parameters and $\mathcal{K}$ is the cone

$$\mathcal{K}=\mathcal{Q}^{m_1}\times\cdots\times\mathcal{Q}^{m_q}\times\{0\}^r, \tag{3.5}$$

where

$$\mathcal{Q}^p=\{(t,\mathbf{x})\in\mathbb{R}\times\mathbb{R}^{p-1}\,|\,\|\mathbf{x}\|_2\le t\}, \tag{3.6}$$

is the second-order cone of dimension p, $\mathcal{Q}^1$ is defined as the cone of nonnegative reals, $\mathbb{R}_+$, and the sum of all the cone dimensions, $m_1+\cdots+m_q+r$, is equal to m.

In order to perform a fast transformation of (3.3) into (3.4), [35] also proposed the use of a technique called matrix stuffing. It works by initially generating a fixed structure that maps the original problem dimensions (RRUs, UEs and antennas) into the new conic form, and then, at running time, by copying the problem data to the previously generated structure.

The process starts by writing a problem equivalent to (3.3). Now, instead of minimizing the sum of the squared norms of $\mathbf{v}_{ji}$, we introduce a relaxed minimization of the norm of the vector $\mathbf{v}$, formed by the composition of all $\mathbf{v}_{ji}$, $\mathbf{v}\triangleq[\mathbf{v}_1^T,\ldots,\mathbf{v}_K^T]^T\in\mathbb{R}^{LNK}$, where $\mathbf{v}_k\triangleq[\mathbf{v}_{k1}^T,\ldots,\mathbf{v}_{kL}^T]^T\in\mathbb{R}^{LN}$. Both objective functions have the same minimum and both are convex. The SINR constraints are still the same, but expressed in a form more convenient to our purpose. Thus, the problems in (3.3) and (3.7) are equivalent for real parameters[1] .

$$\begin{aligned} &\text{minimize} && x_0 \\ &\text{subject to} && \|\mathbf{v}\|_2\le x_0 \\ & && \|\mathbf{C}_k\mathbf{v}+\mathbf{g}_k\|_2\le\beta_k\mathbf{r}_k^T\mathbf{v},\ k=1\ldots K, \end{aligned} \tag{3.7}$$

where $\mathbf{C}_k=[\mathsf{blkdiag}\{\tilde{\mathbf{h}}_{k\tilde{1}},\ldots,\tilde{\mathbf{h}}_{k\tilde{K}}\},\mathbf{0}_{LNK}]^T\in\mathbb{R}^{(K+1)\times LNK}$, $\mathbf{r}_k=[\mathbf{0}_{(k-1)LN}^T,\tilde{\mathbf{h}}_{k\tilde{k}}^T,\mathbf{0}_{(K-k)LN}^T]^T\in\mathbb{R}^{LNK}$, $\beta_k=\sqrt{1+1/\gamma_k}$, $\mathbf{g}_k=[\mathbf{0}_K^T,\sigma_k]^T\in\mathbb{R}^{K+1}$ and $\tilde{\mathbf{h}}_{k\tilde{i}}=[\mathbf{0}_{(\tilde{i}-1)N}^T,\mathbf{h}_{k\tilde{i}}^T,\mathbf{0}_{(L-\tilde{i})N}^T]^T\in\mathbb{R}^{LN}$, $\tilde{i}$ represents the index of the RRU to which user i is allocated to, and $\mathsf{blkdiag}\{\}$ is the block diagonal matrix formed by the sub-matrices on its argument.

The relaxation is applied to the first constraint. Note that in the conventional form it would be $x_0=\|\mathbf{v}\|_2$, however this is not satisfactory, since in a convex problem all equality constraints must be affine [54]. The relaxation does not change the optimal result of the problem, since the relaxed constraint is always active at the optimal point.

[1] Complex parameters need to be rearranged into a real form, as indicated in [35].

At this moment, it is already possible to note the cones formed by the constraints of (3.7). Using the notation of a cone shown in (3.6), we can rewrite them as $(x_0, \mathbf{v}_1) \in Q^{LNK+1}$ and $(\beta_k \mathbf{r}_k^T \mathbf{v}, \mathbf{C}_k \mathbf{v} + \mathbf{g}_k) \in Q^{K+2}$, respectively.

Now, it is necessary to transform this conic problem into the standard SOCP form as the problem in (3.4). For that, we introduce the variable $\boldsymbol{\mu} = [\boldsymbol{\mu}_0; \boldsymbol{\mu}_1]$, that contains the Cartesian product of the cones in the problem, and write the new constraints in a standard form, as the ones in (3.4).

The first new constraint is

$$\underbrace{\left[\begin{array}{c|c} -1 & \\ \hline & -\mathbf{I}_{LNK} \end{array}\right]}_{\mathbf{A}_0} \underbrace{\left[\begin{array}{c} x_0 \\ \hline \mathbf{v} \end{array}\right]}_{\boldsymbol{\nu}_0} + \boldsymbol{\mu}_0 = \underbrace{\left[\begin{array}{c} 0 \\ \hline \mathbf{0}_{LNK} \end{array}\right]}_{\mathbf{b}_0}, \tag{3.8}$$

where $\mathbf{A}_0$ and $\boldsymbol{\nu}_0$ are designed so that $\boldsymbol{\mu}_0$ will be a cone as the one in the first constraint of the problem in (3.7), $\mathbf{I}_{LNK}$ is the identity matrix of dimension LNK, and $\mathbf{0}_{LNK}$ is a vector of dimension LNK with zeros in all positions.

By doing this, $\boldsymbol{\mu}_0$ is obtained as

$$\boldsymbol{\mu}_0 = \left[\begin{array}{c} x_0 \\ \hline \mathbf{v} \end{array}\right]. \tag{3.9}$$

If $\boldsymbol{\mu}_0$ is the cone Q^{LNK+1}, then $\|\mathbf{v}\|_2 \leq x_0$. In this sense, (3.8) with $\boldsymbol{\mu}_0 \in Q^{LNK+1}$ is a constraint of the desired standard conic problem.

Introducing a slack variable t_0^k, the second constraint is

$$\underbrace{\left[\begin{array}{c|c} 1 & \beta_k \mathbf{r}_k^T \\ \hline -1 & \\ & -\mathbf{C}_k \end{array}\right]}_{\mathbf{A}_1^k} \underbrace{\left[\begin{array}{c} t_0^k \\ \hline \mathbf{v} \end{array}\right]}_{\boldsymbol{\nu}_1^k} + \boldsymbol{\mu}_1^k = \underbrace{\left[\begin{array}{c} 0 \\ \hline 0 \\ \hline \mathbf{g}_k \end{array}\right]}_{\mathbf{b}_1^k}, \tag{3.10}$$

where the values of $\mathbf{A}_1^k$ and $\boldsymbol{\nu}_1^k$ are designed in order to make $\boldsymbol{\mu}_1^k$ a cone for the second constraint in (3.7).

In this way, the value of $\boldsymbol{\mu}_1$ can be obtained as

$$\boldsymbol{\mu}_1^k = \left[\begin{array}{c} -t_0^k + \beta_k \mathbf{r}_k^T \\ \hline t_0^k \\ \hline \mathbf{C}_k \mathbf{v} + \mathbf{g}_k \end{array}\right]. \tag{3.11}$$

In this case, if $\boldsymbol{\mu}_1^k$ is formed by the Cartesian product of the cones Q^1 and Q^{K+2}, then $-t_0^k + \beta_k \mathbf{r}_k^T \geq 0$ and $\|\mathbf{C}_k \mathbf{v} + \mathbf{g}_k\|_2 \leq t_0^k$. Combining these two expressions we find that $\|\mathbf{C}_k \mathbf{v} + \mathbf{g}_k\|_2 \leq \beta_k \mathbf{r}_k^T$, that is the desired SINR constraint. Then, (3.10) with $\boldsymbol{\mu}_1^k \in Q^1 \times Q^{K+2}$ is another constraint of the desired standard conic problem.

The variable $\boldsymbol{\mu} \in \mathcal{K}$ is, then, formed by the Cartesian product of the cones within $\boldsymbol{\mu}_0$ and $\boldsymbol{\mu}_1$.

$$\mathcal{K} = Q^{LNK+1} \times \underbrace{Q^1 \times \cdots \times Q^1}_{K} \times \underbrace{Q^{K+2} \times \cdots \times Q^{K+2}}_{K}. \tag{3.12}$$

The last step in the transformation is to arrange the constraints into an unified form, as in (3.4). This is done by defining the matrix $\mathbf{A}$, and the vectors $\boldsymbol{\nu}$, $\mathbf{c}$ and $\mathbf{b}$, based on the constraints in (3.8) and (3.10).

$$\boldsymbol{\nu} = [x_0, t_0^1, \ldots, t_0^K, \mathbf{v}], \quad \mathbf{c} = [1, \mathbf{0}_{n-1}], \tag{3.13}$$

$$\mathbf{A} = \left[\begin{array}{c|cc} -1 & & \\ & & -\mathbf{I}_{LNK} \\ \hline & 1 & -\beta_1 \mathbf{r}_1^T \\ & \ddots & \vdots \\ & 1 & -\beta_K \mathbf{r}_K^T \\ \hline & -1 & \\ & & -\mathbf{C}_1 \\ \hline & \vdots & \vdots \\ \hline & -1 & \\ & & -\mathbf{C}_K \end{array}\right], \mathbf{b} = \left[\begin{array}{c} 0 \\ \mathbf{0}_{LNK} \\ \hline 0 \\ \vdots \\ 0 \\ \hline 0 \\ \mathbf{g}_1 \\ \hline \vdots \\ \hline 0 \\ \mathbf{g}_k \end{array}\right]. \tag{3.14}$$

Matrix Stuffing works by initially defining the dimensions of the problem, n and m, creating the general matrices and vectors in the form of $\mathbf{A}$, $\mathbf{b}$ and $\mathbf{c}$, and defining the cone dimensions. These elements will be used as the "skeleton" of the problem, over which the run time parameters, $\mathbf{C}_k$, $\mathbf{r}_k$ and $\mathbf{g}_k$ will be copied at each problem instance.

3.3.2 Homogeneous Self-Dual Embedding

The HSD embedding is obtained by transforming the *primal-dual* pair of the convex conic optimization problem into an equivalent feasibility problem of finding a nonzero point in the intersection of a subspace and a cone [37]. A very important feature of the HSD embedding is that it can provide certificates of infeasibility if a *primal-dual* pair is not solvable.

The dual of the Problem in (3.4) is

$$\begin{aligned} \text{maximize} \quad & -\mathbf{b}^T \boldsymbol{\eta} \\ \text{subject to} \quad & -\mathbf{A}^T \boldsymbol{\eta} + \boldsymbol{\lambda} = \mathbf{c} \\ & (\boldsymbol{\lambda}, \boldsymbol{\eta}) \in \{0\}^n \times \mathcal{K}^*, \end{aligned} \tag{3.15}$$

where $\boldsymbol{\lambda} \in \mathbb{R}^n$ and $\boldsymbol{\eta} \in \mathbb{R}^m$ are the dual variables and $\mathcal{K}^*$ is the dual cone of $\mathcal{K}$. We define p^* as the optimal primal solution, and d^* as the optimal dual, and we assume that strong duality holds, i.e. $p^* = d^*$, in all cases.

If strong duality holds, the problem is feasible and the following KKT conditions

(embedded into a single system of equations) are necessary and sufficient for optimality

$$\underbrace{\begin{bmatrix} \boldsymbol{\lambda} \\ \boldsymbol{\mu} \\ \kappa \end{bmatrix}}_{\mathbf{y}} = \underbrace{\begin{bmatrix} 0 & \mathbf{A}^T & \mathbf{c} \\ -\mathbf{A} & 0 & \mathbf{b} \\ -\mathbf{c}^T & -\mathbf{b}^T & 0 \end{bmatrix}}_{\mathbf{Q}} \underbrace{\begin{bmatrix} \boldsymbol{\nu} \\ \boldsymbol{\eta} \\ \tau \end{bmatrix}}_{\mathbf{x}}, \tag{3.16}$$
$$(\boldsymbol{\nu}, \boldsymbol{\mu}, \boldsymbol{\lambda}, \boldsymbol{\eta}, \tau, \kappa) \in \mathbb{R}^n \times \mathcal{K} \times \{0\}^n \times \mathcal{K}^* \times \mathbb{R}_+ \times \mathbb{R}_+.$$

The inclusion of the variables τ and κ is made to allow a feasibility analysis based on their values.

The HSD embedding is, then, written as a feasibility problem to find a nonzero point that satisfies the KKT conditions

$$\begin{aligned} &\text{find} && (\mathbf{x}, \mathbf{y}) \\ &\text{subject to} && \mathbf{y} = \mathbf{Q}\mathbf{x} \\ &&& (\mathbf{x}, \mathbf{y}) \in C \times C^*, \end{aligned} \tag{3.17}$$

where $C = \mathbb{R}^n \times \mathcal{K}^* \times \mathbb{R}_+$ and $C^* = \{0\}^n \times \mathcal{K} \times \mathbb{R}_+$.

This approach is shown to be homogeneous and self-dual by [37], which also proposed an ADMM algorithm to solve it, as discussed in the following section.

3.3.3 ADMM Algorithm For The HSD Embedding

The HSD Embedding in (3.17) can be reformulated into an ADMM form, by splitting the optimization variables in $(\mathbf{x}, \mathbf{y})$ and $(\tilde{\mathbf{x}}, \tilde{\mathbf{y}})$, with the objective function separable across this splitting

$$\begin{aligned} &\text{minimize} && \mathcal{I}_{C \times C^*}(\mathbf{x}, \mathbf{y}) + \mathcal{I}_{\mathbf{Q}\tilde{\mathbf{x}} = \tilde{\mathbf{y}}}(\tilde{\mathbf{x}}, \tilde{\mathbf{y}}) \\ &\text{subject to} && (\mathbf{x}, \mathbf{y}) = (\tilde{\mathbf{x}}, \tilde{\mathbf{y}}), \end{aligned} \tag{3.18}$$

where $\mathcal{I}_S(z)$ is the indicator function of the set $\mathcal{S}$, that assumes value 1 if it is applied to an element of the set, and goes to infinity otherwise. The direct application of the ADMM algorithm [37] to problem in (3.18) yields:

$$\begin{aligned} (\tilde{\mathbf{x}}^{k+1}, \tilde{\mathbf{y}}^{k+1}) &= \Pi_{\mathbf{Q}\mathbf{x} = \mathbf{y}}(\mathbf{x}^k + \mathbf{s}^k, \mathbf{y}^k + \mathbf{r}^k), \\ \mathbf{x}^{k+1} &= \Pi_C(\tilde{\mathbf{x}}^k - \mathbf{s}^k), \\ \mathbf{y}^{k+1} &= \Pi_{C^*}(\tilde{\mathbf{y}}^k - \mathbf{r}^k), \\ \mathbf{s}^{k+1} &= \mathbf{s}^k - \tilde{\mathbf{x}}^{k+1} + \mathbf{x}^{k+1}, \\ \mathbf{r}^{k+1} &= \mathbf{r}^k - \tilde{\mathbf{y}}^{k+1} + \mathbf{y}^{k+1}, \end{aligned} \tag{3.19}$$

where $\mathbf{s}$ and $\mathbf{r}$ are the dual variables for the equality constraints on $\mathbf{x}$ and $\mathbf{y}$, respectively, and $\Pi_{\mathcal{S}}(\mathbf{z})$ is the Euclidean projection of $\mathbf{z}$ over the set $\mathcal{S}$.

As the problem in (3.18) is self-dual, we can verify that $\mathbf{s}^k = \mathbf{y}^k$ and $\mathbf{r}^k = \mathbf{x}^k$ if they are equally initialized ($\mathbf{s}^0 = \mathbf{y}^0$, $\mathbf{r}^0 = \mathbf{x}^0$) [37]. This fact allows us to eliminate the dual variable updates in (3.19). It also enables the change of the update of $\mathbf{y}^{k+1}$ using a cone projection by the

equivalent $\mathbf{s}^{k+1}$ update, which is typically computationally less expensive than a projection. The resulting algorithm is

$$\begin{aligned}\tilde{\mathbf{x}}^{k+1} &= \Pi_{\mathbf{Qx}=\mathbf{y}}(\mathbf{x}^k + \mathbf{y}^k),\\ \mathbf{x}^{k+1} &= \Pi_C(\tilde{\mathbf{x}}^k - \mathbf{y}^k),\\ \mathbf{y}^{k+1} &= \mathbf{y}^k - \tilde{\mathbf{x}}^{k+1} + \mathbf{x}^{k+1}.\end{aligned} \tag{3.20}$$

Another simplification that can be done is the projection performed in the first step of the algorithm, replacing it by its matrix form $\Pi_{\mathbf{Qx}=\mathbf{y}}(\mathbf{x}^k + \mathbf{y}^k) = (\mathbf{I} + \mathbf{Q})^{-1}(\mathbf{x}^k + \mathbf{y}^k)$.

The algorithm is then formed by three steps. The first and second steps involve projections over the set $\mathbf{Qx} = \mathbf{y}$ and the cone C, respectively, and the third is a simple running sum of the error at the $(k+1)$th iteration.

3.4 Simulation Results

For the ADMM simulation, we apply the matrix stuffing procedure by creating the base structure for the standard conic problem, and in each realization we copy the problem data into this structure. Afterwards, we use a numerical optimization package based on [37], called SCS, which solves conic programs in the form of the problem in (3.4), using the ADMM algorithm for HSD embedding as defined in Sections 3.3.2 and 3.3.3.

The SDP formulation [16], which is used to assess the ADMM performance, is a well known semidefinite relaxed version of (3.3). To solve it, we use the interior point toolbox *SeDuMi*, from the CVX modeling framework.

Another important feature of the SDP formulation is its ability to determine an optimal RRU-UE allocation [16]. In this sense, both approaches use the same allocation, provided by SDP. However, when SDP is not capable of converging in a reasonable amount of time we use, for simplicity, a minimum RRU-UE distance based allocation for the ADMM approach, i.e. the each UE is allocated to the closest BS.

The simulations parameters are shown in Table 3.1.

Table 3.1 – Simulation Parameters.

Parameters	Value
Number of UE antennas	1
Scenario Area	500 m×500 m
Min. RRU-to-RRU distance	40 m
Min. RRU-to-UE distance	3 m
RRU and UE positioning	uniformly random
Noise Density	−174 dBm/Hz
Min. SINR at each UE	0.9 dB
Path-loss	$30.6 + 36.7\log_{10}(d)$ dB
Channel Model	Rayleigh

Source: Created by the author.

We show results on the amount of time that each of the strategies take to converge on a limited computer based simulation. It is important to highlight that the obtained values of time do not reflect the actual optimization time in a real network application. However, the presented analysis is valid, by comparing the ADMM and SDP algorithms with respect to the difference of speeds of convergence. Also, some of the simulated scenarios may not directly reflect a massive deployment, due to computational limitations. However, we seek to show the behavior of the solutions with the variation from a standard-scale scenario to a larger one, varying one variable (number or antennas, RRUs and UEs) at a time. Thus, our goal is to discuss the trends on how each solution would behave in a scenario with an even larger-scale deployment.

The first simulation is made to assess the time performance for scenarios with 5 RRUs and 10 UEs, varying the number of antennas. For each of the instances, the simulation was run 100 times and the average of the resulting times is analyzed. The results of this simulation are shown in Figure 3.2.

From Figure 3.2, it can be seen that the ADMM based algorithm requires significantly less time than SDP in scenarios with large numbers of antennas. Additionally, SDP was not capable to provide solutions within a reasonable amount of time for scenarios with more than 60 antennas, while ADMM was shown to be very time efficient in these cases. However, the highlighted part of Figure 3.2 shows that when the number of antennas is equal to or less than 5 the ADMM algorithm was slower than SDP, and that the demanded ADMM time decreases when the number of antennas increases from 2 to 5.

Instances of the problem with less antennas offer less degrees of freedom for the beamforming, which makes it hard to find a combination of beamforming vectors that is good enough to meet the SINR constraints. However, when the number of antennas is larger, the solution will have to deal with more variables, and then the problem will have larger scale, which would also increase the time requirement.

An interpretation for the behavior shown by the ADMM based algorithm is related to this trade-off and the fact that, as stated before, ADMM shows slow convergence for scenarios with high accuracy requirements, but it deals well with large-scale problems.

A problem with a very small number of antennas and very strict constraints, can be seen as equivalent to a problem with high accuracy requirements, since in order to find a specific solution that can meet very strict constraints, by only using very few degrees of freedom, it is necessary to reach a really accurate solution. In this sense, ADMM may be slower when dealing with scenarios with a very small number of antennas. However, when the number of antennas is large enough to provide the minimum required amount of degrees of freedom, such impact is reduced and the ADMM strength on dealing well with large-scale problems is reflected in the results.

The next simulation was made by varying the number of RRUs, setting the number of UEs as twice the number of RRUs for each scenario. The results are shown in Figure 3.3, where the numbers of RRU antennas used in each simulation are indicated in the legend box.

Figure 3.2 – Performance for 5 RRUs and 10 UEs.

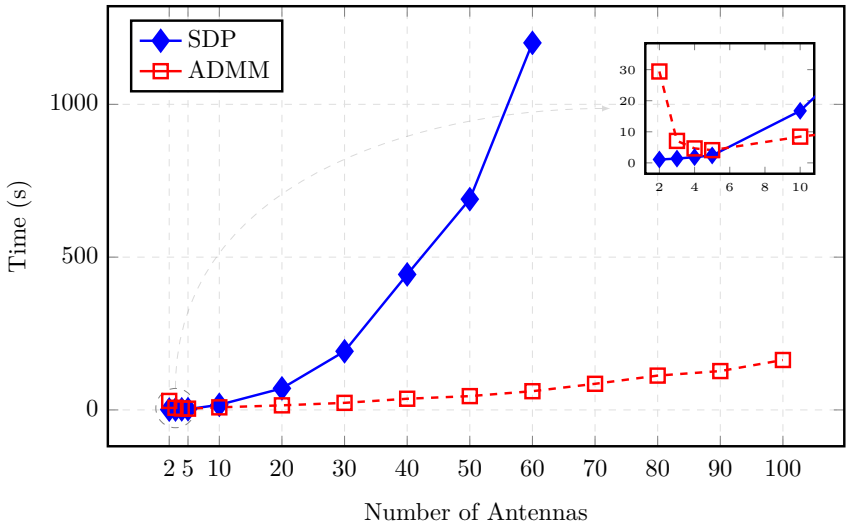

Source: Created by the author.

Figure 3.3 – Performance for x RRUs with y antennas and $2x$ UEs.

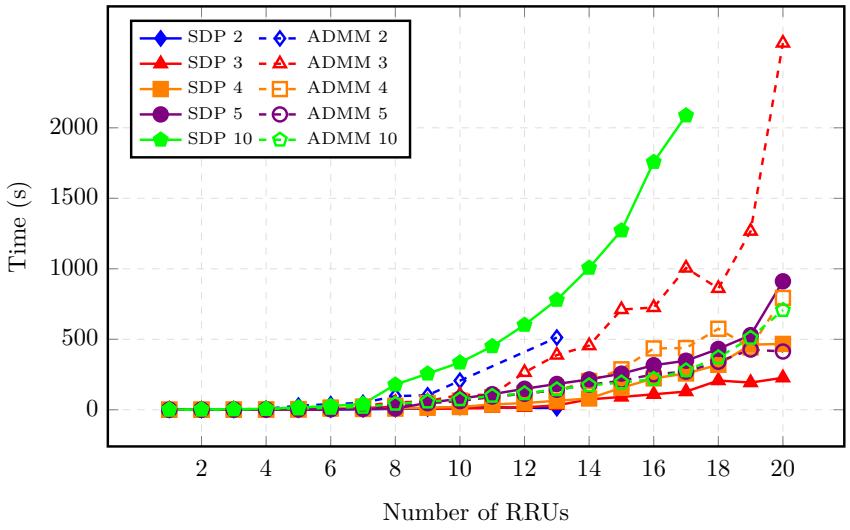

Source: Created by the author.

In Figure 3.3, we see that for all cases the solving time increases when the number of RRUs increases, what makes sense as we are adding more problems to be solved. We also see that when the number of antennas increases from 2 to 5 the demanded SDP time increases, while the ADMM time decreases as in the previous simulation. When the number of antennas is less than 5, ADMM is more time demanding than SDP in all cases, however, the scenario with 5 antennas is the turning point, where ADMM spends more time in scenarios with less than 9 RRUs, but less time with more cells. With 10 antennas, ADMM shows a much better result than SDP, and it can converge in more cases, as SDP failed to converge, within a reasonable amount of time, with more than 17 RRUs.

Another simulation was made by keeping the numbers of RRUs and antennas fixed,

Figure 3.4 – Performance for 7 RRUs with 20 Antennas.

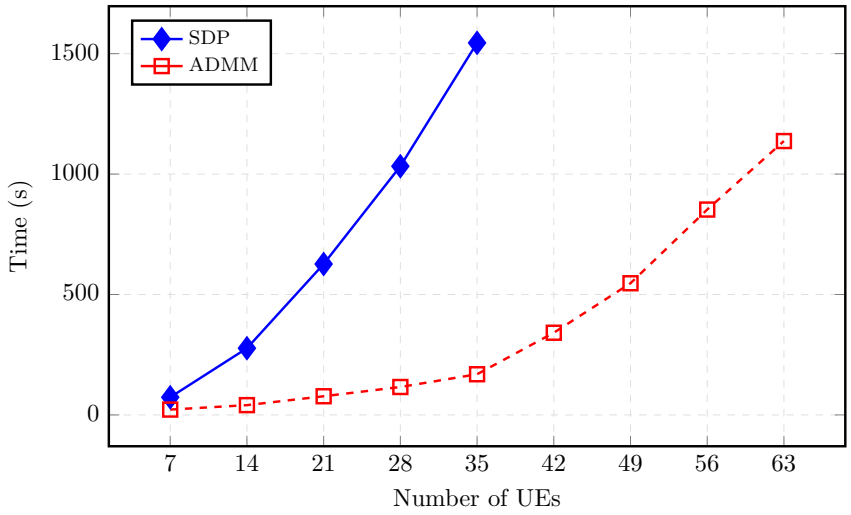

Source: Created by the author.

while varying the number of users. In Figure 3.4 we show the results for the scenario with 7 RRUs with 20 antennas each. It is seen that in all cases ADMM needed less time than SDP, and that both times increase when more users are added. However, SDP did not converge in a reasonable amount of time for cases with more than 35 UEs.

In order to better demonstrate and understand why ADMM provides modest accuracy within a reasonably low amount of time, but fails to provide high accuracy in comparison to other methods, we analyze its convergence behavior in different scenarios. This is done by an inspection of the primal-dual solution gap curve from both approaches, ADMM and SDP. The gap is used for both methods as an accuracy measure and parameter for the stopping criteria, since in convex problems the point with the smallest dual gap is the optimal point.

Figures 3.5 to 3.7 show the gap curves for one realization with 8 UEs and 4 RRUs using 5, 10 and 20 antennas, respectively. In these figures, the gap is simply defined as the modulus of the difference between the squared primal and dual objectives. However, as the objective function of the ADMM problem in (3.7) is only the norm, instead of the squared norm as in the conventional problem, the gap for ADMM is defined as the norm of the difference of the squared primal and dual objectives.

It can be seen in these Figures that ADMM takes longer to converge than SDP only in the case with 5 antennas, in the other scenarios ADMM converges faster, and the time difference increases when more antennas are added, what agrees with the previous results. The interesting result is that ADMM shows a convergence rate smoother than SDP, i.e, the gap reduction rate is almost linear after a small time from the start of the iterations. However, the initial gap values are much smaller than in SDP, what makes ADMM faster, when less accurate solutions are needed.

For example, in the configuration with 5 antennas, if the gap required by the stopping criterion were 10^{-4}, ADMM would have required less time to reach this point and provide a solution. When larger-scale problems are analyzed (10 and 20 antennas), ADMM scaled well

and provided the required accuracy faster than SDP, however, if more accurate solutions are needed, ADMM may require more time than SDP.

Figure 3.5 – Duality gap comparison (5 antennas).

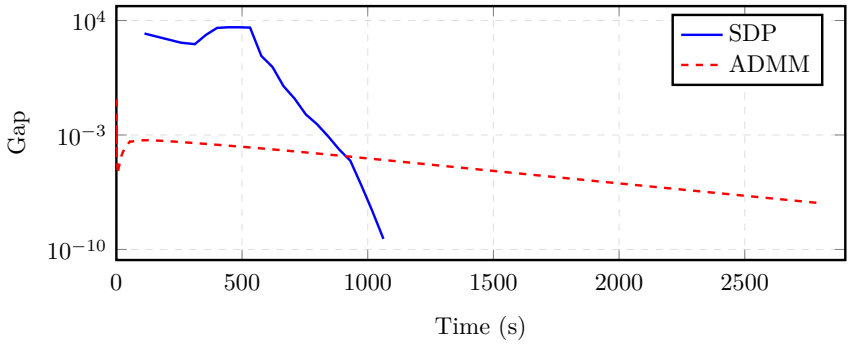

Source: Created by the author.

Figure 3.6 – Duality gap comparison (10 antennas).

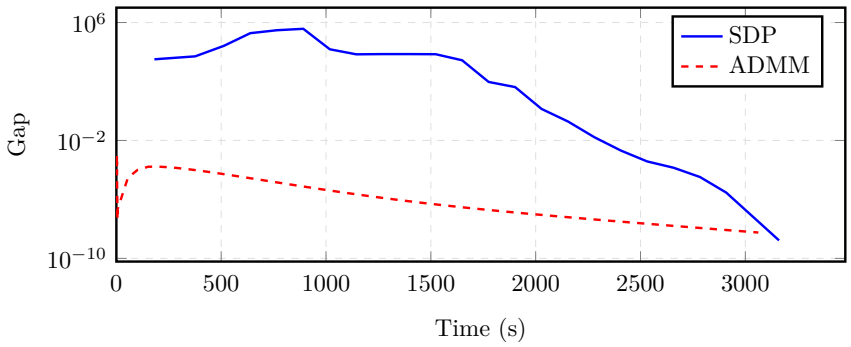

Source: Created by the author.

Figure 3.7 – Duality gap comparison (20 antennas).

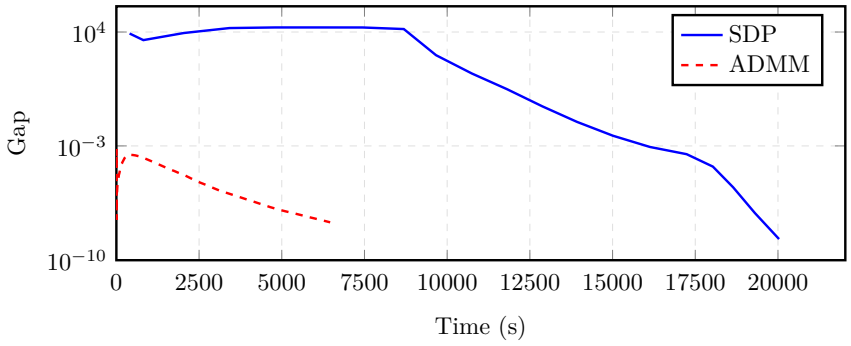

Source: Created by the author.

3.5 Conclusions

In this chapter we have presented a performance analysis of a centralized ADMM based solution for the beamforming problem, which aims to scale well to large-scale problems, providing modest accuracy within a reasonable amount of time.

The simulation results showed that the ADMM based method was able to provide solutions for large-scale scenarios in much less time than the SDP based method. However, for the scenarios with small numbers of antennas, when compared with the number of users, ADMM required more time to converge than SDP. This result corroborates that ADMM has fast convergence for modest accuracy requirement, but it is slow providing high accuracy results.

Another possibility of ADMM is its capability of performing the projection steps in a parallel form, what would represent even greater time reductions in C-RAN systems, where this processing can be distributed in multiple BBUs.

4 DISTRIBUTED BEAMFORMING FOR DYNAMIC TDD NETWORKS WITH BS TO BS INTERFERENCE CONSTRAINTS

4.1 Introduction

In dense networks that employ Dynamic TDD in order to adapt to the unbalanced and varying traffic requirements, an important issue arises related to cross-link interferences, between the neighbor cells transmitting in contrary link directions. In practice, the BS to BS interference is one of the main challenges that limit the dynamic DL and UL reconfiguration [39], since the BS transmits in high power levels and the channel between BSs may present high line-of-sight (LoS) probability. On the other hand, the UE to UE links are typically weaker, considering the randomness of the UE location and surroundings, and the UEs lower transmit power levels [55].

For these reasons, interference management techniques applied to dynamic TDD systems mainly target the BS to BS interference. In this chapter, we propose beamforming strategies for dynamic TDD MIMO systems, which protect the UL transmission from the harmful BS to BS interference by keeping the interference power from the DL BSs to the UL BSs below some maximum tolerable levels, while minimizing the DL sum-power and guaranteeing a minimum SINR for DL UEs.

We propose an iterative centralized solution that requires global CSI at the central node and an iterative decentralized solution with decoupling based on primal decomposition, in which each BS requires only local CSI and uses a lightweight backhaul and over-the-air signaling scheme in order to share the required run-time information. Our solutions for the dynamic TDD scenario are based on the decentralized MIMO solution proposed by [34] for the conventional TDD scenario, which also employs decoupling by primal decomposition with a similar over-the-air signaling scheme, and in the solution proposed by [56] for a MISO cognitive radio network, that also employs a maximum interference constraint (secondary BS to primary UE interference).

The proposed solutions can provide an increase in the UL SINR by keeping the BS to BS interference below tolerable levels, while still guaranteeing quality of service for the DL users, with a minimum SINR threshold. The decentralized solution approaches the same outcome as the centralized one as the algorithm iterates, however after any intermediate iteration of the decentralized algorithm a feasible solution can be extracted for both DL SINR and BS to BS interference constraints, at the cost of suboptimal DL sum-power and UL SINR.

This chapter is organized as follows. Section 4.2 describes the signal model used in this and in the following chapters. Section 4.3 describes the problem and proposes a centralized solution. Section 4.4 presents a decentralized solution based on primal decomposition. Section 4.5 describes the signaling strategies and compares the amount of signaling required by both approaches. Section 4.6 presents and analyzes simulation results, while the main conclusions are

drawn in Section 4.7.

4.2 Signal Model

In this and in the following chapter we consider a dynamic TDD MIMO system with a group formed by B BSs, equipped with N_b antennas each, and K UEs, equipped with N_u antennas each. In a given time slot any BS can operate in UL or DL mode, according to some previous system decision taking into account traffic load and interference situations.

Let $\mathcal{B}_{ul}$, $\mathcal{B}_{dl}$, $\mathcal{K}_{ul}$ and $\mathcal{K}_{dl}$ represent the sets of BSs and UEs in the UL and DL mode, respectively. Then, the signal received by UE $k \in \mathcal{K}_{dl}$ can be written as

$$\mathbf{y}_k^{dl} = \underbrace{\mathbf{H}_{b_k,k}\mathbf{m}_k d_k}_{\text{desired signal}} + \underbrace{\sum_{i\in\mathcal{K}_{dl}\setminus k} \mathbf{H}_{b_i,k}\mathbf{m}_i d_i}_{\text{BS to UE interf.}} + \underbrace{\sum_{j\in\mathcal{K}_{ul}} \mathbf{Q}_{j,k}\mathbf{w}_j d_j}_{\text{UE to UE interf.}} + \underbrace{\mathbf{n}_k}_{\text{noise}}, \tag{4.1}$$

where $\mathbf{H}_{b_i,k} \in \mathbb{C}^{N_u\times N_b}$ denotes the channel between the BS that serves UE i (b_i) and UE k; $\mathbf{m}_i \in \mathbb{C}^{N_b\times 1}$ denotes a beamforming BS filter with respect to UE i, while $\mathbf{w}_i \in \mathbb{C}^{N_u\times 1}$ denotes the beamforming filter at UE i, independently from the link direction; d_i denotes the data symbol relative to UE i, which is assumed to have unit variance; $\mathbf{Q}_{j,k} \in \mathbb{C}^{N_u\times N_u}$ denotes the channel between UEs j and k, and $\mathbf{n}_k \in \mathbb{C}^{N_u\times 1} \sim \mathcal{N}(0, N_0)$ represents the noise at the link of UE k, which is a complex Gaussian random variable with zero mean and unit variance. Figure 4.1 exemplifies a 3-cell system with this structure.

At UE k, the received signal $\mathbf{y}_k^{dl}$ is decoded by the unit norm vector $\mathbf{w}_k^H$, and the SINR at this link can be written as

$$\Gamma_k^{dl} = \frac{|\mathbf{w}_k^H\mathbf{H}_{b_k,k}\mathbf{m}_k|^2}{\sum\limits_{i\in\mathcal{K}_{dl}\setminus k} |\mathbf{w}_k^H\mathbf{H}_{b_i,k}\mathbf{m}_i|^2 + \sum\limits_{j\in\mathcal{K}_{ul}} |\mathbf{w}_k^H\mathbf{Q}_{j,k}\mathbf{w}_j|^2 + ||\mathbf{m}_l||^2 N_0}. \tag{4.2}$$

On the other hand, the signal received by BS $b_l \in \mathcal{B}_{ul}$, sent from its served UE $l \in \mathcal{K}_{ul}$, is written as

$$\mathbf{y}_l^{ul} = \underbrace{\mathbf{H}_{b_l,l}^H\mathbf{w}_l d_l}_{\text{useful signal}} + \underbrace{\sum_{j\in\mathcal{K}_{ul}\setminus l} \mathbf{H}_{b_l,j}^H\mathbf{w}_j d_j}_{\text{UE to BS interf.}} + \underbrace{\sum_{i\in\mathcal{K}_{dl}} \mathbf{G}_{b_i,b_l}\mathbf{m}_i d_i}_{\text{BS to BS interf.}} + \underbrace{\mathbf{n}_l}_{\text{noise}}, \tag{4.3}$$

where, $\mathbf{G}_{b_i,b_l} \in \mathbb{C}^{N_b\times N_b}$ denotes the channel between the BS $b_i \in \mathcal{B}_{dl}$ and b_l. Channel reciprocity is used to obtain the channels between UEs and BSs. The channel in one link direction is the Hermitian of the channel in the other link direction ($\mathbf{H}_{l,b_l} = \mathbf{H}_{b_l,l}^H$).

At the UL BS b_l, the received signal $\mathbf{y}_l^{ul}$ is multiplied by an unit norm receive vector $\mathbf{m}_l^H \in \mathbb{C}^{1\times N_b}$, and the SINR at this link can be written as

$$\Gamma_l^{ul} = \frac{|\mathbf{m}_l^H\mathbf{H}_{b_l,l}^H\mathbf{w}_l|^2}{\sum\limits_{j\in\mathcal{K}_{ul}\setminus l} |\mathbf{m}_l^H\mathbf{H}_{b_l,j}^H\mathbf{w}_j|^2 + \sum\limits_{i\in\mathcal{K}_{dl}} |\mathbf{m}_l^H\mathbf{G}_{b_i,b_l}\mathbf{m}_i|^2 + ||\mathbf{m}_l||^2 N_0}. \tag{4.4}$$

Figure 4.1 – Dynamic TDD system.

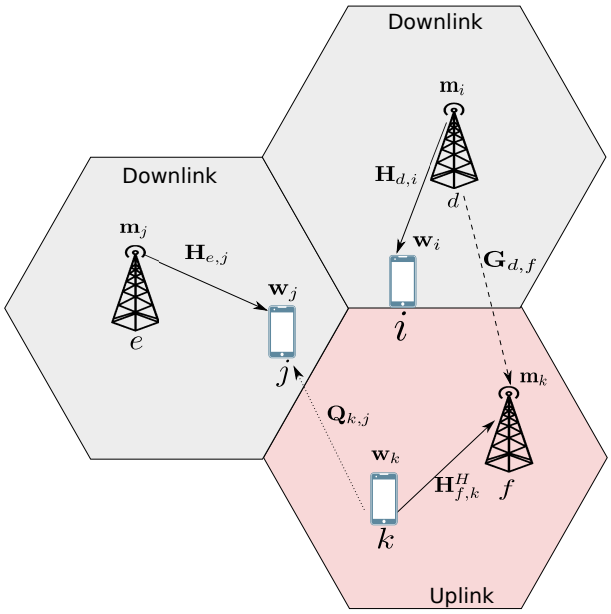

Source: Created by the author.

4.3 Centralized Approach

The target of the DL problem is to minimize the transmit sum power, while satisfying a minimum SINR threshold for the DL UEs and keeping the BS to BS interference power below a maximum target at each link. This problem can be conveniently expressed as an optimization task as

$$\begin{aligned} \min_{\{\mathbf{m}_i, \mathbf{w}_i\}_{i\in\mathcal{K}_{dl}}} \quad & \sum_{i\in\mathcal{K}_{dl}} \|\mathbf{m}_i\|_2^2 \\ \text{s. t.} \quad & \Gamma_k^{dl} \geq \gamma_k, \quad \forall k \in \mathcal{K}_{dl} \\ & \sum_{i\in\mathcal{K}_{dl}} |\mathbf{m}_l^H \mathbf{G}_{b_i,b_l} \mathbf{m}_i|^2 \leq \psi_l, \quad \forall l \in \mathcal{K}_{ul}, \end{aligned} \tag{4.5}$$

where γ_k is the minimum DL SINR threshold of UE k and ψ_l the maximum BS to BS interference power constraint in the decoded signal received from UL UE l, and both are non-negative and chosen accordingly to system requirements.

The problem in (4.5) is not jointly convex in $\{\mathbf{m}_i\}_{i\in\mathcal{K}_{dl}}$ and $\{\mathbf{w}_i\}_{i\in\mathcal{K}_{dl}}$, however it can be solved by an iterative approach [57], in which the transmit and receive beamformers are calculated in an alternate fashion. For the calculation of the DL transmitter, $\{\mathbf{m}_i\}_{i\in\mathcal{K}_{dl}}$, the receivers, $\{\mathbf{w}_i\}_{i\in\mathcal{K}_{dl}}$, must be fixed. On the other hand, for the calculation of the receivers $\{\mathbf{w}_i\}_{i\in\mathcal{K}_{dl}}$, the transmitter variables $\{\mathbf{m}_i\}_{i\in\mathcal{K}_{dl}}$ are fixed. These two steps are done iteratively until some stop criterion is reached, such as the relative power change between iterations or a predefined maximum number of iterations. This approach is inspired on a similar procedure

presented by [33] and [57] for the MIMO sum-power minimization problem with individual SINR constraints.

In one step of this iterative process, the optimization variables are the transmitters, $\{\mathbf{m}_i\}_{i\in\mathcal{K}_{dl}}$, and the problem is written as (4.6), with $\psi_l \geq 0, \forall l \in \mathcal{K}_{ul}$ and $N_b \geq K$ for strict feasibility. This problem can be cast into a standard SOCP form, thus it can be solved by standard convex optimization tools.

$$\begin{aligned} \min_{\{\mathbf{m}_i\}_{i\in\mathcal{K}_{dl}}} \quad & \sum_{i\in\mathcal{K}_{dl}} \|\mathbf{m}_i\|_2^2 \\ \text{s. t.} \quad & \Gamma_k^{dl} \geq \gamma_k, \forall k \in \mathcal{K}_{dl} \\ & \sum_{i\in\mathcal{K}_{dl}} |\mathbf{m}_l^H \mathbf{G}_{b_i,b_l} \mathbf{m}_i|^2 \leq \psi_l, \quad \forall l \in \mathcal{K}_{ul}. \end{aligned} \tag{4.6}$$

In Problem (4.6) the SINR constraint is always tight at the optimal solution, however the BS to BS interference constraint may be below the maximum value, so that in such occasions removing this constraint does not affect the final solution. We consider that problem (4.6) is always feasible, which requires that the value of ψ_k be non-negative ($\psi_k \geq 0$) and the number of BS antennas needs to be greater than or equal to the total number of UEs ($N_b \geq K$).

In the second step, the receive vectors are calculated. The optimal DL receivers $\{\mathbf{w}_i\}_{i\in\mathcal{K}_{dl}}$ are the ones that maximize the DL SINR, and can be calculated using the MMSE approach as follows.

$$\mathbf{w}_k = \frac{\bar{\mathbf{w}}_k}{\|\bar{\mathbf{w}}_k\|}, \quad \forall k \in \mathcal{K}_{dl} \tag{4.7}$$

$$\bar{\mathbf{w}}_k = \left(\sum_{i\in\mathcal{K}_{dl}} \mathbf{H}_{b_i,k} \mathbf{m}_i \mathbf{m}_i^H \mathbf{H}_{b_i,k}^H + \sum_{j\in\mathcal{K}_{ul}} \mathbf{Q}_{j,k} \mathbf{w}_j \mathbf{w}_j^H \mathbf{Q}_{j,k}^H + N_0 \mathbf{I}_{N_u} \right)^{-1} \mathbf{H}_{b_k,k} \mathbf{m}_k. \tag{4.8}$$

The optimality of acMMSE as the DL UE receiver can be verified by a similar analysis to the one presented by [57]. Let us assume that during the iterative procedure to solve (4.5) we have the feasible set of solutions $\{\mathbf{m}_{\mathcal{K}_{dl}(1)}(t), \mathbf{m}_{\mathcal{K}_{dl}(2)}(t), \ldots, \mathbf{m}_{\mathcal{K}_{dl}(|\mathcal{K}_{dl}|)}(t), \mathbf{w}_{\mathcal{K}_{dl}(1)}(t), \mathbf{w}_{\mathcal{K}_{dl}(2)}(t), \ldots, \mathbf{w}_{\mathcal{K}_{dl}(|\mathcal{K}_{dl}|)}(t)\}$ after the (t)th iteration, and $\{\mathbf{m}_{\mathcal{K}_{dl}(1)}(t+1), \mathbf{m}_{\mathcal{K}_{dl}(2)}(t+1), \ldots, \mathbf{m}_{\mathcal{K}_{dl}(|\mathcal{K}_{dl}|)}(t+1), \mathbf{w}_{\mathcal{K}_{dl}(1)}(t+1), \mathbf{w}_{\mathcal{K}_{dl}(2)}(t+1), \ldots, \mathbf{w}_{\mathcal{K}_{dl}(|\mathcal{K}_{dl}|)}(t+1)\}$ after the $(t+1)$th iteration.

To show that this step contributes to a monotonically decreasing sum-power at each iteration, it suffices to prove that the solution set formed during iteration $(t+1)$, after the update of the UL receiver, but before solving the SOCP for the transmitters, $\{\mathbf{m}_{\mathcal{K}_{dl}(1)}(t), \mathbf{m}_{\mathcal{K}_{dl}(2)}(t), \ldots, \mathbf{m}_{\mathcal{K}_{dl}(|\mathcal{K}_{dl}|)}(t), \mathbf{w}_{\mathcal{K}_{dl}(1)}(t+1), \mathbf{w}_{\mathcal{K}_{dl}(2)}(t+1), \ldots, \mathbf{w}_{\mathcal{K}_{dl}(|\mathcal{K}_{dl}|)}(t+1)\}$, forms another feasible solution to the problem. The rationale for that is that the solution set after a receiver update must still obey the constraints in (4.6). This will make the constraints loose (higher than the minimum or lower than the maximum targets), allowing a power reduction, or at least maintenance, after the next transmitters update, when the constraints are tightened.

Thus, analyzing the SINR constraints in Problem (4.6) after the UL receiver update using MMSE, we can see that they are always feasible.

Proof. $\{\mathbf{w}_i\}_{i\in\mathcal{K}_{dl}}$ is given by the MMSE in (4.7), that maximizes the SINR of the DL UE k. This way, if the jth iteration was feasible, it can be guaranteed that for each UE $k \in \mathcal{K}_{dl}$

$$\begin{aligned}&\frac{|\mathbf{w}_k^H(t+1)\mathbf{H}_{b_k,k}\mathbf{m}_k(t)|^2}{\sum\limits_{i\in\mathcal{K}_{dl}\setminus k}|\mathbf{w}_k^H(t+1)\mathbf{H}_{b_i,k}\mathbf{m}_i(t)|^2+\sum\limits_{j\in\mathcal{K}_{ul}}|\mathbf{w}_k^H(t+1)\mathbf{Q}_{j,k}\mathbf{w}_j|^2+N_0}\\ &\geq\frac{|\mathbf{w}_k^H(t)\mathbf{H}_{b_k,k}\mathbf{m}_k(t)|^2}{\sum\limits_{i\in\mathcal{K}_{dl}\setminus k}|\mathbf{w}_k^H(t)\mathbf{H}_{b_i,k}\mathbf{m}_i(t)|^2+\sum\limits_{j\in\mathcal{K}_{ul}}|\mathbf{w}_k^H(t)\mathbf{Q}_{j,k}\mathbf{w}_j|^2+N_0}\geq\gamma_k.\end{aligned} \tag{4.9}$$

Thus, $\{\mathbf{m}_1(t),\mathbf{m}_2(t),\ldots,\mathbf{m}_B(t),\mathbf{w}_{\mathcal{K}_{dl}(1)}(t+1),\mathbf{w}_{\mathcal{K}_{dl}(2)}(t+1),\ldots,\mathbf{w}_{\mathcal{K}_{dl}(|\mathcal{K}_{dl}|)}(t+1)\}$ is a feasible set. □

For simplicity, we consider fixed UL transmitters $\{\mathbf{w}_i\}_{i\in\mathcal{K}_{ul}}$ calculated by an MRT approach, using as transmit vector the singular vector corresponding to the strongest element from the singular value decomposition (SVD) decomposition of the direct channel, multiplied by some fixed transmit power.

For the UL receivers, $\{\mathbf{m}_i\}_{i\in\mathcal{K}_{ul}}$, we propose an iterative approach combined with the steps of the DL beamforming, with the objective of maximizing the UL SINR at each link. In this approach the UL receivers are updated at each iteration, at the same moment as the DL receivers. MMSE can also be used to calculate the UL receive filters, however, it cannot guarantee monotonic convergence. The reason for this is that the UL receiver calculated by MMSE at an iteration, may not obey the interference constraints in (4.6), since MMSE maximizes the SINR, not directly guaranteeing a BS to BS interference reduction. However, results show that such solution iterates towards a point representing the combination of DL power minimization and UL SINR maximization.

An MMSE receiver for the UL UE k can be written as

$$\mathbf{m}_k=\frac{\bar{\mathbf{m}}_k}{\|\bar{\mathbf{m}}_k\|},\quad \forall k\in\mathcal{K}_{ul} \tag{4.10}$$

$$\bar{\mathbf{m}}_k=\left(\sum_{i\in\mathcal{K}_{dl}}\mathbf{G}_{b_i,b_k}\mathbf{m}_i\mathbf{m}_i^H\mathbf{G}_{b_i,b_k}^H+\sum_{j\in\mathcal{K}_{ul}}\mathbf{H}_{b_k,j}^H\mathbf{w}_j\mathbf{w}_j^H\mathbf{H}_{b_k,j}+N_0\mathbf{I}_{N_b}\right)^{-1}\mathbf{H}_{b_k,k}^H\mathbf{w}_k. \tag{4.11}$$

The iterative Algorithm 1 is proposed to solve the problem in (4.5) and it is designed by initially calculating the fixed UL UE precoders using MRT and an initial value for the DL BS precoders (this initialization can also be done using MRT or another approach). After the initialization the algorithm performs iteratively the calculation of the receivers and DL transmit filters until some convergence criterion is met. This algorithm assumes a centralized processing, that requires full knowledge about channels (i.e. global CSI), precoders and decoders available at a central unit or at each BS. This requirement exists because some variables are coupled between many BSs, i.e, the precoder selection by one BS may affect the computation of the precoders from other BSs.

Algorithm 1 Centralized dynamic TDD MIMO BF.

1: Find $\{\mathbf{w}_i\}_{i\in\mathcal{K}_{ul}}$ using MRT and initialize $\{\mathbf{m}_i\}_{i\in\mathcal{K}_{dl}}$.
2: **repeat**
3: Compute $\{\mathbf{w}_i\}_{i\in\mathcal{K}_{dl}}$ and $\{\mathbf{m}_i\}_{i\in\mathcal{K}_{ul}}$ according to (4.7) (4.10).
4: Compute $\{\mathbf{m}_i\}_{i\in\mathcal{K}_{dl}}$ solving the SOCP form of (4.6).
5: **until** Some stop criterion

4.4 Decentralized Approach via Primal Decomposition

In a fully decentralized version of Algorithm 1, the DL BS problem in (4.6) must be divided into subproblems, each solved by one DL BS, and each receiver must be calculated locally, with each node only having access to information about the channel from other nodes to itself, i.e., local CSI. This is possible if we can decouple the inter-cell interference terms related to each DL BS in (4.6) and if the transmitter and receiver vectors computed at the intermediate steps can be shared via over-the-air signaling between nodes by using orthogonal pilot symbols.

In order to decouple the inter-cell interference terms in (4.6) let us introduce two new sets of variables $\boldsymbol{\chi} = \{\chi_{b,k}\}_{b\in\mathcal{B}dl,\, k\in\mathcal{K}_{dl}\setminus\mathcal{K}_b}$ and $\boldsymbol{\psi} = \{\psi_{b,k}\}_{b\in\mathcal{B}dl,\, k\in\mathcal{K}_{ul}}$ ($\mathcal{K}_b$ denotes the set of users served by BS b), which account for the inter-cell interference from each DL BS to DL UE and from each DL BS to the transmission of each UL UE, respectively. By doing this, a primal decomposition method can be used to decentralize the solution by separating the problem in two levels of optimization [50]. In the lower level, the inter-cell interference terms in (4.6) are decoupled by fixing them to the value of the respective element of $\boldsymbol{\chi}$ and $\boldsymbol{\psi}$, while in the higher level a master problem updates each element in these sets.

The local decoupled problem at BS $b \in \mathcal{B}_{dl}$ is given as,

$$
\begin{aligned}
\min_{\{\mathbf{m}_i\}_{i\in\mathcal{K}_b}} \quad & \sum_{i\in\mathcal{K}_b} \|\mathbf{m}_i\|_2^2 \\
\text{s. t.} \quad & \frac{|\mathbf{w}_k^H \mathbf{H}_{b_k,k}\mathbf{m}_k|^2}{\sum\limits_{b'\in\mathcal{B}_{dl}\setminus b} \chi_{b',k} + \sum\limits_{i\in\mathcal{K}_b\setminus k} |\mathbf{w}_k^H \mathbf{H}_{b_i,k}\mathbf{m}_i|^2 + \theta_k + N_0} \geq \gamma_k,\ \forall k \in \mathcal{K}_b \\
& \sum_{i\in\mathcal{K}_b} |\mathbf{w}_j^H \mathbf{H}_{b,j}\mathbf{m}_i|^2 \leq \chi_{b,j}, \quad \forall j \in \mathcal{K}_{dl}\setminus\mathcal{K}_b \\
& \sum_{i\in\mathcal{K}_b} |\mathbf{m}_l^H \mathbf{G}_{b_i,b_l}\mathbf{m}_i|^2 \leq \psi_{b,l}, \quad \forall l \in \mathcal{K}_{ul},
\end{aligned}
\tag{4.12}
$$

where $\theta_k = \sum\limits_{i\in\mathcal{K}_{ul}} |\mathbf{w}_k^H \mathbf{Q}_{i,k}\mathbf{w}_i|^2$ is the UE to UE interference power term, which is constant and assumed to be known at the BS b_k in order to guarantee the SINR constraints.

In (4.12), the transmit power in BS b is minimized, subject to an SINR constraint for each of its users. In this SINR expression the received BS to UE inter-cell interference power terms are fixed to the values determined in the set $\boldsymbol{\chi}$. Another constraint in this problem is a maximum target for the transmitted BS to UE inter-cell interference power from BS b, in order to agree with the fixed maximum interference received by other DL UEs. The constraint on the

BS to BS interference puts a maximum target on the total interference generated by DL BS b to the UL transmission from user l.

Thus, the DL problems are decoupled by the use of the fixed interference sets $\boldsymbol{\chi}$ and $\boldsymbol{\psi}$, which need to be iteratively updated by a network master problem that can be written as

$$\begin{aligned} \min_{\{\boldsymbol{\chi},\boldsymbol{\psi}\}} \quad & \sum_{b\in\mathcal{B}_{dl}} f_b^*(\boldsymbol{\chi}^{(b)},\boldsymbol{\psi}) \\ \text{s. t.} \quad & \boldsymbol{\chi}^{(b)} \in \mathcal{S}, \quad \forall b \in \mathcal{B}_{dl} \\ & \boldsymbol{\psi} \in \mathcal{T}, \end{aligned} \tag{4.13}$$

where $\boldsymbol{\chi}^{(b)} = \{\chi_{b,k}, \chi_{b',k'}\}_{k\in\mathcal{K}_{dl}\backslash\mathcal{K}_b,\, b'\in\mathcal{B}_{dl}\backslash b,\, k'\in\mathcal{K}_b}$ is the set of elements in $\boldsymbol{\chi}$ that are related to BS b, $f_n^*(\boldsymbol{\chi}^{(b)},\boldsymbol{\psi})$ is the optimal objective of subproblem b in (4.12), for fixed sets of interferences, $\boldsymbol{\chi}^{(b)}$ and $\boldsymbol{\psi}$, $\mathcal{S} = \{\boldsymbol{\chi}^{(b)} : \boldsymbol{\chi}^{(b)} \in \mathbb{R}_{++}^{|\mathcal{K}_b|(|\mathcal{B}_{dl}|-1)+|\mathcal{K}_{dl}|-|\mathcal{K}_b|}\}$ is a set of positive reals (interferences should be greater than zero for strict feasibility) and $\mathcal{T} = \{\boldsymbol{\psi} : \boldsymbol{\psi} \in \mathbb{R}_{++}^{|\mathcal{B}_{dl}||\mathcal{K}_{ul}|}, \sum_{b\in\mathcal{B}_{dl}} \psi_{b,l} = \psi_l,\ \forall l \in \mathcal{K}_{ul}\}$ is the set of positive reals that sum up to the maximum BS to BS interference thresholds.

To solve this problem we use a projected subgradient method. This method works by updating at each iteration the inter-cell interference terms $\chi_{b,k}$ and $\psi_{b,k}$ as

$$\chi_{b,k}(t+1) = \mathcal{P}_{\mathcal{S}}\{\chi_{b,k}(t) - \sigma_t s_{b,k}(t)\}, \quad \forall b \in \mathcal{B}_{dl}, \forall k \in \mathcal{K}_{dl}\backslash\mathcal{K}_b, \tag{4.14}$$

$$\psi_{b,l}(t+1) = \mathcal{P}_{\mathcal{T}}\{\psi_{b,l}(t) - \sigma_t v_{b,l}(t)\}, \quad \forall b \in \mathcal{B}_{dl}, \forall l \in \mathcal{K}_{ul}, \tag{4.15}$$

where t is the iteration index, σ_t is the step-size at iteration t, that is required to be nonsummable and diminishing for guaranteed convergence of the subgradient method [51], $\mathcal{P}_{\mathcal{S}}\{\}$ and $\mathcal{P}_{\mathcal{T}}\{\}$ are the projections onto the sets $\mathcal{S}$ and $\mathcal{T}$, respectively. The factors $s_{b,k}(t)$ and $v_{b,l}(t)$ are subgradients of problem (4.13) with respect to the variables $\chi_{b,k}$ and $\psi_{b,l}$, respectively, which are expressed as [56]

$$s_{b,k}(t) = \lambda_k^{(b_k)}(t) - \lambda_k^{(b)}(t), \quad \forall b \in \mathcal{B}_{dl}, \forall k \in \mathcal{K}_{dl}\backslash\mathcal{K}_b, \tag{4.16}$$

$$v_{b,l}(t) = \sum_{b'\in\mathcal{B}_{dl}\backslash b} \lambda_l^{(b')}(t) - \lambda_l^{(b)}(t), \quad \forall b \in \mathcal{B}_{dl}, \forall l \in \mathcal{K}_{ul}, \tag{4.17}$$

where $\lambda_k^{(b_k)}(t)$ is the optimal Lagrange multiplier in (4.12) solved at BS b_k with respect to the SINR constraint of its UE k, and $\lambda_i^{(b)}(t)$, $i \notin \mathcal{K}_b$, is the optimal Lagrange multiplier with respect to the maximum inter-cell interference from BS b to the transmission of UE i in DL or UL directions. Monotonic convergence is not guaranteed for the subgradient method, then the best solutions need to be stored at each intermediate iteration.

Since the SOCP reformulation of (4.12) is a strictly feasible convex problem, thus Slater's condition is fulfilled for it, and it can be proven by a similar procedure as in [56] that strong duality holds for (4.12). This proof is detailed in Appendix A. Thus, a way to find the values of the optimal Lagrange multipliers, $\boldsymbol{\lambda}^{(b)}$, for the master problem update is by solving the

dual of the problem in (4.12). The dual problem is given by (4.18), that is a convex problem, cast in a standard SDP form, which can be efficiently solved by convex optimization tools at each DL BS. The mathematical procedure to find this dual problem formulation is shown in the Appendix B.

$$
\begin{aligned}
\underset{\{\boldsymbol{\lambda}^{(b)}\}}{\text{minimize}} \quad & \sum_{k\in\mathcal{K}_b} \lambda_k^{(b)} \left(\sum_{b'\in\mathcal{B}_{dl}\setminus b} \chi_{b',k} + \theta_k + N_0 \right) - \sum_{k\in\mathcal{K}_{dl}\setminus\mathcal{K}_b} \lambda_k^{(b)} \chi_{b,k} - \sum_{k\in\mathcal{K}_{ul}} \lambda_k^{(b)} \psi_{b,k} \\
\text{subject to} \quad & \mathbf{I} - \frac{\lambda_k^{(b)}}{\gamma_k} \mathbf{H}_{b_k,k}^H \mathbf{w}_k \mathbf{w}_k^H \mathbf{H}_{b_k,k} + \sum_{i\in\mathcal{K}_{dl}\setminus k} \lambda_i^{(b)} \mathbf{H}_{b,i}^H \mathbf{w}_i \mathbf{w}_i^H \mathbf{H}_{b,i} \\
& + \sum_{i\in\mathcal{K}_{ul}} \lambda_i^{(b)} \mathbf{G}_{b_k,b_i}^H \mathbf{m}_i \mathbf{m}_i^H \mathbf{G}_{b_k,b_i} \succeq 0, \forall k \in \mathcal{K}_b \\
& \boldsymbol{\lambda}^{(b)} \geq 0.
\end{aligned}
\tag{4.18}
$$

where, the symbol $\succeq$ is the generalized inequality operator.

Therefore, we can write a decentralized version of the algorithm to perform the beamforming in dynamic TDD MIMO scenarios as Algorithm 2.

Algorithm 2 Decentralized dynamic TDD MIMO BF.

1: Initialize $\boldsymbol{\chi}$ and $\boldsymbol{\psi}$.
2: UE $k, \forall k \in \mathcal{K}_{ul}$: Find $\mathbf{w}_k$ (MRT) and transmit pilots.
3: BS $b, \forall b \in \mathcal{B}_{dl}$: Initialize DL precoders $\{\mathbf{m}_i\}_{i\in\mathcal{K}_b}$.
4: **repeat**
5: BS $b, \forall b \in \mathcal{B}_{dl}$: Use $\{\mathbf{m}_i\}_{i\in\mathcal{K}_b}$ to transmit pilots.
6: UE $k, \forall k \in \mathcal{K}_{dl}$: Compute $\mathbf{w}_k$ using (4.7).
BS $b, \forall b \in \mathcal{B}_{ul}$: Compute $\{\mathbf{m}_i\}_{i\in\mathcal{K}_b}$ using (4.10).
7: UE $k, \forall k \in \mathcal{K}_{dl}$: Use $\mathbf{w}_k$ to transmit pilots.
BS $b, \forall b \in \mathcal{B}_{ul}$: Use $\{\mathbf{m}_i\}_{i\in\mathcal{K}_b}$ to transmit pilots.
8: **repeat**
9: BS $b, \forall b \in \mathcal{B}_{dl}$: Solve (4.18) and send $\boldsymbol{\lambda}^{(b)}$ via backhaul.
10: BS $b, \forall b \in \mathcal{B}_{dl}$: Update $\boldsymbol{\chi}^{(b)}$ and $\boldsymbol{\psi}$ using (4.14) and (4.15).
11: **until** Some stop criterion
12: BS $b, \forall b \in \mathcal{B}_{dl}$: Solve (4.12) for $\{\mathbf{m}_i\}_{i\in\mathcal{K}_b}$.
13: **until** Some stop criterion.

4.5 Signaling and Practical Considerations

For the decentralized beamforming computation we consider that each node only has access to local CSI, however, information still needs to be shared between the nodes in order to coordinate them. Algorithm 2 relies on two types of information sharing, the over-the-air signaling and the backhaul signaling. The over-the-air signaling is used during the iterative transmit-receive beamforming to inform the receivers the precoders used by the transmitters

and to inform the transmitters the decoders used by the receivers. The backhaul signaling is used by the DL BSs to share the dual variables $\lambda_k^{(b)}$ for the subgradient update of the decoupled interference terms $\boldsymbol{\chi}^{(b)}$ and $\boldsymbol{\psi}$.

Figure 4.2 illustrates the signaling strategy proposed for the decentralized beamforming computation, based on the signaling strategies proposed by [47] and [58]. The frame is divided in two main parts, the initial part corresponds to the beamforming setup procedure, in which Algorithm 2 is performed, and in the second part, the actual data transmission takes place in both link directions.

Figure 4.2 – Frame structure for signaling and data of decentralized Algorithm 2.

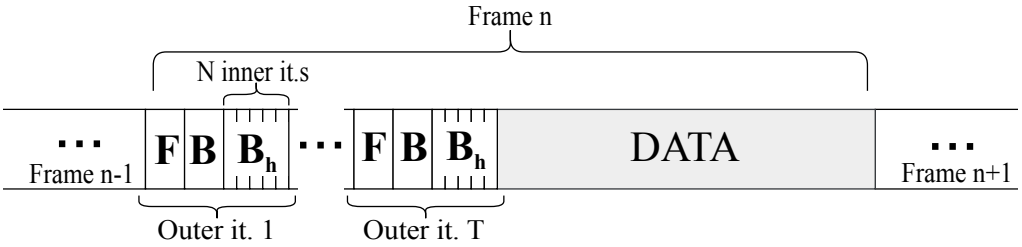

Source: Created by the author.

During the beamforming setup stage, the over-the-air signaling is denoted by the letters **F**, for the forward (transmitters to receivers) pilot signaling, corresponding to steps 2 and 5 of Algorithm 2, and **B** for the backward (receivers to transmitters) pilot signaling, corresponding to step 7. We consider that all nodes (BS and UE) use known orthogonal precoded pilot symbols, allowing perfect signal separation and perfect estimation of the effective channels, and consequently perfect estimation of the precoders and decoders by the opposite nodes.

The backhaul signaling, denoted by $\mathbf{B_h}$, is used by each DL BS to share between themselves, the dual variables $\lambda_k^{(b)}$, that are necessary for the subgradient update of $\boldsymbol{\chi}^{(b)}$ and $\boldsymbol{\psi}$. This signaling exchange is exemplified, for a 3 cell scenario, in Figure 4.3.

Figure 4.3 – Signaling strategy for Algorithm 2.

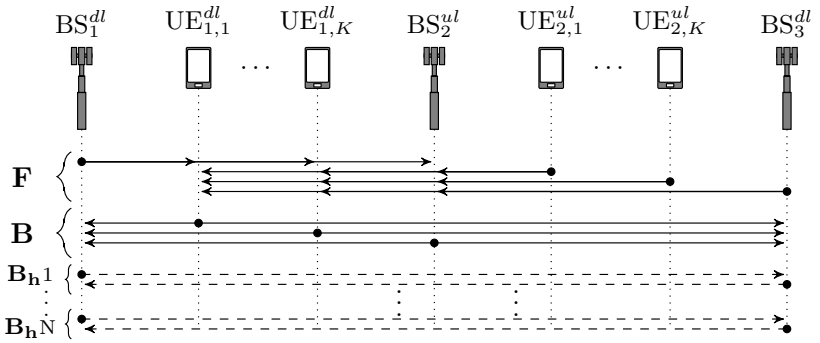

Source: Created by the author.

For the update of $\boldsymbol{\chi}^{(b)}$, the duals related to the SINR constraints $\{\lambda_k^{(b)}\}_{k\in\mathcal{K}_b}$ are sent to all the other DL BSs, thus, in a scenario with users equally divided by all BSs ($K_b = K/B$),

each DL BS sends $(B_{dl}-1)K_b$ real scalars via backhaul, the duals related to the inter-cell DL interference $\{\lambda_k^{(b)}\}_{k\in\mathcal{K}_{dl}\setminus\mathcal{K}_b}$ are sent to the BS serving the interfered user, adding more $(K-K_b)$ real scalar backhaul transmissions per DL BS. The update of $\boldsymbol{\psi}$ requires each DL BS to send the dual variables $\{\lambda_k^{(b)}\}_{k\in\mathcal{K}_{ul}}$ to all the other DL BSs, what means more $(B_{dl}-1)(B_{ul}K_b)$ real scalar backhaul transmissions per DL BS. Thus, at each inner iteration of Algorithm 2 the total number of real scalars sent by all BSs via backhaul is $B_{dl}K_b(B_{dl}-1)(2+B_{ul})$.

In a centralized approach, assuming that each BS exchanges its local CSI with all other BSs via backhaul at setup time, an estimative of the total number of real valued scalars required to be sent is $2KN_bN_u(B-1)B+2B_{dl}N_b^2(B-1)B_{ul}+2K_b^2B_{ul}N_u^2(B-1)B_{dl}$, with each term being related to the exchange of channels $\mathbf{H}$, $\mathbf{G}$ and $\mathbf{Q}$, respectively. Table 4.1 shows a comparison of the number of backhaul symbols transmitted via centralized and decentralized applications, and it can be seen that the amount of backhaul signaling in each iteration of the decentralized algorithm is much smaller than the total centralized load, and the difference in the signaling load increases with the increase of the network dimensions.

The number of Forward-Backward and backhaul stages is determined by the number of outer and inner iterations in Algorithm 2. At each outer iteration a Forward-Backward step is performed and at each inner iteration the backhaul signaling takes place. To achieve the same solution as the centralized case, the subgradient steps (inner iterations 8-11) in Algorithm 2 must be always repeated until convergence. However, feasible solutions can be extracted at any intermediate iteration, at the cost of suboptimal DL sum-power and UL SINR performance. Thus, the signaling load can be controlled by fixing the number of inner and outer iterations, at the cost of suboptimal performance. However, simulation results show that very close to optimal performance can be obtained with small numbers of iterations.

Table 4.1 – Backhaul signaling load.

$\{B_{ul},B_{dl},K_b,N_b,N_u\}$	Centralized	Decentralized per it.
$\{2,2,2,8,2\}$	4992	16 (0.32%)
$\{3,3,2,12,2\}$	31680	60 (0.19%)
$\{4,4,2,16,4\}$	186368	144 (0.08%)

Source: Created by the author.

4.6 Results

In this section we present simulation results in order to assess the performance of the proposed centralized and decentralized algorithms, and we analyze possible scenarios that could benefit from them.

The simulation scenario is formed by 7 cells (4 DL, 3 UL) with 50 m radius each, and 2 UEs randomly placed per cell. Each BS has 14 antennas and each UE has 2 antennas. This scenario is used since it is simple and presents all types of intra-cell and inter-cell interference links. However, performance gains can be obtained for a variety of interference-limited scenarios,

and the higher the BS to BS interference becomes, the higher is the UL SINR gain due to restricting it to tolerable levels. We consider that this cluster of 7 cells is within a larger system whose interference is treated as noise. Flat Rayleigh fading is considered, in which each element of the channels is an i.i.d. complex Gaussian random variable with zero mean and unit variance. The path-loss model is based on [39] and detailed in Table 4.2. The transmit power is 20 dBm for UEs.

Table 4.2 – Propagation characteristics.

Link	Path-loss
BS to BS	If $R < 2/3$km: $\mathrm{PL}(R) = 98.4 + 20\log_{10}(R)$, R in km If $R \geq 2/3$km: $\mathrm{PL}(R) = 101.9 + 40\log_{10}(R)$, R in km
BS to UE UE to BS	LOS: $\mathrm{PL}(R) = 103.8 + 20.9\log_{10}(R)$, R in km NLOS: $\mathrm{PL}(R) = 145.4 + 37.5\log_{10}(R)$, R in km $\mathrm{Prob}_{\mathrm{LOS}}(R) = 0.5 - \min(0.5, 5\exp(-0.156/R))$ $+\min(0.5, 5\exp(-R/0.03))$, R in km.
UE to UE	If $R < 50$m: $\mathrm{PL}(R) = 98.45 + 20\log_{10}(R)$, R in km If $R \geq 50$m: $\mathrm{PL}(R) = 55.78 + 40\log_{10}(R)$, R in m

Source: Based on [59]

Figure 4.4 shows the cumulative distribution function (CDF) of the SINR gains obtained when the UL is protected. In all cases the minimum DL SINR constraint is 20 dB and the number of outer iterations is 10. In the centralized solution, we see that when the BS to BS interference is not controlled, the UL suffers and achieves the worst SINR. However, when this interference is constrained to small values, $\psi_k = -100$ dBm, the UL SINR is greatly increased. We also show the decentralized solutions with 1 and 10 inner iterations (steps 8 to 11 in Algorithm 2), and both achieved a UL SINR close to the centralized. Furthermore, it can also be seen that the DL SINR constraints are always satisfied.

Figure 4.5 shows that when the constraint on ψ_k is included, the DL power increases. This happens because the feasible set of problem (4.6) is reduced when the BS to BS interference constraint is hardened. Figure 4.5 also shows that the decentralized algorithms achieved a slightly higher power due to the reduced number of iterations.

Figures 4.6 and 4.7 show the mean convergence for the scenario with $\gamma_k = 20$ dB, $\forall k \in \mathcal{K}_{dl}$, and $\psi_k = -100$ dBm, $\forall k \in \mathcal{K}_{ul}$. It can be seen that in all situations the UL SINR is increasing, while the DL sum power is decreasing. As expected, the centralized curves show the best solution, while the decentralized approaches with limited number of inner iterations (1, 10 and 100) try to approximate it, and with more inner iterations the closer the decentralized solution gets to the centralized one.

We also present results for other scenarios, in order to show that performance gains can be obtained for a variety of interference-limited scenarios, and the higher the BS to BS interference is, the higher is the UL SINR gain in restricting it to tolerable levels. Therefore,

Figure 4.4 – SINR gains when UL is protected.

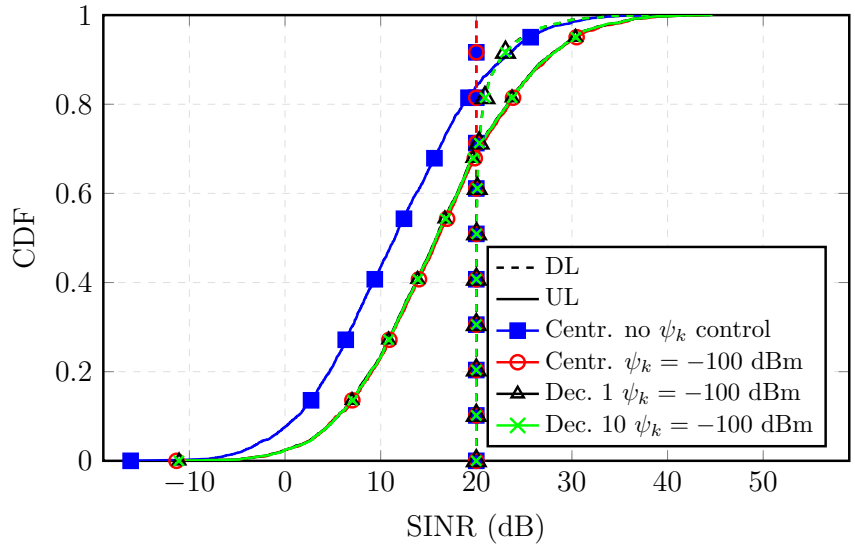

Source: Created by the author.

Figure 4.5 – Increase in DL power to protect UL.

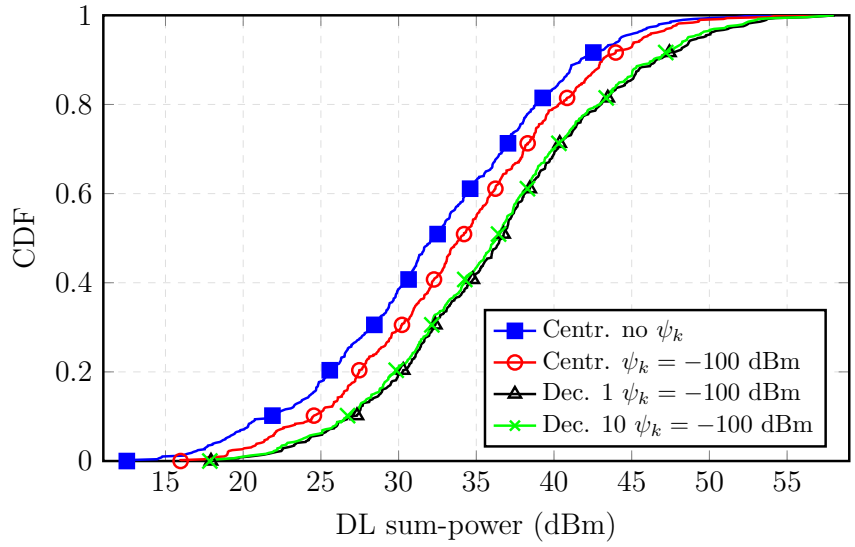

Source: Created by the author.

Figures 4.8 and 4.9 show the resulting SINR and sum-power for the MISO case with 1 antenna per UE and for another MIMO case where UEs have 5 antennas. These results show a similar behavior as the one obtained for the 2 antennas per UE case. The application of our algorithms provided an increase in UL SINR, while guaranteeing a minimum SINR for the DL users. The centralized algorithm achieved the optimum power, while the decentralized with reduced numbers of iterations achieved a slightly higher sum-power.

In Figure 4.10 we consider a different scenario, in which the algorithms are applied to a 4-cell cluster (2 DL, 2UL), each BS has 12 antennas and each cell has 3 UEs, with 3 antennas each. The results also show a similar behavior with regard to the relative performance of the algorithms.

Figure 4.6 – UL SINR convergence.

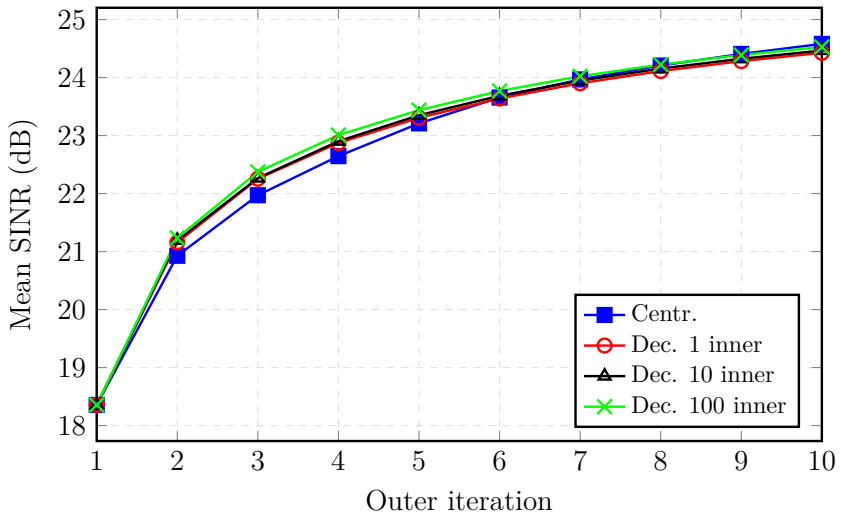

Source: Created by the author.

Figure 4.7 – DL Sum-power convergence.

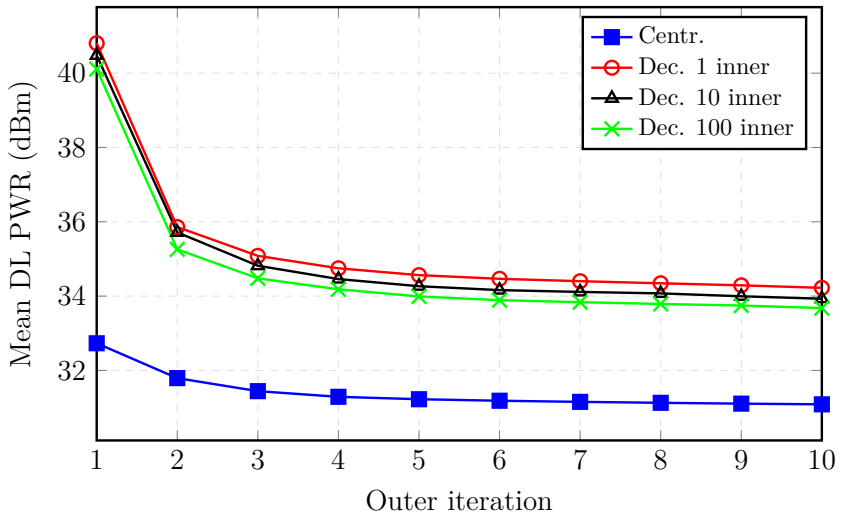

Source: Created by the author.

4.7 Conclusions

This chapter proposed a beamforming solution that can provide an increase in the UL SINR by keeping the BS to BS interference below tolerable levels, while still guaranteeing quality of service for the DL users, with a minimum DL SINR threshold. The decentralized solution converges towards the centralized solution as the algorithm iterates, however after any intermediate iteration of the decentralized algorithm a feasible solution is found for both DL SINR and BS to BS interference constraints, at the cost of suboptimal DL sum-power and UL SINR performance, and good approximations can be obtained with small numbers of iterations.

We also presented simulation results on the convergence of the proposed algorithms and we conclude that, as the algorithms iterate, the UL SINR is increased, while the DL sum

power is decreased. Finally, we verify that even though the centralized curves show the best solution, the decentralized approaches, even with limited number of inner iterations, approximates it.

Figure 4.8 – Performance for UEs with 1 antenna.

(a) SINR gains when DL is protected. (b) Increase in DL Sum-power to protect the UL.

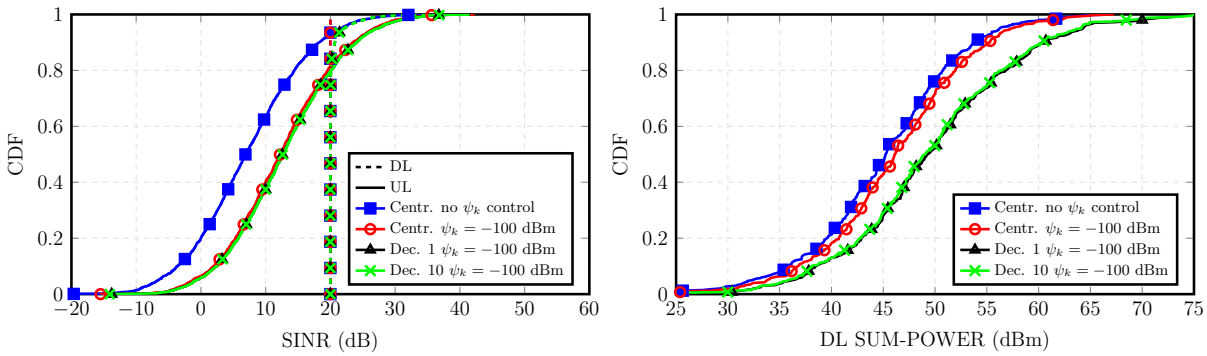

Source: Created by the author.

Figure 4.9 – Performance for UEs with 5 antennas.

(a) SINR gains when DL is protected. (b) Increase in DL Sum-power to protect the UL.

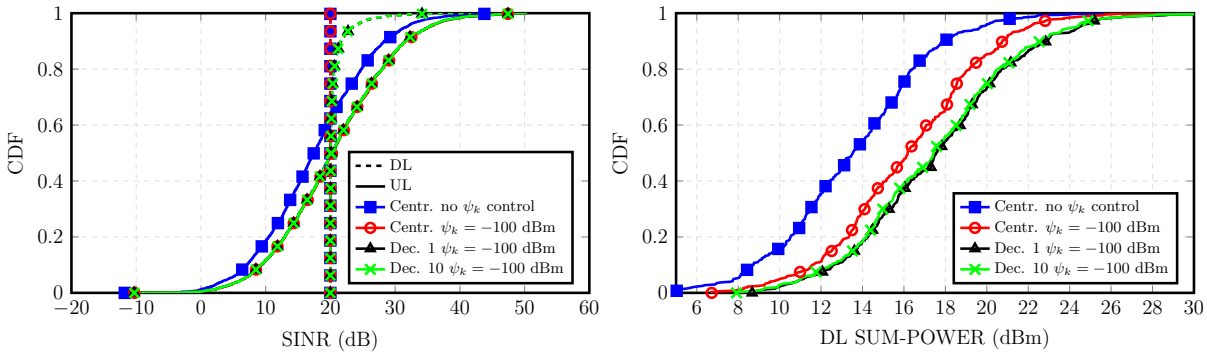

Source: Created by the author.

Figure 4.10 – Performance for a 4 cell scenario.

(a) SINR gains when DL is protected. (b) Increase in DL Sum-power to protect the UL.

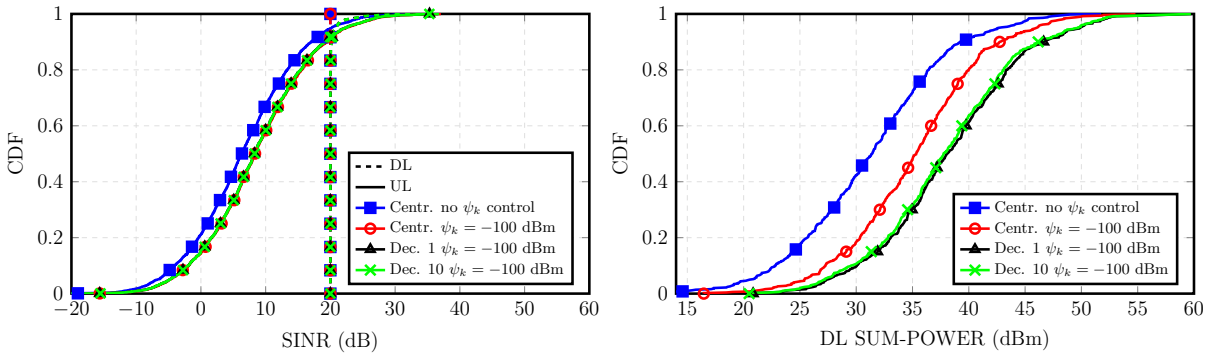

Source: Created by the author.

5 DISTRIBUTED BEAMFORMING FOR DYNAMIC TDD NETWORKS WITH DL AND UL SINR CONSTRAINTS

5.1 Introduction

In this chapter we present a centralized solution for the sum-power minimization beamforming with individual SINR constraints for every user in downlink and uplink, which requires global CSI, and a decentralized solution based on ADMM, which requires local CSI and uses a lightweight backhaul and over-the-air signaling scheme in order to share the required run-time information. It is shown that the decentralized solution approaches the same outcome as the centralized one as the algorithm iterates. Furthermore, the total signaling load can be controlled by fixing the number of inner and outer iterations, at the cost of suboptimal performance. However, simulation results show that very close to optimal performance can be obtained with small numbers of iterations.

The chapter is organized as follows. In Section 5.2, we formulate the problem and describe the centralized beamforming solution. In Section 5.3 we reformulate the problem and describe the ADMM based decentralized solution. In Section **??**, we propose a signaling scheme for the decentralized solution. Section 5.5 provides the numerical examples for the proposed algorithms. Conclusions are drawn in Section 5.6.

5.2 Centralized Approach

The target of the optimization problem is to minimize the total transmit sum power, while satisfying a minimum SINR threshold for all UEs in both UL and DL directions. This problem can be conveniently expressed as an optimization task as

$$\min_{\{\mathbf{m}_i,\,\mathbf{w}_i\}_{\forall i}} \sum_{i\in\mathcal{K}_{dl}} \|\mathbf{m}_i\|_2^2 + \sum_{j\in\mathcal{K}_{ul}} \|\mathbf{w}_j\|_2^2 \tag{5.1}$$

$$\begin{aligned} \text{s. t.} \quad & \Gamma_k^{dl} \geq \gamma_k, \quad \forall k \in \mathcal{K}_{dl} \\ & \Gamma_l^{ul} \geq \gamma_l, \quad \forall l \in \mathcal{K}_{ul}, \end{aligned} \tag{5.2}$$

where γ_k is the minimum SINR constraint for UE k.

Problem (5.1) is not jointly convex in $\{\mathbf{m}_i\}_{\forall i}$ and $\{\mathbf{w}_i\}_{\forall i}$, however, in a centralized case, it can be solved by an iterative approach, in which the transmit and receive beamformers are calculated in an alternate fashion until some stop criterion. For the calculation of the transmit vectors, $\{\mathbf{m}_i\}_{i\in\mathcal{K}_{dl}}$ and $\{\mathbf{w}_i\}_{i\in\mathcal{K}_{ul}}$, the receivers, $\{\mathbf{w}_i\}_{i\in\mathcal{K}_{dl}}$ and $\{\mathbf{m}_i\}_{i\in\mathcal{K}_{ul}}$, must be fixed. On the other side, for the calculation of the receivers $\{\mathbf{w}_i\}_{i\in\mathcal{K}_{dl}}$ and $\{\mathbf{m}_i\}_{i\in\mathcal{K}_{ul}}$, the transmit vectors $\{\mathbf{m}_i\}_{i\in\mathcal{K}_{dl}}$ and $\{\mathbf{w}_i\}_{i\in\mathcal{K}_{ul}}$ are fixed. These two steps are done iteratively until some stop criterion is reached, such as the relative power change between iterations or a predefined maximum number

of iterations. This approach is inspired on a similar procedure presented by [33] and [57] for the MIMO sum-power minimization problem with individual SINR constraints.

In the first step of this iterative process to solve the problem in (5.1), the optimization variables are $\{\mathbf{m}_i\}_{i\in\mathcal{K}_{dl}}$ and $\{\mathbf{w}_i\}_{i\in\mathcal{K}_{ul}}$, and the problem is written as (5.3).

$$\begin{aligned}\min_{\substack{\{\mathbf{m}_i\}_{i\in\mathcal{K}_{dl}}\\ \{\mathbf{w}_i\}_{i\in\mathcal{K}_{ul}}}} \quad & \sum_{i\in\mathcal{K}_{dl}} \|\mathbf{m}_i\|_2^2 + \sum_{j\in\mathcal{K}_{ul}} \|\mathbf{w}_j\|_2^2 \\ \text{s. t.} \quad & \Gamma_k^{dl} \geq \gamma_k, \quad \forall k \in \mathcal{K}_{dl} \\ & \Gamma_k^{ul} \geq \gamma_k, \quad \forall k \in \mathcal{K}_{ul},\end{aligned} \tag{5.3}$$

This problem can be cast into a standard SOCP form or into a relaxed SDP form, and thus it can be efficiently solved by any standard convex optimization tool. The relaxed SDP formulation of the problem in (5.3) can be written as (5.4) by replacing the rank-one matrices $\mathbf{m}_i\mathbf{m}_i^H$ and $\mathbf{w}_i\mathbf{w}_i^H$ by general-rank positive semidefinite matrices $\mathbf{M}_i \succeq 0$ and $\mathbf{W}_i \succeq 0$, respectively.

$$\begin{aligned}\min_{\substack{\{\mathbf{m}_i\}_{i\in\mathcal{K}_{dl}}\\ \{\mathbf{w}_i\}_{i\in\mathcal{K}_{ul}}}} \quad & \sum_{b\in\mathcal{B}_{dl}} \mathrm{Tr}(\tilde{\mathbf{M}}_b) + \sum_{b'\in\mathcal{B}_{ul}} \mathrm{Tr}(\tilde{\mathbf{W}}_b) \\ \text{s. t.} \quad & \mathbf{w}_k^H \mathbf{H}_{b_k,k} \mathbf{D}_k \mathbf{H}_{b_k,k}^H \mathbf{w}_k \geq \sum_{b'\in\mathcal{B}_{dl}\setminus b_k} \mathbf{w}_k^H \mathbf{H}_{b',k} \tilde{\mathbf{M}}_{b'} \mathbf{H}_{b',k}^H \mathbf{w}_k \\ & + \sum_{b''\in\mathcal{B}_{ul}} \mathbf{w}_k^H \left(\sum_{i\in\mathcal{K}_{b''}} \mathbf{Q}_{i,k} \mathbf{W}_i \mathbf{Q}_{i,k}^H \right) \mathbf{w}_k + N_0, \ \forall k \in \mathcal{K}_{dl} \\ & \mathbf{m}_k^H \mathbf{U}_k \mathbf{m}_k \geq \sum_{b'\in\mathcal{B}_{dl}} \mathbf{m}_k^H \mathbf{G}_{b',b_k} \tilde{\mathbf{M}}_{b'} \mathbf{G}_{b',b_k}^H \mathbf{m}_k \\ & + \sum_{b''\in\mathcal{B}_{ul}\setminus b_k} \mathbf{m}_k^H \left(\sum_{i\in\mathcal{K}_{b''}} \mathbf{H}_{b_k,i}^H \mathbf{W}_i \mathbf{H}_{b_k,i} \right) \mathbf{m}_k + N_0, \ \forall k \in \mathcal{K}_{ul} \\ & \mathbf{M}_k \succeq 0, \quad \forall k \in \mathcal{K}_{dl} \\ & \mathbf{W}_k \succeq 0, \quad \forall k \in \mathcal{K}_{ul},\end{aligned} \tag{5.4}$$

where $\mathcal{K}_b$ denotes the set of users served by BS b and

$$\mathbf{D}_i = \frac{1}{\gamma_i}\mathbf{M}_i - \sum_{j\in\mathcal{K}_{b_i}\setminus i} \mathbf{M}_j, \tag{5.5}$$

$$\tilde{\mathbf{M}}_b = \sum_{i\in\mathcal{K}_b} \mathbf{M}_i, \tag{5.6}$$

$$\mathbf{U}_i = \frac{1}{\gamma_i}\mathbf{H}_{b_i,i}^H \mathbf{W}_i \mathbf{H}_{b_i,i} - \sum_{j\in\mathcal{K}_{b_i}\setminus i} \mathbf{H}_{b_i,j}^H \mathbf{M}_j \mathbf{H}_{b_i,j}, \tag{5.7}$$

$$\tilde{\mathbf{W}}_b = \sum_{i\in\mathcal{K}_b} \mathbf{W}_i. \tag{5.8}$$

If perfect CSI is assumed, the solution of (5.4) is shown by [60] to satisfy the rank-one requirement and the optimal $\{\mathbf{m}_i\}_{i\in\mathcal{K}_{dl}}$ and $\{\mathbf{w}_i\}_{i\in\mathcal{K}_{ul}}$ can be extracted from $\{\mathbf{M}_i\}_{i\in\mathcal{K}_{dl}}$ and $\{\mathbf{W}_i\}_{i\in\mathcal{K}_{ul}}$.

In the second step, the receive vectors are calculated. The optimal receivers $\{\mathbf{w}_i\}_{i\in\mathcal{K}_{dl}}$ and $\{\mathbf{m}_i\}_{i\in\mathcal{K}_{ul}}$ are the ones that maximize each user's SINR, and can be calculated using the MMSE approach shown in (4.7) and (4.10).

The optimality of the MMSE filter at the receiver can be verified by an analysis similar to the one presented in Chapter 4. Let us assume that during the iterative procedure to solve (5.1) we obtain the feasible set of solutions $\{\{\mathbf{m}_i(t)\}_{i\in\mathcal{K}_{dl}}, \{\mathbf{m}_j(t)\}_{j\in\mathcal{K}_{ul}}, \{\mathbf{w}_k(t)\}_{k\in\mathcal{K}_{dl}}, \{\mathbf{w}_l(t)\}_{l\in\mathcal{K}_{ul}}\}$ after the (t)th iteration, and $\{\{\mathbf{m}_i(t+1)\}_{i\in\mathcal{K}_{dl}}, \{\mathbf{m}_j(t+1)\}_{j\in\mathcal{K}_{ul}}, \{\mathbf{w}_k(t+1)\}_{k\in\mathcal{K}_{dl}}, \{\mathbf{w}_l(t+1)\}_{l\in\mathcal{K}_{ul}}\}$ after the $(t+1)$th iteration.

Thus, analyzing the SINR constraints in (5.3) after the receivers update using MMSE, we can see that they are always feasible.

Proof. $\{\mathbf{w}_i\}_{i\in\mathcal{K}_{dl}}$ and $\{\mathbf{m}_i\}_{i\in\mathcal{K}_{ul}}$ are given by the MMSE in (4.7) and (4.10), respectively, that maximizes each SINR. This way, if the tth iteration was feasible, it can be guaranteed that

$$\begin{aligned}&\Gamma_k^{dl}\left(\{\mathbf{m}_i(t)\}_{i\in\mathcal{K}_{dl}}, \{\mathbf{w}_j(t+1)\}_{j\in\mathcal{K}_{dl}}, \{\mathbf{w}_l(t)\}_{l\in\mathcal{K}_{ul}}\right) \geq \\ &\Gamma_k^{dl}\left(\{\mathbf{m}_i(t)\}_{i\in\mathcal{K}_{dl}}, \{\mathbf{w}_j(t)\}_{j\in\mathcal{K}_{dl}}, \{\mathbf{w}_l(t)\}_{l\in\mathcal{K}_{ul}}\right) \geq \gamma_k.\end{aligned} \tag{5.9}$$

$$\begin{aligned}&\Gamma_k^{ul}\left(\{\mathbf{m}_i(t)\}_{i\in\mathcal{K}_{dl}}, \{\mathbf{m}_j(t+1)\}_{j\in\mathcal{K}_{ul}}, \{\mathbf{w}_l(t)\}_{l\in\mathcal{K}_{ul}}\right) \geq \\ &\Gamma_k^{ul}\left(\{\mathbf{m}_i(t)\}_{i\in\mathcal{K}_{dl}}, \{\mathbf{w}_j(t)\}_{j\in\mathcal{K}_{dl}}, \{\mathbf{w}_l(t)\}_{l\in\mathcal{K}_{ul}}\right) \geq \gamma_k.\end{aligned} \tag{5.10}$$

Thus, $\{\{\mathbf{m}_i(t)\}_{i\in\mathcal{K}_{dl}}, \{\mathbf{m}_j(t+1)\}_{j\in\mathcal{K}_{ul}}, \{\mathbf{w}_k(t+1)\}_{k\in\mathcal{K}_{dl}}, \{\mathbf{w}_l(t)\}_{l\in\mathcal{K}_{ul}}\}$ is also a feasible set. □

The iterative Algorithm 3 is proposed to solve the problem in (5.1) and it is designed by initializing the transmit vectors using MRT or any another approach. After the initialization the algorithm performs iteratively the calculation of the receivers and transmit filters until some convergence criterion is met. This algorithm assumes a centralized processing, that requires full knowledge about channels (i.e. global CSI), precoders and decoders available at a central unit or at each BS. This requirement exists because some variables are coupled between many BSs, i.e, the precoder and selection by one node may affect the computation of the precoders from another node.

Algorithm 3 Centralized dynamic TDD MIMO beamforming.

1: Initalize the precoders $\{\mathbf{m}_i\}_{i\in\mathcal{K}_{dl}}$ and $\{\mathbf{w}_i\}_{i\in\mathcal{K}_{ul}}$.
2: **repeat**
3: Compute the receivers $\{\mathbf{w}_i\}_{i\in\mathcal{K}_{dl}}$ and $\{\mathbf{m}_i\}_{i\in\mathcal{K}_{ul}}$ according to (4.7) and (4.10).
4: Compute the precoders $\{\mathbf{m}_i\}_{i\in\mathcal{K}_{dl}}$ and $\{\mathbf{w}_i\}_{i\in\mathcal{K}_{ul}}$ according to (5.4).
5: **until** Some convergence criterion

5.3 Decentralized Approach via ADMM

In a decentralized version of Algorithm 3, the problem in (5.4) must be divided into subproblems, each solved by one transmitter, and each receiver must be calculated locally, with each node only having access to channel information from nodes in its vicinity, i.e., local CSI. Beyond that, it is required that the transmitter and receiver vectors computed at the intermediate steps can be shared via over-the-air signaling between nodes by using orthogonal pilot symbols, and some signaling must be exchanged in order to coordinate the nodes. A signaling strategy is discussed in Section 5.4.

In order to reformulate (5.4) into a distributable form, let us first introduce four new sets of real variables shown in Table 5.1, which account for the different types of inter-cell interference in each link.

Table 5.1 – Inter-cell interference sets.

Set	Inter-cell interference
$\boldsymbol{\chi} = \{\chi_{b,k}\}_{b\in\mathcal{B}_{dl},\, k\in\mathcal{K}_{dl}\setminus\mathcal{K}_b}$	DL BS to DL UE
$\boldsymbol{\psi} = \{\psi_{b,k}\}_{b\in\mathcal{B}_{dl},\, k\in\mathcal{K}_{ul}}$	DL BS to UL BS
$\Omega = \{\Omega_{l,k}\}_{l\in\mathcal{K}_{ul},\, k\in\mathcal{K}_{ul}\setminus\mathcal{K}_b}$	UL UE to UL BS
$\boldsymbol{\theta} = \{\theta_{l,k}\}_{l\in\mathcal{K}_{ul},\, k\in\mathcal{K}_{dl}}$	UL UE to DL UE

Source: Created by the author.

This way it is possible to rewrite the constraints in (5.4) in terms of $|\mathcal{B}_{dl}| + |\mathcal{K}_{ul}|$ independent convex sets

$$\begin{aligned}
\mathcal{D}_b = \Bigg\{ \Bigg(\{\mathbf{M}_i\}_{i\in\mathcal{K}_b}, \boldsymbol{\chi}^b, \boldsymbol{\psi}^b, \boldsymbol{\theta}^b, p_b \Bigg) \Bigg| \; & \mathrm{Tr}\{\tilde{\mathbf{M}}_b\} = p_b, \\
& \mathbf{w}_k^H \mathbf{H}_{b_k,k} \mathbf{D}_k \mathbf{H}_{b_k,k}^H \mathbf{w}_k \geq \sum_{b'\in\mathcal{B}_{dl}\setminus b_k} \chi_{b',k} + \sum_{l\in\mathcal{K}_{ul}} \theta_{l,k} + N_0, \; \forall k \in \mathcal{K}_b \\
& \mathbf{w}_k^H \mathbf{H}_{b,k} \tilde{\mathbf{M}}_b \mathbf{H}_{b,k}^H \mathbf{w}_k \leq \chi_{b,k}, \; \forall k \in \mathcal{K}_{dl}\setminus b \\
& \mathbf{m}_k^H \mathbf{G}_{b,b_k} \tilde{\mathbf{M}}_b \mathbf{G}_{b,b_k}^H \mathbf{m}_k \leq \psi_{b,k}, \; \forall k \in \mathcal{K}_{ul} \\
& \mathbf{M}_k \geq 0, \; \forall k \in \mathcal{K}_b \Bigg\}, \quad \forall b \in \mathcal{B}_{dl},
\end{aligned} \tag{5.11}$$

$$\begin{aligned}
\mathcal{U}_l = \Bigg\{ \Bigg(\mathbf{W}_l, \Omega^l, \boldsymbol{\psi}^l, \boldsymbol{\theta}^l, p_l \Bigg) \Bigg| \; & \mathrm{Tr}\{\mathbf{W}_l\} = p_l, \\
& \frac{1}{\gamma_l} \mathbf{m}_l^H \mathbf{H}_{b_l,l}^H \mathbf{W}_l \mathbf{H}_{b_l,l} \mathbf{m}_l \geq \sum_{b\in\mathcal{B}_{dl}} \psi_{b,l} + \sum_{l'\in\mathcal{K}_{ul}\setminus l} \Omega_{l',l} + N_0, \\
& \mathbf{w}_k^H \mathbf{Q}_{l,k} \mathbf{W}_l \mathbf{Q}_{l,k}^H \mathbf{w}_k \leq \theta_{l,k}, \; \forall k \in \mathcal{K}_{dl} \\
& \mathbf{m}_k^H \mathbf{H}_{b_k,l}^H \mathbf{W}_l \mathbf{H}_{b_k,l} \mathbf{m}_k \leq \Omega_{l,k}, \; \forall k \in \mathcal{K}_{ul}\setminus l \\
& \mathbf{W}_l \geq 0, \Bigg\}, \quad \forall l \in \mathcal{K}_{ul},
\end{aligned} \tag{5.12}$$

where p_b is an auxiliary variable that accounts for the total power used by the transmission in cell b and the cell specific non-negative inter-cell interference sets are defined as indicated in Table 5.2.

Table 5.2 – BS b Inter-cell interference sets.

$b \in \mathcal{B}_{dl}$	$\boldsymbol{\chi}^b = \{\chi_{b,i}, \chi_{b',i'}\}_{i\in\mathcal{K}_{dl}\setminus\mathcal{K}_b,\, b'\in\mathcal{B}_{dl}\setminus b, i'\in\mathcal{K}_b}$ $\boldsymbol{\psi}^b = \{\psi_{b,i}\}_{i\in\mathcal{K}_{ul}}$ $\boldsymbol{\theta}^b = \{\theta_{l,i}\}_{l\in\mathcal{K}_{ul},\, i\in\mathcal{K}_b}$
$l \in \mathcal{K}_{ul}$	$\Omega^l = \{\Omega_{l,i}, \Omega_{l',l}\}_{i\in\mathcal{K}_{ul}\setminus l, l'\in\mathcal{K}_{ul}\setminus l}$ $\boldsymbol{\psi}^l = \{\psi_{b,l}\}_{b\in\mathcal{B}_{dl}}$ $\boldsymbol{\theta}^l = \{\theta_{l,i}\}_{i\in\mathcal{K}_{dl}}$

Source: Created by the author.

For each of these node specific interference terms there is are linear mapping matrices $\mathbf{P}_i^{\chi}$, $\mathbf{P}_i^{\Omega}$, $\mathbf{P}_i^{\theta}$ and $\mathbf{P}_i^{\psi} \in \{0,1\}$ such that $\boldsymbol{\chi}^i = \mathbf{P}_i^{\chi}\boldsymbol{\chi}$, $\Omega^i = \mathbf{P}_i^{\Omega}\Omega$, $\boldsymbol{\theta}^i = \mathbf{P}_i^{\theta}\boldsymbol{\theta}$ and $\boldsymbol{\psi}^i = \mathbf{P}_i^{\psi}\boldsymbol{\psi}$ $\forall i \in \mathcal{B}_{dl}\cup\mathcal{K}_{ul}$. This way it is possible to rewrite the problem in (5.4) as

$$\min_{\substack{\boldsymbol{\chi}^b,\Omega^l,\boldsymbol{\theta}^i \\ \boldsymbol{\psi}^i,\boldsymbol{\chi},\Omega,\boldsymbol{\theta},\boldsymbol{\psi},p_i \\ \{\mathbf{M}_i\}_{i\in\mathcal{K}_{dl}},\{\mathbf{W}_i\}_{i\in\mathcal{K}_{ul}}}} \sum_{i\in\mathcal{B}_{dl}\cup\mathcal{K}_{ul}} p_i \tag{5.13}$$

$$\begin{aligned}
\text{s. t.} \quad & \left(\{\mathbf{M}_i\}_{i\in\mathcal{K}_b}, \boldsymbol{\chi}^b, \boldsymbol{\psi}^b, \boldsymbol{\theta}^b, p_b\right) \in \mathcal{D}_b,\ \forall b \in \mathcal{B}_{dl} \\
& \left(\mathbf{W}_l, \Omega^l, \boldsymbol{\psi}^l, \boldsymbol{\theta}^l, p_l\right) \in \mathcal{U}_l,\ \forall l \in \mathcal{K}_{ul} \\
& \boldsymbol{\chi}^b = \mathbf{P}_b^{\chi}\boldsymbol{\chi},\ \forall b \in \mathcal{B}_{dl} \\
& \Omega^l = \mathbf{P}_l^{\Omega}\Omega,\ \forall l \in \mathcal{K}_{ul} \\
& \boldsymbol{\theta}^i = \mathbf{P}_i^{\theta}\boldsymbol{\theta},\ i \in \mathcal{B}_{dl}\cup\mathcal{K}_{ul} \\
& \boldsymbol{\psi}^i = \mathbf{P}_i^{\psi}\boldsymbol{\psi},\ i \in \mathcal{B}_{dl}\cup\mathcal{K}_{ul}.
\end{aligned}$$

The ADMM solutions consider an equivalent penalty augmented formulation of the problem in (5.13) that can be written as,

$$
\begin{aligned}
\min_{\substack{\boldsymbol{\chi}^b,\Omega^l,\boldsymbol{\theta}^i,p_i \\ \boldsymbol{\psi}^i,\boldsymbol{\chi},\Omega,\boldsymbol{\theta},\boldsymbol{\psi},\boldsymbol{\rho}_i \\ \{\mathbf{M}_i\}_{i\in\mathcal{K}_{dl}} \\ \{\mathbf{W}_i\}_{i\in\mathcal{K}_{ul}}}} & \left\{ \begin{array}{l} \left(\displaystyle\sum_{i\in\mathcal{B}_{dl}\cup\mathcal{K}_{ul}} p_i + \frac{c}{2}\sum_{b\in\mathcal{B}_{dl}} \|\mathbf{P}_b^{\chi}\boldsymbol{\chi}-\boldsymbol{\chi}^b\|^2 + \right. \\ \frac{c}{2}\displaystyle\sum_{l\in\mathcal{K}_{ul}} \|\mathbf{P}_l^{\Omega}\Omega-\Omega^l\|^2 + \frac{c}{2}\sum_{i\in\mathcal{B}_{dl}\cup\mathcal{K}_{ul}} \|\mathbf{P}_i^{\theta}\boldsymbol{\theta}-\boldsymbol{\theta}^b\|^2 \\ \left. + \frac{c}{2}\displaystyle\sum_{i\in\mathcal{B}_{dl}\cup\mathcal{K}_{ul}} \|\mathbf{P}_i^{\psi}\boldsymbol{\psi}-\boldsymbol{\psi}^i\|^2 + \frac{c}{2}\sum_{i\in\mathcal{B}_{dl}\cup\mathcal{K}_{ul}} (\rho_i-p_i)^2 \right) \end{array} \right\} \\
\text{s. t.} \quad & \left(\{\mathbf{M}_i\}_{i\in\mathcal{K}_b},\boldsymbol{\chi}^b,\boldsymbol{\psi}^b,\boldsymbol{\theta}^b,p_b\right) \in \mathcal{D}_b,\ \forall b\in\mathcal{B}_{dl} \\
& \left(\mathbf{W}_l,\Omega^l,\boldsymbol{\psi}^l,\boldsymbol{\theta}^l,p_l\right) \in \mathcal{U}_l,\ \forall l\in\mathcal{K}_{ul} \\
& \boldsymbol{\chi}^b = \mathbf{P}_b^{\chi}\boldsymbol{\chi},\ \forall b\in\mathcal{B}_{dl} \\
& \Omega^l = \mathbf{P}_l^{\Omega}\Omega,\ \forall l\in\mathcal{K}_{ul} \\
& \boldsymbol{\theta}^i = \mathbf{P}_i^{\theta}\boldsymbol{\theta},\ i\in\mathcal{B}_{dl}\cup\mathcal{K}_{ul} \\
& \boldsymbol{\psi}^i = \mathbf{P}_i^{\psi}\boldsymbol{\psi},\ i\in\mathcal{B}_{dl}\cup\mathcal{K}_{ul} \\
& p_i = \rho_i,\ i\in\mathcal{B}_{dl}\cup\mathcal{K}_{ul},
\end{aligned}
\tag{5.14}
$$

where $c \geq 0$ is the penalty parameter and $\rho_i \geq 0$, $i \in \mathcal{B}_{dl} \cup \mathcal{K}_{ul}$ are slack variables introduced in order to impose the power penalty parameter term. The problem in (5.14) is equivalent to (5.13), but the addition of the penalty parameters lead to better convergence stability.

The ADMM solution consists of three iterative steps: 1) update of the local primal variables $\boldsymbol{\chi}^b, \Omega^l, \boldsymbol{\theta}^i, \boldsymbol{\psi}^i, p_i$; 2) update of the global primal variables $\boldsymbol{\chi}, \Omega, \boldsymbol{\theta}, \boldsymbol{\psi}, \boldsymbol{\rho}$ and 3) update of the dual variables related to each interference constraint in (5.14) $\boldsymbol{\lambda}_b^{\chi}, \boldsymbol{\lambda}_l^{\Omega}, \boldsymbol{\lambda}_i^{\theta}, \boldsymbol{\lambda}_i^{\psi}, \lambda_i^{\rho}$.

The local variables update at iteration $(t+1)$ is given by the argument of the minimization of the augmented Lagrangian of (5.14) and is given for each DL BS b as

$$
\begin{aligned}
&\{\boldsymbol{\chi}^b(t+1),\boldsymbol{\theta}^b(t+1),\boldsymbol{\psi}^b(t+1),p_b(t+1)\} = \\
&\arg\min_{\substack{\boldsymbol{\chi}^b,\boldsymbol{\theta}^b \\ \boldsymbol{\psi}^b,p_b \\ \{\mathbf{M}_i\}_{i\in\mathcal{K}_b}}} \left\{ \begin{array}{l} \left(p_b + \frac{c}{2}\|\mathbf{P}_b^{\chi}\boldsymbol{\chi}(t)-\boldsymbol{\chi}^b\|^2 + \frac{c}{2}\|\mathbf{P}_b^{\theta}\boldsymbol{\theta}(t)-\boldsymbol{\theta}^b\|^2 + \right. \\ \frac{c}{2}\|\mathbf{P}_b^{\psi}\boldsymbol{\psi}(t)-\boldsymbol{\psi}^b\|^2 + \frac{c}{2}(\rho_b(t)-p_b)^2 - \boldsymbol{\lambda}_b^{\chi T}(t)\boldsymbol{\chi}^b \\ \left. - \boldsymbol{\lambda}_b^{\theta T}(t)\boldsymbol{\theta}^b - \boldsymbol{\lambda}_b^{\psi T}(t)\boldsymbol{\psi}^b - \lambda_b^{\rho}(t)p_b \right) \end{array} \right\} \\
&\qquad \text{s. t.} \quad \left(\{\mathbf{M}_i\}_{i\in\mathcal{K}_b},\boldsymbol{\chi}^b,\boldsymbol{\psi}^b,\boldsymbol{\theta}^b,p_b\right) \in \mathcal{D}_b,
\end{aligned}
\tag{5.15}
$$

and for each UL UE l as

$$\begin{aligned}
&\{\Omega^l(t+1), \boldsymbol{\theta}^l(t+1), \boldsymbol{\psi}^l(t+1), p_l(t+1)\} = \\
&\underset{\substack{\Omega^l, \boldsymbol{\theta}^l \\ \boldsymbol{\psi}^l, p_l \\ \mathbf{W}_l}}{\arg\min} \left\{ \begin{array}{l} \left(p_l + \frac{c}{2} \|\mathbf{P}_l^{\chi} \Omega(t) - \Omega^l\|^2 + \frac{c}{2} \|\mathbf{P}_l^{\theta} \boldsymbol{\theta}(t) - \boldsymbol{\theta}^l\|^2 + \right. \\ \left. \frac{c}{2} \|\mathbf{P}_l^{\psi} \boldsymbol{\psi}(t) - \boldsymbol{\psi}^l\|^2 + \frac{c}{2} (\rho_l(t) - p_l)^2 - \boldsymbol{\lambda}_l^{\Omega^T}(t) \Omega^l \right\} \\ \left. - \boldsymbol{\lambda}_l^{\theta^T}(t) \boldsymbol{\theta}^l - \boldsymbol{\lambda}_l^{\psi^T}(t) \boldsymbol{\psi}^l - \lambda_l^{\rho}(t) p_l \right) \end{array} \right. \\
&\qquad \text{s. t.} \quad \left(\mathbf{W}_l, \Omega^l, \boldsymbol{\psi}^l, \boldsymbol{\theta}^l, p_l \right) \in \mathcal{U}_l, \forall l \in \mathcal{K}_{ul},
\end{aligned} \tag{5.16}$$

The global variables update is also given by the argument of the minimization of the augmented Lagrangian of (5.14), which has closed form solution given as

$$\boldsymbol{\chi}(t+1) = \mathbf{P}_{\chi}{}^{\dagger} \left(\tilde{\boldsymbol{\chi}}(t+1) - \frac{1}{c} \tilde{\boldsymbol{\lambda}}_{\chi}(t) \right), \tag{5.17}$$

$$\Omega(t+1) = \mathbf{P}_{\Omega}{}^{\dagger} \left(\tilde{\Omega}(t+1) - \frac{1}{c} \tilde{\boldsymbol{\lambda}}_{\Omega}(t) \right), \tag{5.18}$$

$$\boldsymbol{\theta}(t+1) = \mathbf{P}_{\theta}{}^{\dagger} \left(\tilde{\boldsymbol{\theta}}(t+1) - \frac{1}{c} \tilde{\boldsymbol{\lambda}}_{\theta}(t) \right), \tag{5.19}$$

$$\boldsymbol{\psi}(t+1) = \mathbf{P}_{\psi}{}^{\dagger} \left(\tilde{\boldsymbol{\psi}}(t+1) - \frac{1}{c} \tilde{\boldsymbol{\lambda}}_{\psi}(t) \right), \tag{5.20}$$

$$\rho_b(t+1) = p_b(t+1) - \frac{1}{c} \lambda_{\psi}(t), \forall b, \tag{5.21}$$

where $(.)^{\dagger}$ represents the pseudoinverse operation, $\mathbf{P}_{\chi} = [\mathbf{P}_1^{\chi^T}, \ldots, \mathbf{P}_B^{\chi^T}]^T$, $\tilde{\boldsymbol{\chi}} = [\boldsymbol{\chi}^{1^T}, \ldots, \boldsymbol{\chi}^{B^T}]^T$, $\tilde{\boldsymbol{\lambda}}_{\chi} = [\boldsymbol{\lambda}_1^{\chi^T}, \ldots, \boldsymbol{\lambda}_B^{\chi^T}]^T$ and the other variables are defined similarly.

The last step is the update of the dual variables, that can be expressed as

$$\boldsymbol{\lambda}_b^{\chi}(t+1) = \boldsymbol{\lambda}_b^{\chi}(t) + c(\boldsymbol{P}_b^{\chi} \boldsymbol{\chi}(t+1) - \boldsymbol{\chi}^b(t+1)), \tag{5.22}$$

$$\boldsymbol{\lambda}_l^{\Omega}(t+1) = \boldsymbol{\lambda}_l^{\Omega}(t) + c(\boldsymbol{P}_l^{\Omega} \Omega(t+1) - \Omega^l(t+1)), \tag{5.23}$$

$$\boldsymbol{\lambda}_i^{\theta}(t+1) = \boldsymbol{\lambda}_i^{\theta}(t) + c(\boldsymbol{P}_i^{\theta} \boldsymbol{\theta}(t+1) - \boldsymbol{\theta}^i(t+1)), \tag{5.24}$$

$$\boldsymbol{\lambda}_i^{\psi}(t+1) = \boldsymbol{\lambda}_i^{\psi}(t) + c(\boldsymbol{P}_i^{\psi} \boldsymbol{\psi}(t+1) - \boldsymbol{\psi}^i(t+1)), \tag{5.25}$$

$$\lambda_i^{\rho}(t+1) = \lambda_i^{\rho}(t) + c(\rho_i(t+1) - p_i(t+1)). \tag{5.26}$$

The second step of the ADMM solution can be further simplified by noticing that a specific node does not need to compute all the elements of the global variables, since the other two ADMM steps only use these global variables multiplied by the linear mapping matrices of each node, i.e. each node only requires the elements of the global variables that have information about interference related to itself. This way, each of the global variables elements can be computed at as

$$\chi_{b,i}(t+1) = \frac{1}{2}\left(\chi^{b}_{b,i}(t+1) - \frac{1}{c}\lambda^{\chi_{b,i}}_{b}(t)\right) + \frac{1}{2}\left(\chi^{b_i}_{b,i}(t+1) - \frac{1}{c}\lambda^{\chi_{b,i}}_{b_i}(t)\right), \tag{5.27}$$

$$\Omega_{l,i}(t+1) = \frac{1}{2}\left(\Omega^{l}_{l,i}(t+1) - \frac{1}{c}\lambda^{\Omega_{l,i}}_{l}(t)\right) + \frac{1}{2}\left(\Omega^{i}_{l,i}(t+1) - \frac{1}{c}\lambda^{\Omega_{l,i}}_{i}(t)\right), \tag{5.28}$$

$$\theta_{l,i}(t+1) = \frac{1}{2}\left(\theta^{l}_{l,i}(t+1) - \frac{1}{c}\lambda^{\theta_{l,i}}_{l}(t)\right) + \frac{1}{2}\left(\theta^{i}_{l,i}(t+1) - \frac{1}{c}\lambda^{\theta_{l,i}}_{i}(t)\right), \tag{5.29}$$

$$\psi_{b,i}(t+1) = \frac{1}{2}\left(\psi^{b}_{b,i}(t+1) - \frac{1}{c}\lambda^{\psi_{b,i}}_{b}(t)\right) + \frac{1}{2}\left(\psi^{i}_{b,i}(t+1) - \frac{1}{c}\lambda^{\psi_{b,i}}_{i}(t)\right). \tag{5.30}$$

By using this approach, each node only needs to have access to the result of the local expression of the coupled nodes in order to calculate the global variables that are necessary to it. For example, BS b needs to have access to the result of the expression $(\chi^{b_i}_{b,i}(t+1) - \frac{1}{c}\lambda^{\chi_{b,i}}_{b_i}(t))$ computed locally at BS b_i, in order to compute $\chi_{b,i}$.

Thus, a decentralized version of Algorithm 3 can be written as the Algorithm 4.

Algorithm 4 Distributed dynamic TDD MIMO SPmin.

Initialize $\boldsymbol{\chi}$, Ω, $\boldsymbol{\theta}$, $\boldsymbol{\psi}$ and $\boldsymbol{\rho}$.
BS $b, \forall b \in \mathcal{B}_{dl}$: Initialize DL precoders $\{\mathbf{m}_i\}_{i\in\mathcal{K}_b}$.
UE $l, \forall l \in \mathcal{K}_{ul}$: Initialize UL precoders $\mathbf{w}_l$.
repeat
    BS $b, \forall b \in \mathcal{B}_{dl}$: Use $\{\mathbf{m}_i\}_{i\in\mathcal{K}_b}$ to transmit pilots
    UE $l, \forall l \in \mathcal{K}_{ul}$: Use $\mathbf{w}_l$ to transmit pilots.
    BS $b, \forall b \in \mathcal{B}_{ul}$: Compute $\{\mathbf{m}_i\}_{i\in\mathcal{K}_b}$ (4.10) and send precoded pilots.
    UE $k, \forall k \in \mathcal{K}_{dl}$: Compute $\mathbf{w}_k$ (4.7) and send precoded pilots.
    repeat
        BS $b, \forall b \in \mathcal{B}_{dl}$: Compute $\boldsymbol{\chi}^b, \boldsymbol{\theta}^b, \boldsymbol{\psi}^b$ and p_b (5.15).
        UE $l, \forall l \in \mathcal{K}_{ul}$: Compute $\Omega^l, \boldsymbol{\theta}^l, \boldsymbol{\psi}^l$ and p_l (5.16).
        BS $b, \forall b \in \mathcal{B}_{dl}$ and UE $l, \forall l \in \mathcal{K}_{ul}$: Share the values of $(primal_{local} - \frac{1}{c}dual_{local})$ with the coupled nodes.
        BS $b, \forall b \in \mathcal{B}_{dl}$ and UE $l, \forall l \in \mathcal{K}_{ul}$: Update its global variables terms in $\boldsymbol{\chi}$, Ω, $\boldsymbol{\theta}$, $\boldsymbol{\psi}$ and $\boldsymbol{\rho}$ (5.27) to (5.30) and (5.21).
        BS $b, \forall b \in \mathcal{B}_{dl}$: Update the dual variables $\boldsymbol{\lambda}^{\chi}_b, \boldsymbol{\lambda}^{\theta}_b, \boldsymbol{\lambda}^{\psi}_b$ and λ^{ρ}_b (5.22) to (5.26)
        UE $l, \forall l \in \mathcal{K}_{ul}$: Update the dual variables $\boldsymbol{\lambda}^{\Omega}_l, \boldsymbol{\lambda}^{\theta}_l, \boldsymbol{\lambda}^{\psi}_l$ and λ^{ρ}_l (5.22) to (5.26).
    until Some stop criterion
    BS $b, \forall b \in \mathcal{B}_{dl}$: Solve (5.15) for $\{\mathbf{M}_i\}_{i\in\mathcal{K}_b}$.
    UE $l, \forall l \in \mathcal{K}_{ul}$: Solve (5.16) for $\{\mathbf{W}_l\}$.
until Some stop criterion.

5.4 Signaling and Practical Considerations

For the decentralized approach we consider that each node only has access to local CSI, however, information still needs to be shared between the nodes, in order to coordinate

Figure 5.1 – Frame structure for Algorithm 4.

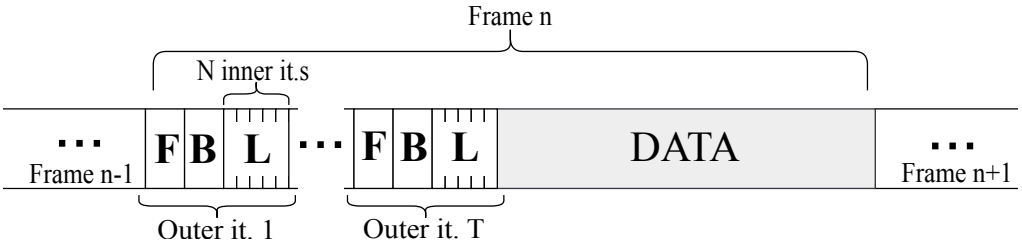

Source: Created by the author.

them. Algorithm 4 relies on two types of information sharing, over-the-air pilot signaling and local primal variables sharing. Figure 5.1 shows the proposed frame structure based on [47].

The frame is divided in two main parts, the beamforming setup and the data transmission in both directions. During the beamforming setup, the over-the-air signaling is denoted by the letter F, for the forward (transmitters to receivers) pilot signaling, corresponding to step 4 in Algorithm 4, and B for the backward (receivers to transmitters) pilot signaling, corresponding to step 5. We consider that all nodes use known orthogonal precoded pilot symbols, allowing perfect signal separation and estimation of effective channels, and consequently perfect estimation of the precoders and decoders by the opposite nodes.

The local primal variables sharing, denoted by the letter L, which occurs in step 8, is proposed to take place via both backhaul and over-the-air control channel, since information needs to be shared among all transmitting nodes (DL BSs and UL UEs). This way, all BSs must share their information by using the backhaul and each UL UE must send its data to its respective BS, and receive the updates from the other nodes also hearing from its BS. This signaling scheme is shown in Figure 5.2.

Figure 5.2 – Local variables signaling strategy.

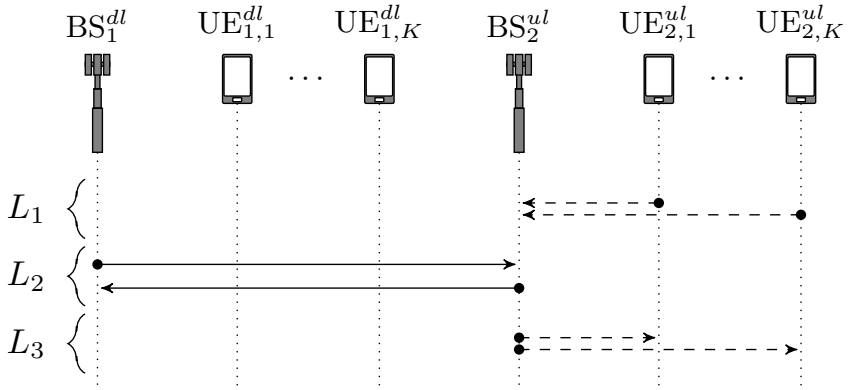

Source: Created by the author.

In this procedure, the UL UE information about its local variables (Ω^l, $\boldsymbol{\psi}^l$ and $\boldsymbol{\theta}^l$) must be sent, in time L_1, by each UL UE to its respective BS, thus, a total of $2(|\mathcal{K}_{ul}|-1)+|\mathcal{B}_{dl}|+|\mathcal{K}_{dl}|$ scalars to be sent per UE. In Time L_2 each DL BS sends the information about its local variables

($\boldsymbol{\chi}^b, \boldsymbol{\psi}^b$ and $\boldsymbol{\theta}^b$) to the coupled BSs, with a total of $2(|\mathcal{K}_{dl}| - |\mathcal{K}_b|) + |\mathcal{K}_{ul}| + |\mathcal{K}_{ul}||\mathcal{K}_b|$ scalars per DL BS, and the UL BSs sends the terms from its users to each coupled BS. In time L_3 the UL BSs send to each of its UEs the other nodes variables.

In a centralized approach, if we assume that each BS exchanges its local CSI with all other BSs via backhaul at setup time, an estimative of the total number of real valued scalars required to be sent is $2KN_bN_u(B-1)B + 2|\mathcal{B}_{dl}|N_b^2(B-1)|\mathcal{B}_{ul}| + 2K_b^2|\mathcal{B}_{ul}|N_u^2(B-1)|\mathcal{B}_{dl}|$, with each term being related to the exchange of the channels $\mathbf{H}$, $\mathbf{G}$ and $\mathbf{Q}$, respectively. Besides that, the calculated precoders and decoders must still be sent to their respective nodes. Table 5.3 shows a comparison of the amount of signaling for centralized and decentralized applications, and it can be seen that the the decentralized algorithm requires much less signaling per iteration than the total centralized load, and this difference increases with the increase of the network dimensions.

Table 5.3 – Signaling load.

$\{B_{ul}, B_{dl}, K_b, N_b, N_u\}$	Centralized	Decentralized per it.
$\{2,2,2,6,3\}$	5184	90 (1.54%)
$\{3,3,2,8,4\}$	34560	192 (0.56%)
$\{4,4,2,10,5\}$	131600	320 0.24%)

Source: Created by the author.

The number of Foward-Backward and local variables sharing stages is determined by the number of outer and inner iterations in the Algorithm 4. At each outer iteration a Foward-Backward step is performed and at each inner iteration the local variables sharing takes place. In order to achieve the same solution as the centralized case, the Algorithm 4 must iterate until convergence. However, approximate solutions can be extracted at intermediate iterations, at the cost of suboptimal sum-power and SINR. Thus, the signaling load can be controlled by fixing the number of inner and outer iterations, at the cost of suboptimal performance. However, simulation results show that very close to optimal performance can be obtained with small numbers of iterations.

Beyond that, since the ADMM solution does not require that the local variables be equal to the global ones before convergence, an intermediate solution may not fulfil all the SINR contraints. However, a solution that strictly respects the minimum SINR constraints can be obtained by solving (5.15) and (5.16) including to the problem a constraint to force the local variables to be equal to the global ones. In this situation feasibility is not always guaranteed, and when infeasibility is declared in an iteration, the algorithm is required to iterate more in order to reach a possible feasible solution.

Another interesting feature of the ADMM decentralized solution is that it can converge, or at least provide approximate solutions, even when the centralized solution is infeasible. This happens, because the centralized solution requires feasibility in all iterations, so, for example, if the first iteration is not feasible, then the centralized algorithm fails to provide a solution. On the other hand, since ADMM does not require feasibility at all iterations, it can

Figure 5.3 – SINR comparison.

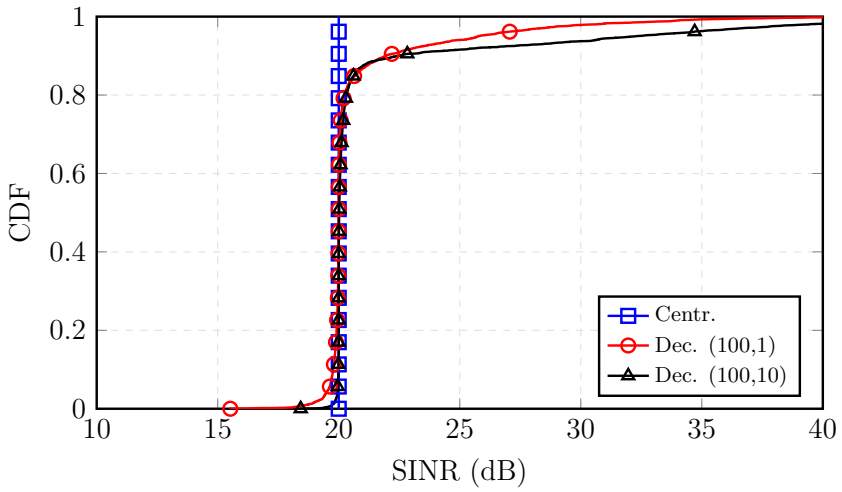

Source: Created by the author.

converge or provide good solutions in far more situations.

5.5 Results

The simulation scenario is formed by 4 cells (2 DL, 2 UL) with 100 m radius each, and 2 UEs per cell. Each BS has 6 antennas and each UE has 3 antennas. This scenario is considered for its simplicity and presents all types of intra-cell and inter-cell interference link. We consider a flat Rayleigh fading scenario with uncorrelated channels, in which each element of the channels is an i.i.d. complex Gaussian random variable with zero mean and unit variance, the pathloss model is based on [39] and it is detailed in Table 4.2, and the required SINR for all users is 20 dB. The simulation results shown are obtained after 500 Monte-Carlo snapshots.

In Figure 5.3, we compare the SINR obtained by all users, by analysing the CDF plot for the centralized algorithm, and for the decentralized algorithm after 100 outer iterations, with 1 and 10 inner iterations. The coordinate pair in the legend show the number of outer and inner iterations, respectively. It can be seen that the centralized algorithm attains the required SINR in all feasible cases, while the decentralized algorithms approximate this value allowing some variation from the target, but mainly with SINR values greater than the minimum. We can also see that the decentralized approach with more inner iterations tends to better fulfill the minimum required SINR, but both decentralized curves achieve a good approximation of the required values. Furthermore, the minimum SINR can still be attained by forcing the local variables to be equal to the global ones.

Figure 5.4 compares the transmit power for the same three approaches. It can be seen that the centralized one obtains the lowest power, but the decentralized algorithm approximates it well, and they obtain a very close outcome. It can also be seen that the decentralized approach with 1 inner iteration achieved smaller power than the approach with 10 inner iterations. This

Figure 5.4 – Power comparison.

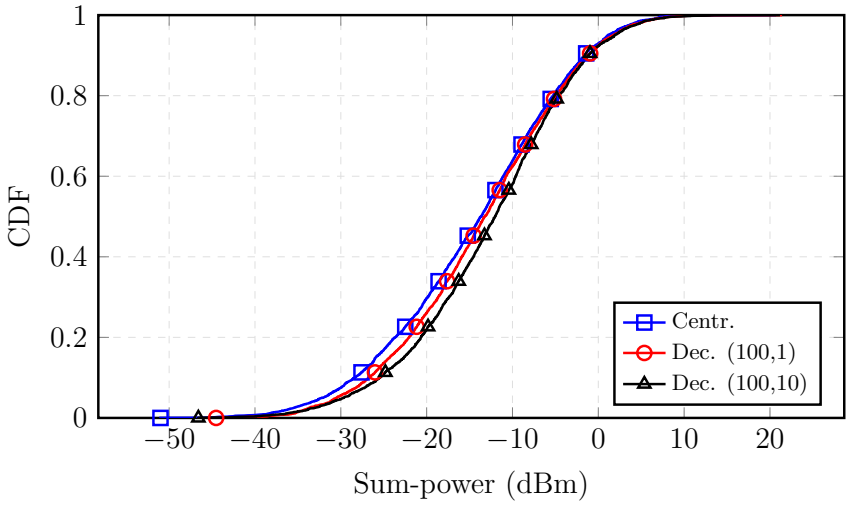

Source: Created by the author.

Figure 5.5 – Power convergence.

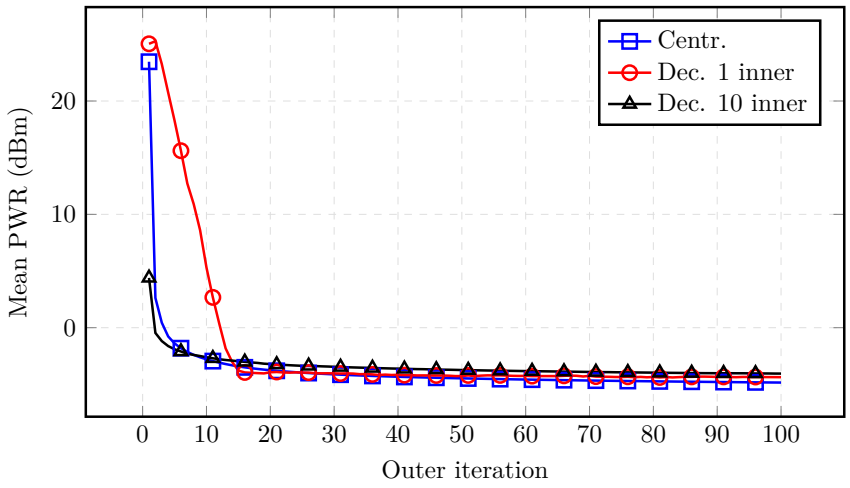

Source: Created by the author.

can happen since the decentralized algorithm does not require the SINR bound to be strictly attained, so if the SINR obtained by the decentralized with 1 inner iteration is smaller, then the power can also be. However, both of them still approximate well the centralized curve.

To show the convergence for the proposed algorithms, Figure 5.5 shows the mean transmit power after each step of the centralized algorithm and after each outer step for the decentralized one. It can be seen that all approaches iterate in direction to a very close minimum power point, and that up from the 15th iteration all algorithms already obtain a good approximation of the optimum value. The centralized algorithm converges to the smallest power, as expected, and the decentralized approach with 1 inner iteration seems to be slower at the very initial iterations, but it provided the best final approximation, while the approach with 10 inner iterations obtains the smallest power at the initial iterations, but afterwards, its convergence saturates.

Figure 5.6 – SINR convergence, 1 inner iteration.

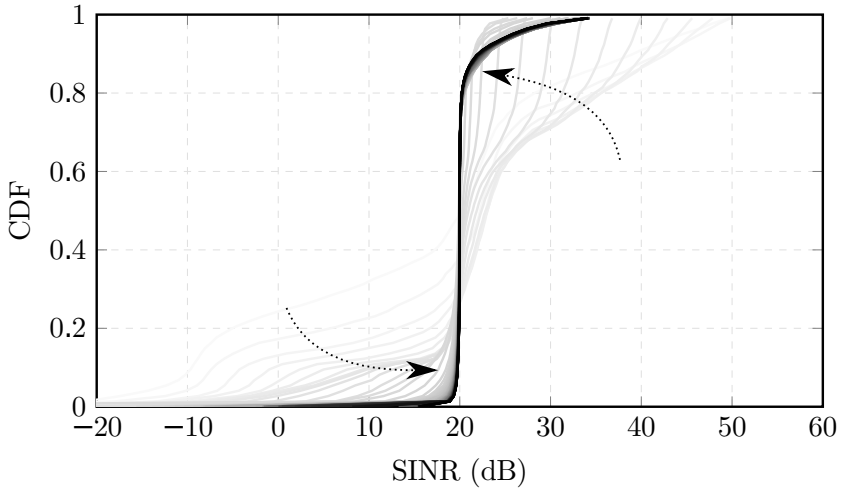

Source: Created by the author.

Figure 5.7 – SINR convergence, 10 inner iterations.

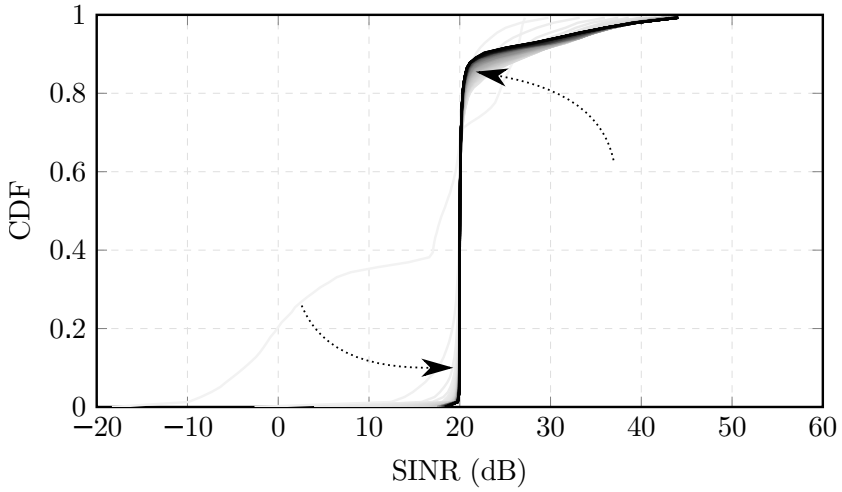

Source: Created by the author.

For the decentralized algorithms it is also important to show how the SINR behaves at each iteration, and how it converges to the required value, since the ADMM solution does not guarantee that the SINR constraints are respected at all iterations. For this reason, we show for both cases in figures 5.6 and 5.7, with 1 and 10 inner iterations, curves that show the CDF of the SINRs at each outer iteration. The plot is shown in a gray-scale, in which the initial iterations are shown in light gray, and the final iterations are the dark gray. The arrows indicate the main convergence directions.

From 5.6 and 5.7, we see that as the algorithm iterates the variance of the SINR values is reduced and the results go in the direction of the desired value (20 dB). It can also be seen that the approach with more inner iterations shows faster approximation of the minimum required SINR, while the approach with 1 inner iteration takes more iterations to approximate the target. However, both approaches required less than 15 iterations to achieve a good approximation.

5.6 Conclusions

In this chapter, we proposed a Beamforming solution for Dynamic TDD Networks, which guarantees a minimum SINR for each link while minimizing the total transmitter Sum-power. Two solutions were presented, a centralized version that requires full CSI, and a decentralized version based on ADMM that requires local CSI and a lightweight signaling procedure. It is shown that both approaches converge to the same solution, and that the decentralized one can approximate the optimal solution with a reduced amount of iterations. Thus, by using this approach, the higher interference in Dynamic TDD can be overcome, since users can have guaranteed their SINR requirements.

6 CONCLUSIONS AND FUTURE WORK

In this master's thesis we have presented ways to deal with interference in dense scenarios. More specifically we have studied solutions based on coordinated sum-power minimization beamforming for large-scale optimization and for Dynamic TDD scenarios. In order to better solve these problems we used the ADMM and primal decomposition methods described in Chapter 2.

Chapter 3 presented an ADMM based solution for the coordinated bemforming optimization with a large number of variables. We used simulations to compare it to a well known SDP solution and analyzed the convergence behavior for a variety of scenarios. The simulation results showed that the ADMM solution provided much faster convergence with modest accuracy, however it could not be faster than SDP with high accuracy requirements. We also presented results on the convergence by analyzing the duality gap, these results also illustrated how ADMM solution converges faster with modest accuracy.

Chapter 4 proposed a coordinated beamforming problem for Dynamic TDD MIMO networks which minimizes the transmit sum-power while guaranteeing a minimum SINR for DL users and limits the BS to BS interference power. We derived two solutions for this problem, one centralized and one decentralized based on primal decomposition, which required local CSI and a lightweight over-the-air and backhaul signaling infrastructure. We showed that the decentralized solution iterates towards the same solution as the centralized one. However, feasible solutions can be obtained at each intermediate iteration, at the cost of suboptimal power. The presented solutions show that the UL capacity can be improved by applying the BS to BS interference constraint while a minimum DL SINR target is guaranteed, at the cost of increased DL power consumption. Convergence results show that with more inner and outer iterations the decentralized algorithm achieves solutions closer to the centralized one.

Chapter 5 proposed another coordinated beamforming problem for Dynamic TDD MIMO networks, which aims to minimize the transmit power while guaranteeing a minimum SINR threshold for both DL and UL users. Two solutions were presented, a centralized and a decentralized based on ADMM, which requires local CSI and lightweight backhaul and over-the-air signaling scheme. We show that both solutions can satisfy the SINR requirements and achieve values close to the minimum power. We also show that the decentralized solution iterates towards the centralized one and that signaling load can be controlled by fixing the number of iterations at the cost of close to optimal power and SINR performance.

In summary, this work presented relevant results related to interference management in 5G dense scenarios regarding large-scale optimization and Dynamic TDD. Nevertheless, there are still extensions and several open issues to be investigated by further works in this area, such as:

- The study of the parallel implementation of the large-scale ADMM algorithms, in order to speed up even more the optimization by using multiple BBUs to compute the bemforming.
- The search for large-scale optimization methods that can provide fast convergence also when high accuracy is needed.
- The study of robust methods to perform the beamforming in Dynamic TDD scenarios considering CSI imperfections.
- The analysis of the joint application of dense networks and other 5G technologies such as massive MIMO and millimeter waves, mainly regarding Dynamic TDD interference management techniques.
- The search for other beamforming solutions for Dynamic TDD MIMO systems using objectives other than sum-power minimization.

BIBLIOGRAPHY

1 ERICSSON. **Ericsson mobility report**. [S.l.], June 2015. Available from: http://www.ericsson.com/res/docs/2015/ericsson-mobility-report-june-2015.pdf.

2 SOLDANI, D.; MANZALINI, A. Horizon 2020 and beyond: on the 5G operating system for a true digital society. **IEEE Vehicular Technology Magazine**, v. 10, n. 1, p. 32–42, Mar. 2015. ISSN 1556-6072.

3 ERICSSON. **5G radio access: tecnologies and capabilities**. [S.l.], Feb. 2015. Available from: http://www.ericsson.com/res/docs/whitepapers/wp-5g.pdf.

4 BHUSHAN, N. et al. Network densification: the dominant theme for wireless evolution into 5G. **IEEE Communications Magazine**, IEEE, v. 52, n. 2, p. 82–89, 2014.

5 NOKIA. **5G radio access: system design aspects**. [S.l.], Jan. 2015. Available from: http://www.networks.nokia.com/file/37611/5g-radio-access.

6 RAPPAPORT, T. S. et al. Millimeter wave mobile communications for 5G cellular: it will work! **IEEE Access**, v. 1, p. 335–349, 2013. ISSN 2169-3536.

7 NIU, Y. et al. A survey of millimeter wave communications (mmWave) for 5G: opportunities and challenges. **Wireless Networks**, Springer, v. 21, n. 8, p. 2657–2676, 2015.

8 BOCCARDI, F. et al. Five disruptive technology directions for 5G. **IEEE Communications Magazine**, v. 52, n. 2, p. 74–80, Feb. 2014. ISSN 0163-6804.

9 LARSSON, E. et al. Massive MIMO for next generation wireless systems. **IEEE Communications Magazine**, IEEE, v. 52, n. 2, p. 186–195, 2014.

10 LIU, J. et al. Interference management in ultra-dense networks: challenges and approaches. **IEEE Network**, v. 31, n. 6, p. 70–77, Nov. 2017. ISSN 0890-8044.

11 RAPPAPORT, T. S. et al. **Wireless communications: principles and practice**. 2. ed. New Jersey: prentice hall, 1996.

12 AFROZ, F.; SANDRASEGARAN, K.; AL KIM, H. Interference management in LTE downlink networks. **International Journal of Wireless & Mobile Networks**, Academy & Industry Research Collaboration Center (AIRCC), v. 7, n. 1, p. 91, 2015.

13 NAM, W. et al. Advanced interference management for 5G cellular networks. **IEEE Communications Magazine**, IEEE, v. 52, n. 5, p. 52–60, 2014.

14 MIRIDAKIS, N. I.; VERGADOS, D. D. A survey on the successive interference cancellation performance for single-antenna and multiple-antenna OFDM systems. **IEEE Communications Surveys & Tutorials**, IEEE, v. 15, n. 1, p. 312–335, 2013.

15 DIVSALAR, D.; SIMON, M. K.; RAPHAELI, D. Improved parallel interference cancellation for CDMA. **IEEE Transactions on Communications**, v. 46, n. 2, p. 258–268, Feb. 1998. ISSN 0090-6778.

16 GERSHMAN, A. B. et al. Convex optimization-based beamforming: from receive to transmit and network designs. **IEEE Signal Processing Magazine**, v. 27, n. 3, p. 62–75, 2010.

17 LO, T. K. Y. **Maximum ratio transmission**. In: 1999 IEEE International Conference on Communications. [S.l.]: IEEE, 1999. v. 2, p. 1310–1314.

18 WIESEL, A.; ELDAR, Y. C.; SHAMAI, S. Zero-forcing precoding and generalized inverses. **IEEE Transactions on Signal Processing**, v. 56, n. 9, p. 4409–4418, Sept. 2008. ISSN 1053-587X.

19 SERBETLI, S.; YENER, A. Transceiver optimization for multiuser MIMO systems. **IEEE Transactions on Signal Processing**, v. 52, n. 1, p. 214–226, Jan. 2004. ISSN 1053-587X.

20 VENTURINO, L.; PRASAD, N.; WANG, X. Coordinated linear beamforming in downlink multi-cell wireless networks. **IEEE Transactions on Wireless Communications**, v. 9, n. 4, p. 1451–1461, Apr. 2010. ISSN 1536-1276.

21 NEGRO, F. et al. **Weighted sum rate maximization in the MIMO Interference Channel**. In: 21ST Annual IEEE International Symposium on Personal, Indoor and Mobile Radio Communications. [S.l.]: IEEE, Sept. 2010. p. 684–689.

22 BOGALE, T. E.; VANDENDORPE, L. Weighted sum rate optimization for downlink multiuser MIMO coordinated base station systems: centralized and distributed algorithms. **IEEE Transactions on Signal Processing**, IEEE, v. 60, n. 4, p. 1876–1889, 2012.

23 VENTURINO, L.; BUZZI, S. **Energy-efficient coordinated beamforming in downlink OFDMA cellular networks**. In: 2014 IEEE Workshop on Statistical Signal Processing. [S.l.]: IEEE, June 2014. p. 492–495.

24 HUANG, Y. et al. Decentralized energy-efficient coordinated beamforming for multicell systems. **IEEE Transactions on Vehicular Technology**, IEEE, v. 63, n. 9, p. 4302–4314, 2014.

25 HE, S. et al. Coordinated beamforming for energy efficient transmission in multicell multiuser systems. **IEEE Transactions on Communications**, IEEE, v. 61, n. 12, p. 4961–4971, 2013.

26 HE, S. et al. Coordinated multicell multiuser precoding for maximizing weighted sum energy efficiency. **IEEE Transactions on Signal Processing**, v. 62, n. 3, p. 741–751, Feb. 2014. ISSN 1053-587X.

27 RASHID-FARROKHI, F.; LIU, K. J. R.; TASSIULAS, L. Transmit beamforming and power control for cellular wireless systems. **IEEE Journal on Selected Areas in Communications**, v. 16, n. 8, p. 1437–1450, Oct. 1998. ISSN 0733-8716.

28 BENGTSSON, M.; OTTERSTEN, B. **Optimal downlink beamforming using semidefinite optimization**. In: 37TH Annual Allerton Conference on Communication, Control, and Computing. [S.l.]: [s.n.], 1999. p. 987–996.

29 WIESEL, A.; ELDAR, Y. C.; SHAMAI, S. Linear precoding via conic optimization for fixed MIMO receivers. **IEEE Transactions on Signal Processing**, v. 54, n. 1, p. 161–176, Jan. 2006. ISSN 1053-587X. DOI: 10.1109/TSP.2005.861073.

30 PENNANEN, H.; TOLLI, A.; LATVA-AHO, M. Decentralized coordinated downlink beamforming via primal decomposition. **IEEE Signal Processing Letters**, IEEE, v. 18, n. 11, p. 647–650, 2011.

31 TOLLI, A.; PENNANEN, H.; KOMULAINEN, P. Decentralized minimum power multi-cell beamforming with limited backhaul signaling. **IEEE Transactions on Wireless Communications**, IEEE, v. 10, n. 2, p. 570–580, 2011.

32 CHANG, J.-H.; TASSIULAS, L.; RASHID-FARROKHI, F. Joint transmitter receiver diversity for efficient space division multiaccess. **IEEE transactions on wireless communications**, IEEE, v. 1, n. 1, p. 16–27, 2002.

33 BENGTSSON, M. **A pragmatic approach to multi-user spatial multiplexing**. In: SENSOR Array and Multichannel Signal Processing Workshop Proceedings, 2002. [S.l.]: IEEE, 2002. p. 130–134.

34 PENNANEN, H.; TÖLLI, A.; LATVA-AHO, M. **Pragmatic multi-cell MIMO beamforming with decentralized coordination**. In: 2012 Conference Record of the Forty Sixth Asilomar Conference on Signals, Systems and Computers (ASILOMAR). [S.l.]: IEEE, 2012. p. 1996–2000.

35 SHI, Y. et al. Large-scale convex optimization for dense wireless cooperative networks. **IEEE Transactions on Signal Processing**, IEEE, v. 63, n. 18, p. 4729–4743, 2015.

36 GRANT, M.; BOYD, S.; YE, Y. **CVX: MATLAB software for disciplined convex programming**. [S.l.], 2008.

37 O'DONOGHUE, B. et al. Conic optimization via operator splitting and homogeneous self-dual embedding. **Journal of Optimization Theory and Applications**, Springer, p. 1–27, 2016.

38 PAULI, V.; LI, Y.; SEIDEL, E. Dynamic TDD for LTE-A and 5G. **Nomor Research GmbH, Munich, Germany, Tech. Rep**, 2015.

39 SHEN, Z. et al. Dynamic uplink-downlink configuration and interference management in TD-LTE. **IEEE Communications Magazine**, v. 50, n. 11, 2012.

40 INTEL. **Performance analysis of DL-UL interference management and traffic adaptation in multi-cell Pico-Pico deployment scenario**. Jeju, Korea, Mar. 2012.

41 3GPP. **R1-132350: DL power control based interference mitigation for eIMTA**. Fukuoka, Japan, May 2013.

42 _____. **R1-132351: UL power control based interference mitigation for eIMTA**. Fukuoka, Japan, May 2013.

43 CHOI, Y. S.; SOHN, I.; LEE, K. B. **A novel decentralized time slot allocation algorithm in dynamic TDD system**. In: CCNC 2006. 2006 3rd IEEE Consumer Communications and Networking Conference, 2006. [S.l.]: IEEE, Jan. 2006. v. 2, p. 1268–1272.

44 YOON, C.; CHO, D. H. Energy efficient beamforming and power allocation in dynamic TDD based C-RAN system. **IEEE Communications Letters**, v. 19, n. 10, p. 1806–1809, Oct. 2015. ISSN 1089-7798.

45 GUIMARÃES, F. R. V. et al. Pricing-based distributed beamforming for dynamic time division duplexing systems. **IEEE Transactions on Vehicular Technology**, PP, n. 99, p. 1–1, 2017. ISSN 0018-9545.

46 ARDAH, K. et al. **An ADMM approach to distributed coordinated beamforming in dynamic TDD networks**. In: p. 705–709.

47 JAYASINGHE, P. et al. **Bi-directional signaling for dynamic TDD with decentralized beamforming**. In: 2015 IEEE International Conference on Communication Workshop (ICCW). [S.l.]: IEEE, 2015. p. 185–190.

48 BOYD, S. et al. Distributed optimization and statistical learning via the alternating direction method of multipliers. **Foundations and Trends in Machine Learning**, Now Publishers Inc., v. 3, n. 1, p. 1–122, 2011.

49 BERTSEKAS, D. P.; TSITSIKLIS, J. N. **Parallel and distributed computation: numerical methods**. [S.l.]: Prentice hall Englewood Cliffs, NJ, 1989. v. 23.

50 PALOMAR, D. P.; CHIANG, M. A tutorial on decomposition methods for network utility maximization. **IEEE Journal on Selected Areas in Communications**, v. 24, n. 8, p. 1439–1451, 2006.

51 BOYD, S.; XIAO, L.; MUTAPCIC, A. Subgradient methods. **lecture notes of EE392o, Stanford University, Autumn Quarter**, v. 2004, p. 2004–2005, 2003.

52 BERTSEKAS, D. P. **Nonlinear programming**. [S.l.]: Athena scientific Belmont, 1999.

53 CHECKO, A. et al. Cloud RAN for mobile networks: a technology overview. **IEEE Communications surveys & tutorials**, IEEE, v. 17, n. 1, p. 405–426, 2015.

54 CHU, E. et al. **Code generation for embedded second-order cone programming**. In: CONTROL Conference (ECC), 2013 European. [S.l.]: IEEE, 2013. p. 1547–1552.

55 NA, C.; HOU, X.; JIANG, H. **Interference alignment based dynamic TDD for small cells**. In: 2014 IEEE Globecom Workshops (GC Wkshps). [S.l.]: IEEE, 2014. p. 700–705.

56 PENNANEN, H.; TOLLI, A.; LATVA-AHO, M. Multi-cell beamforming with decentralized coordination in cognitive and cellular networks. **IEEE Transactions on Signal Processing**, v. 62, n. 2, p. 295–308, 2014.

57 WONG, K.-K.; ZHENG, G.; NG, T.-S. **Convergence analysis of downlink MIMO antenna systems using second-order cone programming**. In: PROC. of the IEEE Vehic. Tech. Conf. (VTC). [S.l.]: IEEE, 2005. v. 1, p. 492–496.

58 SHI, C.; BERRY, R. A.; HONIG, M. L. Bi-directional training for adaptive beamforming and power control in interference networks. **IEEE Transactions on Signal Processing**, v. 62, n. 3, p. 607–618, 2014.

59 3GPP. **R1-120948: Simulation assumptions for multi-cell scenarios for TDD IMTA**. [S.l.], Feb. 2012.

60 SHEN, C. et al. Distributed robust multicell coordinated beamforming with imperfect CSI: An ADMM approach. **IEEE Transactions on Signal Processing**, v. 60, n. 6, p. 2988–3003, June 2012. ISSN 1053-587X.

61 BOYD, S.; VANDENBERGHE, L. **Convex optimization**. [S.l.]: Cambridge university press, 2004.

APPENDIX A – STRONG DUALITY PROOF

Proof of strong duality for Problem (4.12) . First, observe that an arbitrary phase rotation on the beamformers does not affect the resulting SINR. Thus, if $\{\mathbf{m}_k\}$ is optimal, then so is $\{\mathbf{m}_k e^{j\phi_k}\}$. Hence, we can consider an arbitrary ϕ_k such as $\mathbf{w}_k^H \mathbf{H}_{b_k,k}\mathbf{m}_k$ is real.

Then, since we assume and guarantee the conditions for strict feasibility ($\chi_{b,j} \geq 0, \psi_{b,l} \geq 0, N_b \geq K, \forall b,j,l$), strong duality holds for the convex reformulation of Problem (4.12), which can be written as

$$
\begin{aligned}
&\min_{\{\mathbf{m}_i\}_{i\in\mathcal{K}_b}} \sum_{i\in\mathcal{K}_b} \|\mathbf{m}_i\|_2^2 \qquad\qquad (A.1)\\
&\text{s. t.} \left\| \begin{array}{c} \mathbf{w}_k^H \mathbf{H}_{b_{\mathcal{K}_b(1)},k}\mathbf{m}_{\mathcal{K}_b(1)} \\ \vdots \\ \mathbf{w}_k^H \mathbf{H}_{b_{\mathcal{K}_b(|K_b|)},k}\mathbf{m}_{\mathcal{K}_b(|K_b|)} \\ \bar{\boldsymbol{\chi}}_k \\ \sqrt{\theta_k} \\ \sqrt{N_0} \end{array} \right\|_2 \leq \sqrt{1+\frac{1}{\gamma_k}}\mathbf{w}_k^H \mathbf{H}_{b_k,k}\mathbf{m}_k, \quad \forall k \in \mathcal{K}_b\\
&\sum_{i\in\mathcal{K}_b} |\mathbf{w}_j^H \mathbf{H}_{b,j}\mathbf{m}_i|^2 \leq \chi_{b,j}, \quad \forall j \in \mathcal{K}_{dl}\backslash\mathcal{K}_b\\
&\sum_{i\in\mathcal{K}_b} |\mathbf{m}_l^H \mathbf{G}_{b_i,b_l}\mathbf{m}_i|^2 \leq \psi_{b,l}, \quad \forall l \in \mathcal{K}_{ul},
\end{aligned}
$$

where $\bar{\boldsymbol{\chi}}_k = [\sqrt{\chi_{\bar{\mathcal{B}}_{dl}^{b_k}(1),k}}, \ldots, \sqrt{\chi_{\bar{\mathcal{B}}_{dl}^{b_k}(|\bar{\mathcal{B}}_{dl}^{b_k}|),k}}]^T$, with $\bar{\mathcal{B}}_{dl}^{b_k}$ defining the set of all BSs in DL excluding b_k.

This reformulated problem is convex since its objective is convex, the SINRs constraint is written in a convex conic form, and the other two constraints are convex. Therefore, in order to prove strong duality for problem (4.12) we must still show that the Lagrangians for both the original and the reformulated convex versions of Problem (4.12) are equivalent. The Lagrangian of Problem (4.12) and its convex reformulation are given, respectively, as:

$$
\begin{aligned}
&L(\mathbf{m}_{\mathcal{K}_b(1)}, \ldots, \mathbf{m}_{\mathcal{K}_b(|\mathcal{K}_b|)}, \boldsymbol{\lambda}^{(b)}) = \sum_{i\in\mathcal{K}_b} \mathbf{m}_i^H \mathbf{m}_i + \sum_{k\in\mathcal{K}_{dl}\backslash\mathcal{K}_b} \lambda_k^{(b)} \left(\sum_{i\in\mathcal{K}_b} |\mathbf{w}_k^H \mathbf{H}_{b,k}\mathbf{m}_i|^2 - \chi_{b,k} \right)\\
&+ \sum_{k\in\mathcal{K}_{ul}} \lambda_k^{(b)} \left(\sum_{i\in\mathcal{K}_b} |\mathbf{m}_k^H \mathbf{G}_{b_i,b_k}\mathbf{m}_i|^2 - \psi_{b,k} \right) - \sum_{k\in\mathcal{K}_b} \lambda_k^{(b)} \left(\frac{1}{\gamma_k} |\mathbf{w}_k^H \mathbf{H}_{b_k,k}\mathbf{m}_k|^2 - \sum_{i\in\mathcal{K}_b\backslash k} |\mathbf{w}_k^H \mathbf{H}_{b_i,k}\mathbf{m}_i|^2 \right.\\
&\left. \sum_{b'\in\mathcal{B}_{dl}\backslash b} \chi_{b',k} - \theta_k - N_0 \right), \qquad\qquad (A.2)
\end{aligned}
$$

$$L(\mathbf{m}_{\mathcal{K}_b(1)},\ldots,\mathbf{m}_{\mathcal{K}_b(|\mathcal{K}_b|)},\boldsymbol{\mu}^{(b)}) = \sum_{i\in\mathcal{K}_b}\mathbf{m}_i^H\mathbf{m}_i + \sum_{k\in\mathcal{K}_{dl}\setminus\mathcal{K}_b}\mu_k^{(b)}\left(\sum_{i\in\mathcal{K}_b}|\mathbf{w}_k^H\mathbf{H}_{b,k}\mathbf{m}_i|^2 - \chi_{b,k}\right)$$
$$+\sum_{k\in\mathcal{K}_{ul}}\mu_k^{(b)}\left(\sum_{i\in\mathcal{K}_b}|\mathbf{m}_k^H\mathbf{G}_{b_i,b_k}\mathbf{m}_i|^2 - \psi_{b,k}\right) - \sum_{k\in\mathcal{K}_b}\mu_k^{(b)}\left(\left\|\vdots\right\|_2 - \sqrt{1+\frac{1}{\gamma_k}}\mathbf{w}_k^H\mathbf{H}_{b,k}\mathbf{m}_k\right), \tag{A.3}$$

where, $\left\|\vdots\right\|_2$ represents the term on the left side of the first constraint in Problem (A.1).

Let, us define a new term:

$$t_k = \left\|\vdots\right\|_2 + \sqrt{1+\frac{1}{\gamma_k}}\mathbf{w}_k^H\mathbf{H}_{b,k}\mathbf{m}_k. \tag{A.4}$$

Then, the last term in the Lagrangian (A.3) can be rewritten as:

$$\begin{aligned}
&\mu_k^{(b)}\left(\left\|\vdots\right\|_2 - \sqrt{1+\frac{1}{\gamma_k}}\mathbf{w}_k^H\mathbf{H}_{b,k}\mathbf{m}_k\right)\\
=&\frac{\mu_k^{(b)}}{t_k}\left(\left\|\vdots\right\|_2^2 - \left(1+\frac{1}{\gamma_k}\right)|\mathbf{w}_k^H\mathbf{H}_{b,k}\mathbf{m}_k|^2\right)\\
=&\frac{\mu_k^{(b)}}{t_k}\left(\sum_{i\in\mathcal{K}_b}|\mathbf{w}_k^H\mathbf{H}_{b_i,k}\mathbf{m}_i|^2 + \sum_{b'\in\mathcal{B}_{dl}\setminus b}\chi_{b',k} + \theta_k + N_0 - \left(1+\frac{1}{\gamma_k}\right)|\mathbf{w}_k^H\mathbf{H}_{b,k}\mathbf{m}_k|^2\right)\\
=&\frac{\mu_k^{(b)}}{t_k}\left(\sum_{i\in\mathcal{K}_b\setminus k}|\mathbf{w}_k^H\mathbf{H}_{b_i,k}\mathbf{m}_i|^2 - \frac{1}{\gamma_k}|\mathbf{w}_k^H\mathbf{H}_{b,k}\mathbf{m}_k|^2 + \sum_{b'\in\mathcal{B}_{dl}\setminus b}\chi_{b',k} + \theta_k + N_0\right)
\end{aligned}$$

Substituting this into the Lagrangian (A.3):

$$L(\mathbf{m}_{\mathcal{K}_b(1)},\ldots,\mathbf{m}_{\mathcal{K}_b(|\mathcal{K}_b|)},\boldsymbol{\lambda}^{(b)}) = \sum_{i\in\mathcal{K}_b}\mathbf{m}_i^H\mathbf{m}_i + \sum_{k\in\mathcal{K}_{dl}\setminus\mathcal{K}_b}\mu_k^{(b)}\left(\sum_{i\in\mathcal{K}_b}|\mathbf{w}_k^H\mathbf{H}_{b,k}\mathbf{m}_i|^2 - \chi_{b,k}\right)$$
$$+\sum_{k\in\mathcal{K}_{ul}}\mu_k^{(b)}\left(\sum_{i\in\mathcal{K}_b}|\mathbf{m}_k^H\mathbf{G}_{b_i,b_k}\mathbf{m}_i|^2 - \psi_{b,k}\right) - \sum_{k\in\mathcal{K}_b}\frac{\mu_k^{(b)}}{t_k}\left(\frac{1}{\gamma_k}|\mathbf{w}_k^H\mathbf{H}_{b_k,k}\mathbf{m}_k|^2 - \sum_{i\in\mathcal{K}_b\setminus k}|\mathbf{w}_k^H\mathbf{H}_{b_i,k}\mathbf{m}_i|^2\right.$$
$$\left.\sum_{b'\in\mathcal{B}_{dl}\setminus b}\chi_{b',k} - \theta_k - N_0\right), \tag{A.5}$$

Since t_k is strictly positive, we can change the optimization variable to $\lambda_k = \gamma_k/t_k$ and the Lagrangians of the original and the convex reformulated problems are the same. Therefore, the dual problems of the two equivalent problems are the same, and strong duality holds for both of them.

□

APPENDIX B – DUAL PROBLEM FORMULATION

To find the the dual Problem of (4.12), let us first write its Lagrangian as

$$
\begin{aligned}
L(\mathbf{m}_{\mathcal{K}_b(1)},\ldots,\mathbf{m}_{\mathcal{K}_b(|\mathcal{K}_b|)},\boldsymbol{\lambda}^{(b)}) &= \sum_{i\in\mathcal{K}_b}\mathbf{m}_i^H\mathbf{m}_i - \sum_{k\in\mathcal{K}_b}\lambda_k^{(b)}\Bigg(\frac{1}{\gamma_k}|\mathbf{w}_k^H\mathbf{H}_{b_k,k}\mathbf{m}_k|^2 - \sum_{i\in\mathcal{K}_b\setminus k}|\mathbf{w}_k^H\mathbf{H}_{b_i,k}\mathbf{m}_i|^2 \\
&- \sum_{b'\in\mathcal{B}_{dl}\setminus b}\chi_{b',k} - \theta_k - N_0\Bigg) + \sum_{k\in\mathcal{K}_{dl}\setminus\mathcal{K}_b}\lambda_k^{(b)}\Bigg(\sum_{i\in\mathcal{K}_b}|\mathbf{w}_k^H\mathbf{H}_{b,k}\mathbf{m}_i|^2 - \chi_{b,k}\Bigg) \\
&+ \sum_{k\in\mathcal{K}_{ul}}\lambda_k^{(b)}\Bigg(\sum_{i\in\mathcal{K}_b}|\mathbf{m}_k^H\mathbf{G}_{b_i,b_k}\mathbf{m}_i|^2 - \psi_{b,k}\Bigg) \qquad \text{(B.1)} \\
&= \sum_{k\in\mathcal{K}_b}\lambda_k^{(b)}\Bigg(\sum_{b'\in\mathcal{B}_{dl}\setminus b}\chi_{b',k} + \theta_k + N_0\Bigg) - \sum_{k\in\mathcal{K}_{dl}\setminus\mathcal{K}_b}\lambda_k^{(b)}\chi_{b,k} - \sum_{k\in\mathcal{K}_{ul}}\lambda_k^{(b)}\psi_{b,k} \\
&+ \sum_{k\in\mathcal{K}_b}\mathbf{m}_k^H\Bigg(\mathbf{I} - \frac{\lambda_k^{(b)}}{\gamma_k}\mathbf{H}_{b_k,k}^H\mathbf{w}_k\mathbf{w}_k^H\mathbf{H}_{b_k,k} + \sum_{i\in\mathcal{K}_{dl}\setminus k}\lambda_i^{(b)}\mathbf{H}_{b,i}^H\mathbf{w}_i\mathbf{w}_i^H\mathbf{H}_{b,i} \\
&+ \sum_{i\in\mathcal{K}_{ul}}\lambda_i^{(b)}\mathbf{G}_{b_k,b_i}^H\mathbf{m}_i\mathbf{m}_i^H\mathbf{G}_{b_k,b_i}\Bigg)\mathbf{m}_k \qquad \text{(B.2)}
\end{aligned}
$$

The dual problem is defined as the infimum of the Lagrangian [61], that is given as

$$
g(\boldsymbol{\lambda}^{(b)}) = \inf_{\mathbf{m}_{\mathcal{K}_b(1)},\ldots,\mathbf{m}_{\mathcal{K}_b(|\mathcal{K}_b|)}} L(\mathbf{m}_{\mathcal{K}_b(1)},\ldots,\mathbf{m}_{\mathcal{K}_b(|\mathcal{K}_b|)},\boldsymbol{\lambda}^{(b)})
$$

$$
g(\boldsymbol{\lambda}^{(b)}) = \begin{cases} \begin{pmatrix} \sum_{k\in\mathcal{K}_b}\lambda_k^{(b)}\Big(\sum_{b'\in\mathcal{B}_{dl}\setminus b}\chi_{b',k} \\ +\theta_k + N_0\Big) \\ -\sum_{k\in\mathcal{K}_{dl}\setminus\mathcal{K}_b}\lambda_k^{(b)}\chi_{b,k} \\ -\sum_{k\in\mathcal{K}_{ul}}\lambda_k^{(b)}\psi_{b,k} \end{pmatrix}, & \text{if } \begin{pmatrix} \mathbf{I} - \frac{\lambda_k^{(b)}}{\gamma_k}\mathbf{H}_{b_k,k}^H\mathbf{w}_k\mathbf{w}_k^H\mathbf{H}_{b_k,k} \\ +\sum_{i\in\mathcal{K}_{dl}\setminus k}\lambda_i^{(b)}\mathbf{H}_{b,i}^H\mathbf{w}_i\mathbf{w}_i^H\mathbf{H}_{b,i} \\ +\sum_{i\in\mathcal{K}_{ul}}\lambda_i^{(b)}\mathbf{G}_{b_k,b_i}^H\mathbf{m}_i\mathbf{m}_i^H\mathbf{G}_{b_k,b_i} \end{pmatrix} \succeq 0, \forall k\in\mathcal{K}_b \\ -\infty, & \text{otherwise} \end{cases} \qquad \text{(B.3)}
$$

Then, the dual of (4.12) is given as (4.18).